CALORIC MEASUREMENTS ON LIQUID AND MELTING HELIUM BELOW 1.5 KELVIN

J. WIEBES

CALORIC MEASUREMENTS ON LIQUID AND MELTING HELIUM BELOW 1.5 KELVIN

PROEFSCHRIFT

TER VERKRIJGING VAN DE GRAAD VAN DOCTOR IN DE WISKUNDE EN NATUURWETENSCHAPPEN AAN DE RIJKSUNIVERSITEIT TE LEIDEN, OP GEZAG VAN DE RECTOR MAGNIFICUS DR L. KUKENHEIM EZN, HOOGLERAAR IN DE FACULTEIT DER LETTEREN, TEN OVERSTAAN VAN EEN COMMISSIE UIT DE SENAAT TE VERDEDIGEN OP WOENSDAG 23 APRIL 1969 TE KLOKKE 14.15 UUR

DOOR

JACOB WIEBES

GEBOREN TE ROTTERDAM IN 1931

1969

BEUGELSDIJK — LEIDEN

PROMOTOR: PROF. DR K. W. TACONIS

DIT PROEFSCHRIFT IS BEWERKT ONDER
LEIDING VAN DR H. C. KRAMERS

STELLINGEN

1. De resultaten van Karra e.a. voor de polarisatie- en relaxatietijden van de protonspins in verdunde kopertuttonzouten zijn niet in overeenstemming met de metingen van Wenckebach e.a.; tegen hun konklusies over de elektronspin-roosterrelaxatietijd zijn ernstige bedenkingen in te brengen.
   J.S.Karra, R.Clarkson en T.Sato, Phys.Rev.175(1968)479;
   W.Th.Wenckebach, T.J.B.Swanenburg, H.Hoogstraate en N.J.Poulis, Phys.Letters 26(1968)203.

2. In de uitdrukking voor de voortplantingssnelheid van het zgn. second sound in helium II:

$$u_{II} = \sqrt{(\rho_s/\rho_n)\ T\ S^2/\ C}$$

   is de benadering van de soortelijke warmte C door die bij konstante druk, C_p, beter dan door die bij konstant volume, C_v.

3. Een indeling van faseovergangen anders dan de oorspronkelijke van Ehrenfest, heeft slechts zin wanneer de verschillende soorten van diskontinuïteiten nader worden onderscheiden.
   M.E.Fisher, Reports on Progress in Physics, ed.A.C.Stickland (The Institute of Physics and The Physical Society, London 1967) Vol.XXX,Part II,p.617.

4. De resultaten van de expansiemetingen aan vloeibaar helium onder druk van Mills en Sydoriak zijn dermate onbevredigend, dat ze niet meer toelaten dan een schatting van de entropie van kompressie.
   R.L.Mills en S.G.Sydoriak, Ann.Phys.(NY)34(1965)276.

5. De verschillen tussen effektieve rotonparameters, die met behulp van de benadering volgens Landau uit verschillende thermodynamische grootheden van helium zijn afgeleid, worden voornamelijk veroorzaakt doordat de excitatiekromme symmetrische afwijkingen van een parabolisch verloop vertoont.

6. Na het beschikbaar komen van de gegevens over de excitatiekrommen uit de experimenten aan inelastische verstrooiing van neutronen, is het niet langer zinvol om de thermodynamische grootheden van helium II met behulp van de parabolische benadering voor rotonen volgens Landau te analyseren.
R.L.Mills, Ann.Phys.(NY)35(1965)410;
dit proefschrift.

7. Het is gewenst dat er eisen worden geformuleerd, waaraan studenten na het volbrengen van een practicum natuurkunde behoren te kunnen voldoen.

8. Het is voor het opdoen van elementair experimenteel inzicht niet gewenst, dat de studenten op het practicum natuurkunde uitsluitend met moderne geautomatiseerde apparatuur in aanraking komen.

9. Onder de wet op het voortgezet onderwijs (de mammoetwet) zijn in de voorbereiding tot het wetenschappelijke onderwijs in de fysika verbeteringen mogelijk; hierbij dient aan het meer bevorderen van een experimentele instelling bij de leerlingen een belangrijke plaats te worden ingeruimd.

10. Tegen de proeven waarmee tot 1964 bij TNO vochtdoorlating van bouwmaterialen is bepaald, zijn bezwaren in te brengen.

11. De verklaring van de werking van een roterende tuinsproeier (reaktierad van Segner) kan direkter worden gegeven via de impuls van de uittredende vloeistof dan via de drukkrachten op de wand; een kwadratisch verband tussen het stuwende koppel en de uittreesnelheid is eenvoudig experimenteel te demonstreren.
J.Wiebes, Faraday 36(1966)49,106.

12. Het is niet vanzelfsprekend dat in de nabije toekomst die maatregelen zullen kunnen worden genomen, die nodig zijn om katastrofale veranderingen in de biosfeer te voorkomen.

Stellingen behorende bij het proefschrift van J.Wiebes.

CURRICULUM VITAE

Teneinde te voldoen aan de wens van de Faculteit der Wiskunde en Natuurwetenschappen laat ik hier een overzicht van mijn studie volgen.

Nadat ik het eindexamen B aan de Rijks Hogere Burgerschool te Vlissingen had afgelegd, ving ik in 1949 mijn studie in Leiden aan. In 1953 legde ik het kandidaatsexamen D in de vakken wiskunde en natuurkunde met scheikunde af.

In september 1953 begon ik mijn werkzaamheden op het Kamerlingh Onnes Laboratorium onder leiding van dr H.C. Kramers. Na de bestaande elektronische apparatuur daartoe te hebben gerevideerd, assisteerde ik bij de metingen aan warmtepulsen in vloeibaar helium en bij de uitwerking daarvan. Vervolgens deed ik in samenwerking met mevrouw dra. C.G. Niels-Hakkenberg een onderzoek aan het fononbijdrage van de soortelijke warmte van helium. Ook hielp ik dr G.J.C. Bots bij diens metingen over het fonteineffekt en het mechanokalorische effekt. Ik legde de tentamens in de wiskunde en de theoretische natuurkunde af na het volgen van colleges van de hoogleraren dr J. Droste, dr N.G. van Kampen, dr S.R. de Groot, dr J. van Kranendonk en dr ir. F.A.W. van den Burg. In juli 1957 legde ik het doctoraal examen experimentele natuurkunde met wiskunde af.

Mijn medewerking aan een nader onderzoek van warmtepulsen werd in augustus 1957 afgebroken doordat ik werd opgeroepen voor de vervulling van mijn militaire dienstplicht. Ingelijfd bij de Koninklijke Luchtmacht, werd ik opgeleid tot weerdienstofficier en was ik als zodanig een jaar werkzaam.

In augustus 1959 keerde ik terug naar het Kamerlingh Onnes Laboratorium waar ik als hoofdassistent, in de rang van wetenschappelijk ambtenaar, werd belast met de dagelijkse leiding van het practicum natuurkunde voor praekandidaten (van 1954 tot 1957

was ik daaraan als assistent verbonden geweest). Sinds 1962 ben ik speciaal belast met het beheer over de Practicum Dependance in het Provisorium Schelpenkade, en met het eerstejaars practicum voor de kandidaatsexamens W, A en N. Ik maakte deel uit van de kommissies voor het examen Natuurkundig Assistent A van 1962 tot 1965, en voor het examen N I (akte voor nijverheidsonderwijs) sinds 1964, in het bijzonder voor de experimentele gedeelten daarvan.

In 1961 ontwikkelde ik in samenwerking met drs. W.S. Hulscher een nieuwe kompensator voor wederkerige induktie voor het meten met magnetische thermometers. Met behulp van deze apparatuur werden in 1963 de metingen over de soortelijke warmte van vloeibaar helium onder druk en over het minimum in de smeltkromme begonnen. Bij deze metingen werd ik terzijde gestaan door drs. W.S. Hulscher, die een belangrijk aandeel heeft gehad in de bouw van de magnetische thermometer, en later door de heer P. van 't Zelfde en door drs. A. de Bakker, die de metingen ook heeft helpen uitwerken.

De leden van de technische staf van het Kamerlingh Onnes Laboratium die in het bijzonder hebben bijgedragen tot het welslagen van de experimenten, zijn de heren A.R.B. Gerritse en H. van Zanten voor het glastechnische gedeelte, de heer J.W. Groenewold voor het metaaltechnische deel en vooral de heer T. Nieboer voor de bouw van het apparaat en de kryogeentechnische verzorging. Dr J.K. Hoffer ben ik dank verschuldigd voor het verbeteren van de Engelse tekst. De heer W.F. Tegelaar verzorgde o.m. de tekeningen van dit proefschrift; mevrouw E.C. Kaper-van Gent heeft een belangrijk gedeelte van het typewerk gedaan.

CONTENTS

LIST OF SYMBOLS

Quantities

α = coefficient of thermal expansion
c = specific heat
ε = energy of elementary excitation
Δ = operator denoting increase during a measurement; minimum roton energy
F = free energy
$h = 2\pi\hbar$ = Planck's constant
k = Boltzmann's constant
$\varkappa$ = compressibility
l = specific latent heat
M = mutual inductance
m = mass; mass of ^{4}He atom
μ = roton parameter
N = number of excitations
p = pressure; momentum of excitation
Q = amount of heat
ρ = density
S = entropy
$s = S/m$ = specific entropy
T = temperature
u = velocity of first sound
V = volume
$v = 1/\rho = V/m$ = specific volume
$W = m\,c$ = heat capacity

Subscripts

	Examples
c : calorimeter	S_c, W_c
f : final value at a measuring point	M_f, m_{tf}, S_{cf}, s_{lf}, T_f, v_{lf}
g : gas	c_{pg}, m_g, s_g, V_g, v_g
i : initial value at a measuring point	M_i, m_{ti}, S_{ci}, s_{si}, T_i, v_{si}
l : liquid	α_{pl}, $c_{\mu l}$, c_{pl}, $c_{\sigma l}$, c_{vl}, m_l, ρ_l, V_l, v_l, s_l
μ : along the melting curve	c_μ, l_μ, p_μ, $(d/dT)_\mu$
p : at constant pressure (isobaric)	α_p, c_p, $(\partial/\partial T)_p$, $[\rho_l - \rho_{lo}]_p$
ph: phonon	C_{vph}, ε_{ph}, F_{ph}, N_{ph}, ρ_{nph}, S_{ph}
r : roton	C_{vr}, ε_r, F_r, N_r, ρ_{nr}, S_r
ρ : at constant density (isopycnal)	$[p - p_o]_\rho$
s : solid	$c_{\mu s}$, m_s, ρ_s, s_s, V_s, v_s
σ : along the vapour pressure curve	c_σ, p_σ, $(d/dT)_\sigma$
T : at constant temperature (isothermal)	$\varkappa_T$
t : total	m_t, S_t, V_t, W_t
v : at constant volume (isochoric)	c_v
0 : at zero (or low) temperature	p_o, ρ_{lo}
1 : at the lowest bath temperature (1.1 K)	T_1, M_1
2 : just after total melting	m_{l2}, m_{s2}, T_2, v_{l2}, v_{s2}

CHAPTER I

GENERAL INTRODUCTION

1-1. Introduction

Although, next to water, liquid helium-four is perhaps the most investigated of all liquids, our knowledge about it, up to 1963, consisted mainly of the properties along its vapour pressure curve. Of course, the liquid had been studied also under higher pressures but those measurements were performed at temperatures above 1 K. One of the few exceptions to this is the measurement by Mayper and Herlin[1,1]) (1953) of the velocity of second sound at several pressures down to 0.2 K. As for the equation of state and the thermodynamic properties, the area in the phase diagram extending below a temperature of 1 K was "terra incognita"(see fig. 1,1). One reason for this is that equipment for measurements under pressure is more complicated than equipment for experiments at saturated vapour pressure. Perhaps another reason is that many of the interesting features of helium II can be displayed and studied

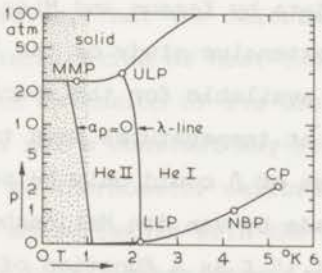

Fig. 1,1. Phase diagram of ^{4}He; vapour pressure curve with critical point (CP), normal boiling point (NBP) and lower lambda point (LLP); λ-line; melting curve with upper lambda point (ULP) and shallow minimum in the melting pressure (MMP); locus of zero coefficient of thermal expansion α_p.

without the necessity for going to pressures higher than that of the saturated vapour.

However, reasonable estimates for the thermodynamic quantities could be made from extrapolations of results obtained at temperatures above 1 K. First, the density as a function of the pressure has been known since the work of Keesom and Miss Keesom[1,2] (1933) on the isopycnals above 1.15 K. Secondly, the velocity of ordinary or first sound, which could have been calculated quite well from those data, was measured by Atkins and Stasior[1,3] (1953) above 1.2 K as a function of the pressure. From higher temperatures towards 1 K, it clearly becomes almost independent of temperature. Now at temperatures below about 0.5 K, the thermodynamic properties are almost exclusively due to thermal excitations called phonons [1,4]. Since the phonons are essentially sound waves described by the velocity of first sound, the thermodynamic quantities at low temperatures could be calculated.

At increasing temperatures above roughly 0.5 K, the contributions of another kind of excitations called rotons[1,4][1,5] become rapidly important. In contrast to phonons giving contributions that vary as the third or the fourth power of temperature, the contributions of the rotons vary essentially as the exponential $e^{-\Delta/kT}$. Here Δ is the minimum energy required to excite a roton. Ignoring some early and limited data by Keesom and Miss Keesom[1,6], it was not before Lounasmaa's extensive study of the lambda line[1,7][1,8] (1959) that data became available for the specific heat as a function of the density at temperatures down to 1.5 K. However, a calculation of the values of Δ could only be performed after measurements had been made by van den Meijdenberg et al.[1,9] (1961) of the entropy down to 1.15 K as a function of the pressure (from the fountain effect). Based on these values the roton contributions at temperatures below 1.1 K may be estimated but, due to the steep exponential function, the accuracy obtained is considerably less than that for the phonons.

In the mean time, the understanding of the nature of the elementary excitations[1,10-13]) had been greatly improved by direct determinations of the excitation spectra from experiments on inelastic neutron scattering[1,14-18]). From these the thermodynamic quantities may be computed directly[1,19])[1,20]). Apart from data at saturated vapour pressure, unfortunately, only one spectrum, at the melting pressure, has been reported.

In more recent years (since 1963) much work has been reported on helium under pressures higher than that of the saturated vapour and at temperatures below 1 K. By the use of ^{3}He cryostats a temperature of 0.4 K can be reached easily. In addition to the equation of state and the thermodynamic quantities of the liquid [1,21-26]) and the solid phase[1,27-29]), special attention has been given to the melting curve since the theoretical[1,30-33]) and the experimental discovery[1,29])[1,34-39]) of a shallow minimum in the melting pressure at a temperature of 0.77 K.

The present measurements were undertaken to extend the data on the specific heat of the liquid under pressure to temperatures as low as 0.3 K. The results enable one to calculate, by means of extrapolations into the pure phonon region, the thermodynamic quantities from the absolute zero of temperature. As an interesting by-product, results on the melting curve could be obtained. It must be borne in mind, however, that the calorimeter has been designed primarily for the determination of heat capacities of the liquid at constant pressure. The extension of its use to measurements in which the pressure is not a constant may be accompanied by difficulties with respect to thermometer calibration. In the next section the possible measurements with the calorimeter will be reviewed. In contrast to all other recent experiments (in which ^{3}He cryostats are used) the method of cooling by adiabatic demagnetization was employed.

1-2. Measurements with an open calorimeter

A calorimeter is generally used for the determination of heat capacities under specified conditions. A known amount of heat ΔQ is added and the resulting increase ΔT of the temperature T is measured. However, if the calorimeter is not closed there is the possibility of changing its content by a known amount Δm_t, or its pressure by Δp, through adiabatic compression or expansion, i.e. without the addition of heat. By means of the heat capacity the resulting change of temperature ΔT can be translated into an amount of heat. The thermodynamic quantity to be calculated from this depends on the composition of the contents.

The calorimeter used in the present experiments is connected to the pressurizing apparatus by a filling capillary. The amount of helium can therefore be changed. In table 1,I the present experiments have been compiled. Small effects, e.g. those originating from thermal expansion, have been omitted here but will be taken fully into account in the actual evaluations (see chapter III). The various experiments will now be reviewed in succession.

Experiment A. Since all results have to be corrected for the heat capacity W_c of the calorimeter, the latter must be determined separately. This is done with a small amount m_1 of helium in the calorimeter in order to enhance internal equilibrium of temperature. Consequently, the calorimeter contains both liquid and vapour. The contributions of these can be calculated if the specific heat $c_{\sigma l}$ of the liquid along the vapour pressure curve and the saturated vapour pressure p_σ are known as functions of temperature.

Experiment B. When the calorimeter of volume V_t is filled with the liquid under the pressure p, the specific heat c_{pl} of the liquid at constant pressure can be found if the density ρ_l is known.

Experiment C. From the change of temperature resulting from an adiabatic change of pressure, the coefficient of isobaric

Table 1,I. Experiments with a calorimeter of heat capacity W_c, filled with helium of total volume V_t of 15.8 cm^3.

exp.	phases	process	accepted quantities	measured quantities	calculated quantities
A	vapour and liquid	closed $\Delta m_t = 0$	$c_{\sigma l}$ p_σ	T ΔQ , ΔT m_l	$W_c = \frac{\Delta Q}{\Delta T} - m_l c_{\sigma l} - W_{vap}(p_\sigma)$
B	liquid	closed $\Delta m_t = 0$	ρ_l W_c (from A)	p , T ΔQ , ΔT	$c_{pl} = (\frac{\Delta Q}{\Delta T} - W_c)/ V_t \rho_l$
C	liquid	adiabatic $\Delta Q = 0$	ρ_l W_c (from A) c_{pl} (from B)	p , T Δp , ΔT	$\alpha_{pl} = \frac{W_c + V_t \rho_l c_{pl}}{V_t T} \frac{\Delta T}{\Delta p}$
D	solid and liquid	closed $\Delta m_t = 0$	ρ_l , ρ_s W_c (from A) $c_{\mu l}$ (from B)	p_μ , T ΔQ , ΔT m_{melt}	$m_s = m_{melt}\rho_s /(\rho_s - \rho_l)$ $m_l = V_t\rho_l - m_{melt}\rho_l /(\rho_s - \rho_l)$ $c_{\mu s} = (\frac{\Delta Q}{\Delta T} - W_c - m_l c_{\mu l})/ m_s$
E	solid and liquid	adiabatic $\Delta Q = 0$	ρ_l , ρ_s W_c (from A) $c_{\mu l}$ (from B) $c_{\mu s}$ (from D)	T Δm_t , ΔT m_{melt}	$m_s = m_{melt}\rho_s /(\rho_s - \rho_l)$ $m_l = V_t\rho_l - m_{melt}\rho_l /(\rho_s - \rho_l)$ $\frac{dp_\mu}{dT} = (W_c + m_l c_{\mu l} + m_s c_{\mu s}) \frac{\rho_l}{T} \frac{\Delta T}{\Delta m_t}$

thermal expansion α_{pl} may be calculated if the total heat capacity $W_c + V_t \rho_l c_{pl}$ is known.

Experiment D. When the calorimeter contains both the solid and the liquid phase, the total heat capacity is composed of contributions from both phases. The amounts of the solid and the liquid phases, m_s and m_l, are determined separately from the amount m_{melt} that has to be released in order to melt the solid. The specific heat $c_{\mu l}$ of the liquid along the melting curve can be extrapolated from experiment B if the melting pressure p_μ is known. The specific heat $c_{\mu s}$ of the solid along the melting curve may now be calculated from the heat capacity

remaining after subtraction of the contributions of the liquid and the calorimeter.

Experiment E. When a small amount Δm_t is released from a two-phase system of solid and liquid, some of the solid will melt. The heat needed for this process causes a change of temperature. Consequently, the heat of melting l_μ (or the slope dp_μ/dT of the melting curve related to l_μ by Clapeyron's equation) can be determined.

The results from experiments B and C, as well as those from experiments D and E, are connected by simple thermodynamic relations. This is shown in table 1,II where the manner of evaluation has been indicated. The measurements of the heat capacities as performed in the experiments B and D yield provisional values c_{lprov} and c_{sprov} for the specific heats of the liquid and the solid. Corrections calculated by means of these provisional results have to be applied in order to find the desired specific heats c_{pl} and $c_{\mu s}$. By simple integration, the specific entropies s_l and s_s can be found from the specific heats. The entropies can now be related to the results of the expansion experiments C and E by application of the second law of thermodynamics.

For the pure liquid phase the Maxwell relation:

$$\left(\frac{\partial s_l}{\partial p}\right)_T = -\left(\frac{\partial v_l}{\partial T}\right)_p = -\alpha_{pl}/\rho_l \qquad (1,1)$$

is used connecting the dependence of the entropy on the pressure with the dependence of the specific volume v_l on the temperature. Consequently, the coefficient of thermal expansion α_{pl} can be computed from the entropy as found in experiment B, and compared with the results of experiment C.

For the two-phase system of solid and liquid Clapeyron's equation applies:

Table 1,II. Scheme of calculations.

exp.	phases	process	calculated from measurements	used for
B	liquid	closed $\Delta m_t \approx 0$	$c_{lprov} \xrightarrow{cor} c_{pl}(p,T) \xrightarrow{cor} c_{vl}(\rho_l,T)$ $\downarrow$ $s_l(p,T) = \int_0^T \frac{c_{pl}}{T} dT \xrightarrow{cor} s_l(\rho_l,T)$ $\downarrow$ $\alpha_{pl}(p,T) = -\rho_l \left(\frac{\partial s_l}{\partial p}\right)_T$ $\downarrow$ $[\rho_l - \rho_{lo}]_p = -\rho_{lo} \int_0^T \alpha_{pl} dT$	theory comparison with exp. C corrections
D	solid and liquid	closed $\Delta m_t = 0$	$c_{sprov} \xrightarrow{cor} c_{\mu s}(T)$ $\downarrow$ $s_s(p_\mu,T) = \int_0^T \frac{c_{\mu s}}{T} dT$ $\downarrow$ $\frac{dp_\mu}{dT} = \frac{s_l - s_s}{v_l - v_s}$ $\downarrow$ $p_\mu(T) - p_\mu(0) = \int_0^T \frac{dp_\mu}{dT} dT$	theory comparison with exp. E $\rho_l(p_\mu,T)$ $s_l(p_\mu,T)$ $c_{\mu l}(T)$

$$dp_\mu/dT = (s_l - s_s) / (v_l - v_s) = l_\mu / T\,(v_l - v_s) \qquad (1,2)$$

relating the entropy difference between the liquid and the solid to the slope of the melting curve. The results as calculated from experiment D may be compared with the more direct determination from experiment E.

In the case of the liquid, the results of the entropy as a function of the density may be compared with theory. For the solid the specific heat may be used to compute the corresponding effective Debije temperatures.

1-3. Survey

In chapter II the experimental arrangement will be given. The measuring apparatus will be described and the cooling and measuring procedures discussed.

In chapter III the appropriate thermodynamic formulae will be derived. Data to be taken from other experiments will be discussed and the various corrections will be indicated. Since the main scheme of calculations has been outlined above, sections 3-2 and 3-4 of this chapter serve only as a more detailed derivation of the formulae and the corrections.

In chapter IV the contribution of the empty calorimeter will be calculated and discussed (experiment A), and the experiments B and C on the liquid will be evaluated. The results will be compared with existing data.

In chapter V the experiments D and E on the two-phase system of solid and liquid will be presented. The results on the melting curve will be discussed.

In chapter VI the entropy of the liquid will be analysed in terms of constants relating to the excitation curves. The results will be compared with the existing data.

REFERENCES

1,1) V.Mayper and M.A.Herlin, Phys.Rev.89(1953)523.

1,2) W.H.Keesom and A.P.Keesom, Commun.Kamerlingh Onnes Lab.,Leiden No.224d,e; Proc. roy.Acad.Amsterdam 36(1933)482,612.

1,3) K.R.Atkins and R.A.Stasior, Canad.J.Phys.31(1953)1156.

1,4) L.D.Landau, J.Phys.U.S.S.R.5(1941)71.

1,5) L.D.Landau, J.Phys.U.S.S.R.11(1947)91; see also D.ter Haar in Selected Readings in Physics, Vol.I, Low Temperature and Solid State Physics; Men of Physics: L.D.Landau (Pergamum Press 1965).

1,6) W.H.Keesom and A.P.Keesom, Commun.Leiden No.235d; Physica 2(1935)557.

1,7) O.V.Lounasmaa and E.Kojo, Ann.Acad.Sci.fenn.A VI,No.36(1959).

1,8) O.V.Lounasmaa and L.Kaunisto, Ann.Acad.Sci.fenn.A VI,No.59(1960).

1,9) C.J.N.van den Meijdenberg, K.W.Taconis and R.de Bruyn Ouboter, Commun.Leiden No.326c; Physica 27(1961)197.

1,10) R.P.Feynman, Phys.Rev.91(1953)1301.

1,11) R.P.Feynman, Phys.Rev.94(1954)262.

1,12) R.P.Feynman and M.Cohen, Phys.Rev.102(1956)1189.

1,13) M.Cohen and R.P.Feynman, Phys.Rev.107(1957)13.

1,14) H.Palevsky, K.Otnes and K.E.Larsson, Phys.Rev.112(1958)11.

1,15) K.E.Larsson and K.Otnes, Ark.Fys.15(1959)49.

1,16) J.L.Yarnell, G.P.Arnold, P.J.Bendt and E.C.Kerr, Phys.Rev.113(1959)1379.

1,17) D.G.Henshaw and A.D.B.Woods, Proc. VIIth intern.Conf.on Low Temp.Phys.(Toronto 1961)p.539.

1,18) D.G.Henshaw and A.D.B.Woods, Phys.Rev.121(1961)1266.

1,19) P.J.Bendt, R.D.Cowan and J.L.Yarnell, Phys.Rev.113(1959)1386.

1,20) M.Cohen, Phys.Rev.118(1960)27.

1,21) J.Wiebes and H.C.Kramers, Proc.IXth intern.Conf.on Low Temp.Phys.(Columbus 1965)p.258.

1,22) R.L.Mills and S.G.Sydoriak, Ann.Phys.(NY)34(1965)276.

1,23) R.L.Mills, Ann.Phys.(NY)35(1965)410.

1,24) C.Boghosian and H.Meyer, Phys.Rev.152(1966)200.

1,25) J.Wiebes and H.C.Kramers, Proc.Xth intern.Conf.on Low Temp.Phys.(Moscow 1967) Vol.I,p.243.

1,26) C.G.Waterfield and J.K.Hoffer, to be published.

1,27) D.O.Edwards and R.C.Pandorf, Phys.Rev.140(1965)816.

1,28) J.Jarvis and H.Meyer, Proc.Xth intern.Conf.on Low Temp.Phys.(Moscow 1967)Vol.I, p.258.

1,29) J.K.Hoffer, Ph.D.Thesis (Berkeley 1968).

1,30) L.Goldstein, Phys.Rev.Letters 5(1960)104.

1,31) L.Goldstein, Phys.Rev.122(1961)726.

1,32) L.Goldstein, Phys.Rev.128(1962)1520.

1,33) L.Goldstein and R.L.Mills, Phys.Rev.159(1967)136.

1,34) J.Wiebes and H.C.Kramers, Phys.Letters 4(1963)298.

1,35) C.le Pair, K.W.Taconis, R.de Bruyn Ouboter and P.Das, Physica 29(1963)755.

1,36) G.O.Zimmerman, Proc.IXth intern.Conf.on Low Temp.Phys.(Columbus 1965)p.240.

1,37) S.G.Sydoriak and R.L.Mills, Proc.IXth intern.Conf.on Low Temp.Phys.(Columbus 1965)p.273.

1,38) C.le Pair, R.de Bruyn Ouboter and J.Pit, Commun.Leiden No.344a; Physica 31 (1965)813.

1,39) G.C.Straty and E.D.Adams, Phys.Rev.Letters 17(1966)290,505.

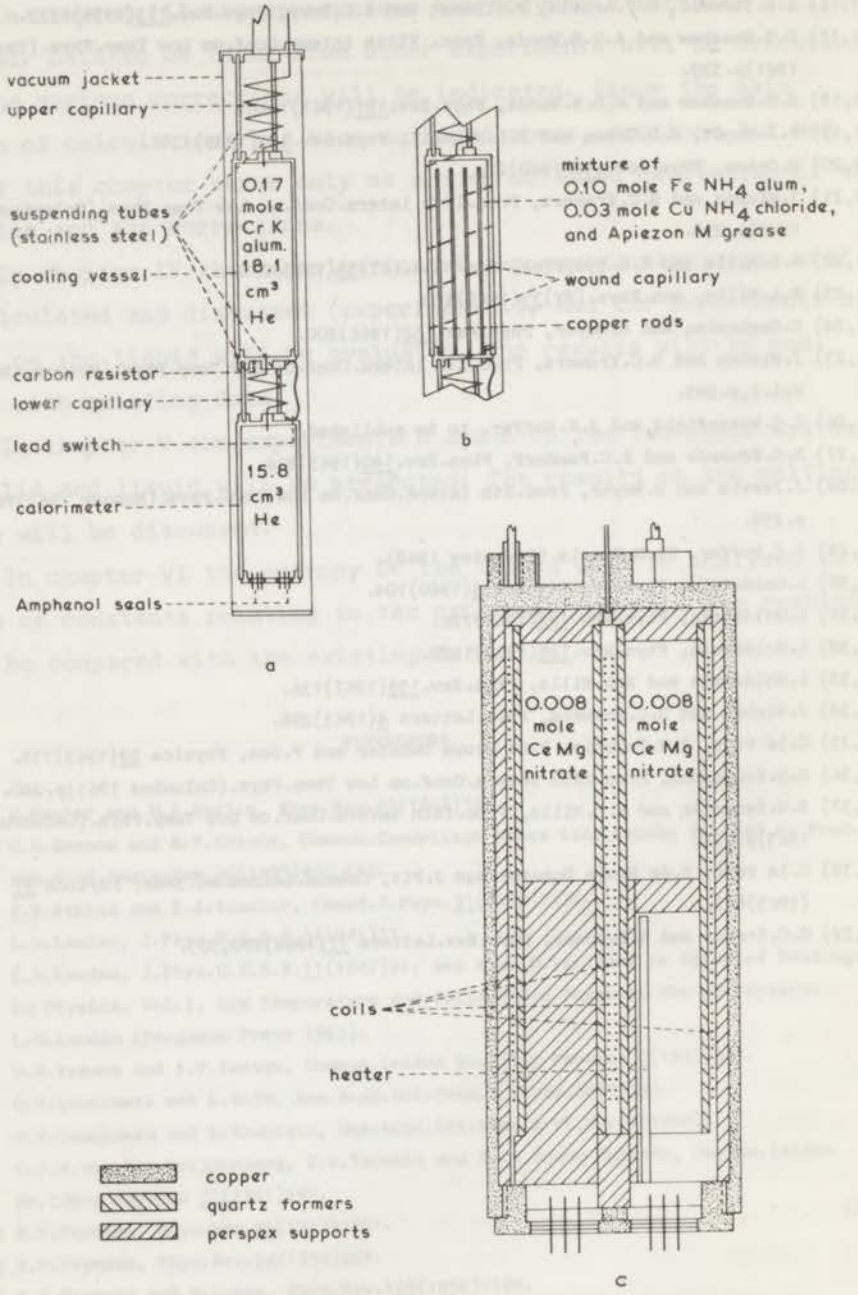

Fig. 2,1. Apparatus; a. first cooling arrangement;
b. second cooling arrangement; c. calorimeter.

CHAPTER II

EXPERIMENTAL ARRANGEMENT

2-1. Introduction

In this chapter the experimental arrangement will be presented. In sec. 2-2 the measuring equipment will be described; special attention will be given to the mutual-inductance compensator and to the magnetic thermometer. The cooling and measuring procedures will be treated in secs. 2-3 and 2-4 respectively.

2-2. Apparatus

a. C o o l i n g a r r a n g e m e n t s . Caloric measurements on ^{4}He under pressure and at temperatures below 1.6 K, are performed in a calorimeter which can be filled by means of a capillary connected to a helium storage cylinder. The calorimeter is enclosed in a vacuum vessel (see fig. 2,1a). When this vessel has been evacuated, the calorimeter is thermally insulated from its surroundings except for unavoidable heat leaks. The vessel is immersed in a ^{4}He bath that can be pumped down to a pressure of about 0.3 mm of mercury; the corresponding temperature is approximately 1.1 K. The part of the capillary immediately outside the vacuum vessel is kept in good thermal contact with the bath; in this way the heat leaking in from parts of the apparatus at room temperature is absorbed by the bath and does not reach the calorimeter.

Cooling to temperatures below 1.1 K is accomplished by adiabatic demagnetization of a sample of a paramagnetic salt that is contained in a separate vessel (see fig. 2,1a). In order to facilitate heat flow from the calorimeter during this cooling procedure, a lead thermal switch is placed between the calorimeter and the

cooling vessel; the switch is operated by the field that also magnetizes the cooling salt (see sec. 2-3).

When the helium within the calorimeter is at temperatures below 1.7 K and at pressures between that of the bath and the melting pressure, the part of the capillary below the bath level contains liquid helium II. The well-known ability of this liquid to provide for good heat transport, renders the thermal insulation of the calorimeter rather poor. Consequently, for the maintenance of calorimeter temperatures different from that of the bath for some reasonable length of time, a thermal buffer has to be located somewhere on the capillary within the vacuum vessel. In addition to its original function, the cooling vessel serves as this buffer. For that reason it has to be furnished with a substantial heat capacity at all temperatures within the measuring range. Moreover, a sufficient heat contact within this vessel must be ensured in order that its cooling capacity is fully utilized. These requirements have been fulfilled in two different designs for the cooling vessel, used in succession.

In the first design the stainless steel capillary with a 200 μ ID within the vacuum vessel was simply cut into a lower part of 30 cm and an upper part of 100 cm in length; the cooling vessel was connected in between (fig. 2,1a). Approximately 18 cm^3 of liquid helium, under the same pressure as that in the calorimeter, is present in the cooling vessel; it fulfils both requirements at temperatures above 0.6 K. Below that temperature a sufficient heat capacity is provided for by the electrical and magnetical interactions between the magnetic spins of the cooling salt itself. This arrangement was used in the measurements of the heat capacity when the calorimeter was completely filled with the liquid.

This construction of the cooling vessel could not be used for measurements if two different phases of helium were contained in the calorimeter. The large dead volume within the cooling vessel, in addition to the volume of the calorimeter, prevents the

determination of the amounts of the two phases that are contained in the calorimeter itself; only the amounts in the combined volumes of calorimeter and cooling vessel can be found. For that reason, the dead helium volume at low temperatures must be kept as small as possible in those measurements.

Therefore, in the second version of the apparatus the filling capillary was made out of one piece connected to the calorimeter only. The cooling vessel was filled with a mixture of a paramagnetic salt as a cooling agent, a salt with a ferromagnetic transition point at 0.7 K as a thermal buffer, and stopcock grease as a heat conducting agent (see fig. 2,1b). In order to enhance internal heat contact, copper rods have been soldered to the cover. Part of the capillary has been wound around the cooling vessel and soldered into a 95 cm long groove. In this way direct heat flow from the bath to the calorimeter is prevented. The cooling efficiency appeared to be somewhat less than that of the former arrangement (see sec. 2-3).

b. T h e c a l o r i m e t e r . The calorimeter is a thick-walled copper vessel (see fig. 2,1c). The temperature is determined from the mutual inductance between two sets of coils that contain a sample of a paramagnetic salt as a core. In order to ensure the best possible heat contact, the entire salt and coil system of the magnetic thermometer has been built within the calorimeter.

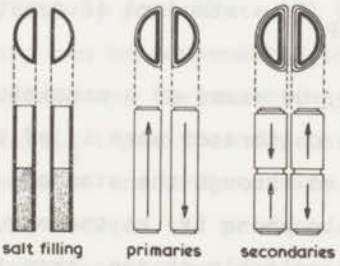

Fig. 2,2. Construction of magnetic thermometer.

The mutual-inductance coils have been wound on two D-shaped quartz formers both half filled with cerium magnesium nitrate (see fig. 2,2); both formers carry one primary of three layers of 50 μ Nb wire, and two equal secondaries of five layers of 50 μ Cu wire wound in mutually opposite senses. The primary fields in the two formers have opposite directions minimizing the resulting flux through a cross-section of the calorimeter, and thereby the influence of eddy currents. The electrical wiring enters through Amphenol seals and consists of 50 μ Nb wire within the vacuum vessel. Perspex supports reduce the remaining helium volume which was determined to be $(15.8 \pm 0.1)\text{cm}^3$.

c. The mutual-inductance compensator. The mutual inductance of the coils is measured by means of an ac mutual-inductance compensator with a variable primary current [2,1]) (see fig. 2,3a). This compensator was developed especially for the measurement of rather impure mutual inductances, such as may occur if eddy currents in metallic parts of the apparatus cause large losses. Like the Hartshorn bridge[2,2]) (fig. 2,3b) which is of common use in low-temperature physics, it balances in principle the voltage across the secondary coils of the cryostat CR by the voltage across the secondary of its own standard mutual inductance ST. In contrast to Hartshorn's method, however, the compensating voltage is varied not by switching secondary turns changing the standard's mutual inductance $\mathcal{M}$, but by variation of the primary current i_p in a standard of constant mutual inductance M_o.

For this purpose, by means of a precision potentiometer of total resistance D, a calibrated part i_p of the current i in the cryostat primary is led through the standard primary. The currents i_p and i can be kept in phase if, at the angular frequency ω, a series capacitor C is suitably chosen; then the remaining impedance is the effective resistance R_p of the primary of the standard. At a fraction p, read on the potentiometer, one now has:

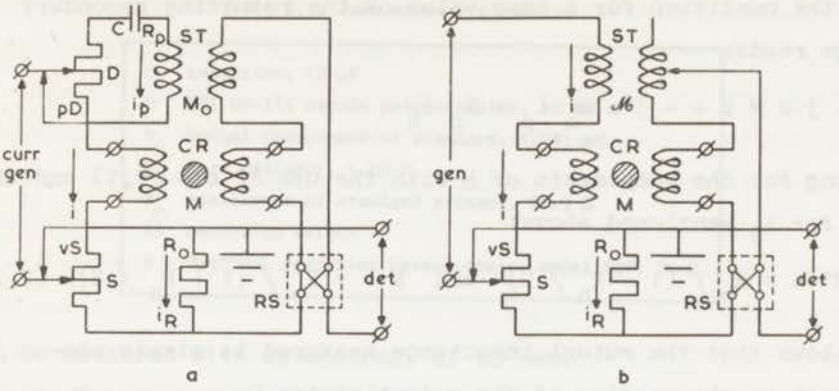

Fig. 2,3. Simplified diagrams of mutual-inductance compensator (a) and Hartshorn bridge (b); for explanation of the symbols see text.

$$i_p = p\, i \,/\, (1 + R_p \,/\, D) \qquad (2.1)$$

which is strictly linear in p; the denominator can be chosen close to 1 for the values that may occur in practice (see table 2,I). At low frequencies, the phase shift between the two currents caused by the self-inductance of the primary of the standard is negligibly small so that the capacitor C may be omitted.

At a zero value of the secondary current, the voltage across the cryostat secondary will be $-j\omega M i$ in which the effective mutual inductance M is in general complex, containing a real part M' and an imaginary (resistive) part that will be written as jR/ω. The inductive part only can be compensated by the voltage $-j\omega M_o i_p$ across the standard secondary; the small imaginary part of M_o originating from parasitic impurities may be neglected for the present purpose. The losses in the cryostat are compensated by means of a resistive coupling between the primary and the secondary circuits through a resistance R_o and a potentiometer with resistance S. WHen a fraction v is read on this potentiometer, the current i_R in the loss resistor R_o amounts to $v\, i \,/\, (1 + R_o \,/\, S)$.

Hence the condition for a zero value of the resulting secondary voltage reads:

$$- j \omega M i = - j \omega M_o i_p + R_o i_R$$

yielding for the components of M with the use of eq. (2,1) and the value for i_R mentioned above:

$$M' = p M_o / (1 + R_p / D) \quad \text{and} \quad R = v R_o / (1 + R_o / S). \quad (2.2)$$

It follows that the mutual inductance measured is simply proportional to the reading of the potentiometer D.

The compensator has two advantages over the Hartshorn bridge. First, the frequency range permitted is of the order of tens of kHz owing to the use of resistive circuit elements and a constant standard that can be constructed in an optimal way with respect to purity. In the usual variable standards the parasitary capacitances and coil resistances reduce the operating frequencies to 500 Hz at most; variable standards with better frequency specifications can be built[2,3]), but only at the expense of elaborate initial adjustment and calibration. Secondly, the compensator can easily be assembled from commercially available precision potentiometers and standards of mutual inductance.

Since the use of the current dividing device involves large variations of the total primary impedance, a current source with a high internal resistance is required for a reasonable constancy of the primary current. In their design Pillinger, Jastram, and Daunt[2,4]) have achieved this by employing an electronic "artificial primary circuit" for the standard mutual inductance. An obvious disadvantage of their method is the use of a vacuum tube, which puts a limit to linearity and stability, necessitating frequent calibration.

The compensator is operated at a frequency of 175 Hz and a primary current of 0.6 mA. The sensitivity of voltage detection in the secondary circuit amounts to 10^{-8} V so that mutual inductances

Table 2,I. Some network elements.

C	capacitor, 19 μF
D	ESI DP-311 decade potentiometer, 10 kΩ
M_o	mutual inductance of standard, 1.041 mH
R_o	loss resistor, 1.00 Ω
R_p	resistance of standard primary, 21.5 Ω
RS	reversing switch
S	Spectrol precision potentiometer model 860, 25 Ω

can be measured with an accuracy of 10^{-5}mH.

d. The magnetic thermometer. In view of the unconventional design of the thermometer, an estimate of the principal calibration constant will be given in this section.

The magnetic susceptibility of cerium magnesium nitrate is used as a thermometric parameter. Except for a diamagnetic part that is independent of the temperature, it obeys Curie's law very accurately down to the millidegree region of temperatures. The crystal is known to exhibit strongly anisotropic values of the splitting factor[2,5]), to be distinguished in $g_{\perp}$ (= 1.84) and $g_{//}$ (= 0.024 [2,6])) for directions with respect to the trigonal crystal axis. A powdered sample was used with a filling factor of 72 %; by the averaging over all directions due to the powdering, another factor of 67 % is contributed to the paramagnetic part. From this, the paramagnetic part χ of the effective (volume) susceptibility is calculated to be $40 \times 10^{-5} T^{-1}$ K; the diamagnetic part equals -47×10^{-6}.

A measure of the susceptibility is found from the mutual inductance M between the two sets of coils that are partly filled with the salt (see fig. 2,2). From the dimensions of the coils it follows that:

$$M = 420 \text{ mH } f \chi T / (T + \theta), \qquad (2.3)$$

in which f and θ are constants. A factor f has been introduced to account for the inhomogeneity of the magnetic field, the

demagnetization effects, and the effects of eddy currents in metallic parts of the calorimeter. From measurements of the field in an enlarged model to scale, it is expected to be of the order of 0.6. The constant θ equals $N\chi T$, where N ($< 4\pi$) is an effective coefficient of demagnetization. This coefficient is estimated to be of the order of 2 so that θ is of the order of 10^{-3} K. Since all temperatures were higher than 0.28 K, this very small correction has been neglected.

With increasing temperatures, the mutual inductance approaches a constant value M_∞. A temperature independent contribution originates in principle from diamagnetism which contributes 0.020 f mH in the present case. In practice, however, it arises mainly from an unbalance of the mutual inductances of the various coils within the calorimeter. Consequently the expected dependence of the mutual inductance on the temperature is:

$$M = M_\infty + C\, T^{-1} , \qquad (2.4)$$

where C equals 0.17 f mH.

The thermometer is calibrated in the usual manner against the saturated vapour pressure of the helium bath at temperatures of about 1.1, 1.4, 1.8, and 2.4 K (T^{-1} equal to approximately 0.9, 0.7, 0.55, and 0.4 K^{-1}) according to the 1958 scale[2,7]. The mutual inductance M was found to vary linearly with T^{-1} within the experimental error. In a graph of M versus T^{-1}, the straight line is drawn through the lowest calibration point with a mutual inductance M_1 and a temperature T_1 (approximately 1.1 K). Its slope equal to C amounts to about 0.070 mH K and can be determined with an accuracy of 0.3 %. Consequently, the factor f in eq. (2.3) is approximately 0.4 which is an acceptable value. The constant M_∞ is found from:

$$M_\infty = M_1 - C / T_1 . \qquad (2.5)$$

It amounts to 1.5 mH approximately; the greater part of this

constant is balanced by a constant mutual inductance of 1.4 mH outside the cryostat.

e. O t h e r e q u i p m e n t . An auxiliary carbon resistor is mounted on the side of the cooling vessel from which the calorimeter is suspended. Its resistance is measured in a Wheatstone bridge.

Heating in the calorimeter is done by feeding a dc current through a 167 Ω Constantan heater during 10.00 s; the current and the voltage across the heater are measured. The energies supplied range from 0.006 to 600 mJ and are known accurately to 0.3 %.

The pressure is measured with a calibrated Bourdon gauge indicating from 0 to 100 atm with an accuracy of 0.05 atm, or with a mercury column for pressures up to 5 atm. The helium is expanded through a throttle valve which leads to a calibrated collecting volume. The pressure of the latter is determined by means of a mercury manometer.

2-3. Cooling procedure

Owing to the various heat links that may occur, the cooling procedure requires special precautions and will be considered in some detail here.

For obtaining temperatures below 1.1 K, cooling is effected by demagnetization of the sooling salt after the evacuation of the vacuum vessel. Since the heat contact between the salt and the other parts of the cooling vessel is good, the temperature of this vessel itself is lowered almost immediately. Under the resulting temperature difference, heat is transported from the calorimeter to the cooling vessel via the lead switch and the lower part of the filling capillary. As a consequence the temperature of the calorimeter decreases and that of the cooling vessel increases demonstrating the rather irreversible way of cooling.

An isentropic way of cooling is approximated by lowering the magnetic field in six steps and allowing for the re-establishment

of temperature equilibrium during five minutes after each step. In that case the temperature of the cooling vessel shows only small rises between the periods in which the field is lowered. In all steps except the last one, the field is strong enough to keep the switch in the normal state where the heat conduction is appreciable. Immediately after total demagnetization, the temperature of the calorimeter has become about 0.65 K. Further cooling is effected by conduction of heat via the capillary during the next sixty minutes. The temperature finally obtained was about 0.25 K when the first cooling vessel was used and about 0.35 K for the one employed in the melting experiments. With a calorimeter filled only partly with the liquid, temperatures down to about 0.28 K were obtained with the latter cooling vessel.

For the cooling to be at all successful, it is necessary to reduce the heat leakage along the upper part of the filling capillary. The helium II in this part of the capillary would present a prohibitive heat contact with the helium bath. Consequently this reduction is achieved, previously to demagnetization, by solidification of the helium contained in the capillary. This is done in two different ways depending on the type of measurements to be made.

At the start the liquid in the calorimeter is brought to a pressure of about 24 atm at the lowest bath temperature of about 1.1 K. In the preparation for the melting experiments, helium was added very carefully at an overpressure of 0.5 atm at most, in order to obtain a strainfree solid. After some time the pressure indicated on the manometer rose, showing that the capillary was blocked. In this way calorimeter fillings with a fraction of solid up to 80 % could be obtained.

In the preparation for the measurements of the heat capacity of the liquid, however, the fractions of solid in the calorimeter and the cooling vessel (first arrangement) must be kept small. Otherwise, owing to the larger specific entropy of the solid at

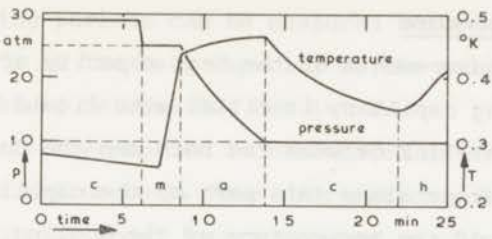

Fig. 2,4. Final part of cooling procedure;
c: cooling; m: melting; a: adjustment of pressure; h: heating.

temperatures below 0.76 K[2,8]) the necessary melting at low temperatures will be accompanied by a large rise of temperature. For that reason the helium is compressed quickly and the external pressure allowed to rise up to about 28 atm, thus blocking the capillary. After evacuation of the vacuum vessel, demagnetization, and cooling to nearly the lowest temperature, the pressure is adjusted to the desired value. The behaviour of the apparatus during this adjustment is shown in fig. 2,4. At the end of the first cooling period (c), helium is released through the throttle valve in order to melt the solid present (period m) and to adjust the pressure (period a). During the release, the pressure decreases to its value at melting of 25.0 atm and remains a constant for some time. The temperature of the calorimeter still decreases for a while. Consequently, at first melting occurs in the cooling vessel only. Later on, the temperature of the calorimeter starts to rise indicating melting there. When the melting is completed, the pressure decreases again, and the steep rise of the temperature comes abruptly to a stop. A slower increase, or even a decrease of temperature is observed if the rate of blowing off is small enough. At the desired pressure the valve is closed. A further cooling takes place during about ten minutes (second cooling period c). Apparently, after the melting the cooling vessel is left colder than the calorimeter owing to the larger heat capacity of the former at these temperatures. The measurements can usually be started at a temperature of about 0.33 K (period h).

2-4. Measuring procedure

During the measurements of the heat capacity of the liquid, part of the filling capillary is filled with liquid helium II. It forms a direct heat link between the bath and the cooling vessel. The large heat leakage along this part of the capillary determines mainly the course of the temperature of the cooling vessel in time. This temperature rises from 0.3 to 1.0 K within about twenty minutes. In the measurements of the heat capacity of the calorimeter itself and of that of the solid, the upper part of the capillary contained gas or solid instead of liquid. As a consequence, in those cases the heat leakages are appreciably smaller, causing the warming-up times to be longer by at least a factor of two.

Also, the heat leak between the cooling vessel and the calorimeter is brought about mainly by the helium within the connecting capillary. It can be kept small if the calorimeter temperature is made to follow the temperature of the cooling vessel as closely as possible. It is found empirically that the heat leakages remain within reasonable bounds if heating is done at a special rate. It amounts to one heating period every minute; the supplied energy must be increased by a factor of two every second or third period. Then it is observed that the heat leakage is negative in the lower temperature region and above 0.9 K, and zero or positive at temperatures between roughly 0.6 and 0.9 K.

Temperature measurements are made at a rate of one every three to five seconds, tape-recorded, and read back afterwards. In one run usually thirty to fourty heating periods, with steps of about 20 mK at 0.3 K increasing to about 50 mK at 1.6 K, are measured within thirty to fourty minutes. The pressure remains a constant up to a temperature of 1.3 K and decreases by about 1 % between 1.3 and 1.6 K, the temperature of the cooling vessel becoming around 1.4 K. In the case that the calorimeter is filled partly with the liquid under its saturated vapour pressure, the same

number of heating periods can be measured between 0.3 and 0.7 K. In the measurements on the heat capacity of the solid, this number of periods is measured between 0.4 and 1.1 K.

The magnetic thermometer is calibrated afterwards against the pressure of the helium bath. Four calibration points are taken, each point requiring about twenty minutes in order to obtain thermal equilibrium.

In two cases the helium is collected. First it is necessary to determine the amount of helium when the calorimeter is filled only partly. No better accuracy than 0.01 g of helium is required in this case. Secondly, since the temperature effects in the melting experiments are proportional to the amounts of helium that are blown off, those amounts are determined accurately to 0.5 mg. The helium is released through the throttle valve at rates ranging from 0.5 to 5 mg/s. The amounts vary from 15 to 50 mg and are collected within 10 to 60 seconds.

REFERENCES

2,1) J.Wiebes, W.S.Hulscher and H.C.Kramers, Commun.Kamerlingh Onnes Lab.,Leiden No. 341c; Appl.sci.Res.11(1964)213.

2,2) L.Hartshorn, J.sci.Instr.2(1925)145.

2,3) R.A.Erickson, L.D.Roberts and J.W.T.Dabbs, Rev.sci.Instr.25(1954)1178.

2,4) W.L.Pillinger, P.S.Jastram and J.G.Daunt, Rev.sci.Instr.29(1958)159.

2,5) A.H.Cooke, H.J.Duffus and W.P.Wolfe, Phil.Mag.44(1953)623.

2,6) J.Lubbers and W.J.Huiskamp, Commun.Leiden No.353b; Physica 34(1967)193.

2,7) F.G.Brickwedde, H.van Dijk, M.Durieux, J.R.Clement and J.K.Logan, J.Res.Nat.Bur. Stand.64A(1960)1.

2,8) J.Wiebes and H.C.Kramers, Phys.Letters 4(1963)298.

CHAPTER III

FORMULAE AND CORRECTIONS

3-1. Introduction

In this chapter it will be shown how the results are obtained from the measurements. The measurements are carried out in two ways. First, heat capacities are measured in a nearly closed calorimeter. Secondly, expansion experiments are performed under nearly adiabatic conditions. From a more general point of view both experiments may be considered as combinations of the two processes of heating and expanding; each experiment consists of one of these processes disturbed by the other. The appropriate thermodynamic formulae will be derived in sec. 3-2. A survey of data from other experiments to be used in the calculation of the results will be given in sec. 3-3. In sec. 3-4 the evaluation of temperatures and the parts of the calculation in the nature of corrections will be considered.

3-2. Derivation of thermodynamic formulae

Some of the thermodynamics of a helium one component system, contained in a calorimeter, will be considered here. Formulae for a one-phase as well as for a two-phase system will be derived. The calorimeter itself is not in general closed; during the measurements of the heat capacity it may be considered as nearly closed but in the expansion experiments it is essentially open. Hence an open process[3,1]) is considered with a variable total helium mass m_t, a fixed total helium volume V_t, and an added quantity of heat dQ. Helium mass, helium volume, entropy, and heat capacity are represented by m, V, S, and W; v, s, and c_p represent specific volume, specific entropy, and specific heat at constant pressure

respectively. Subscripts σ and μ refer to the vapour pressure curve and the melting curve; c, l, g, s, and t refer to calorimeter, liquid, gas, solid, and total quantities respectively.

a. L i q u i d . The one-phase system to be considered here is the liquid under various pressures. The total entropy consists of the contributions of the liquid and the calorimeter:

$$S_t = m_t s_l + S_c \,. \tag{3.1}$$

It is changed by the reversible addition of an infinitesimal quantity of heat dQ and of mass dm_t at the temperature T as follows:

$$dS_t = \frac{1}{T}\, dQ + s_l dm_t \,, \text{ giving } dQ = m_t T\, ds_l + T\, dS_c \,. \tag{3.2}$$

A change dT of the temperature and a change dp of the pressure will result. The following abbreviations are introduced: W_c for the heat capacity of the calorimeter TdS_c/dT which does not depend on the pressure; c_{pl} for the specific heat of the liquid at constant pressure $T(\partial s_l/\partial T)_p$; and α_{pl} for the coefficient of isobaric thermal expansion $v_l^{-1}(\partial v_l/\partial T)_p$ which is equal to $-v_l^{-1}(\partial s_l/\partial p)_T$ by one of Maxwell's relations. Equation (3.2) then yields:

$$\frac{dQ}{dT} - W_c = m_t\, T \frac{ds_l}{dT} = \frac{V_t}{v_l} c_{pl} - V_t\, \alpha_{pl}\, T \frac{dp}{dT} \,. \tag{3.3}$$

Here m_t equals V_t/v_l , where v_l is the specific volume of the liquid at the actual values of the temperature and the pressure.

Relation (3.3) can be used to calculate c_{pl} from the measurement of the effective heat capacity dQ/dT under nearly isobaric conditions:

$$c_{pl} = \frac{v_l}{V_t}\left(\frac{dQ}{dT} - W_c\right) + v_l\, \alpha_{pl}\, T \frac{dp}{dT} \,. \tag{3.4}$$

The small variation of the pressure is caused by the dependence of

v_l on temperature; for a further evaluation of this correction see sec. 3-4,d.

One may also use eq. (3.3) to calculate α_{pl} from dT/dp as measured in a nearly adiabatic expansion experiment, if the heat leak can be eliminated (dQ = 0):

$$\alpha_{pl} = \frac{W_t}{V_t T} \frac{dT}{dp} . \tag{3.5}$$

The total heat capacity $m_t c_{pl} + W_c$ has been abbreviated by W_t here.

b. L i q u i d a n d s o l i d . Let a two-phase system consist of the liquid and the solid in equilibrium along the melting curve. A formula is needed relating the amount of heat that is added and the amount of liquid that escapes to the resulting change of temperature. A somewhat formal derivation will be given based on the change of the entropy for the process mentioned[3,2]), when it is performed in a reversible way.

The following relations apply to the total helium mass, the total helium volume, and the total entropy:

$$m_t = m_l + m_s , \quad V_t = m_l v_l + m_s v_s , \quad S_t = m_l s_l + m_s s_s + S_c . \tag{3.6}$$

The open process is now performed along the melting curve. The changes are:

$$dm_t = dm_l + dm_s , \quad dV_t = 0 , \quad dS_t = \frac{1}{T} dQ + s_l dm_t , \tag{3.7}$$

yielding after elimination of dV_t , dS_t , dm_l , and dm_s by means of eqs. (3.6):

$$dQ + T \frac{s_l - s_s}{v_l - v_s} v_l dm_t = [m_l T(\frac{ds_l}{dT})_\mu + m_s T(\frac{ds_s}{dT})_\mu + T \frac{dS_c}{dT} -$$
$$- T \frac{s_l - s_s}{v_l - v_s} \{m_l (\frac{dv_l}{dT})_\mu + m_s (\frac{dv_s}{dT})_\mu\}]dT. \tag{3.8}$$

To elucidate the meaning of these terms, the specific heat of

melting l_μ and the specific heats along the melting curve $c_{\mu l}$ and $c_{\mu s}$ are introduced:

$$l_\mu = T(s_l - s_s) \ , \ c_{\mu l} = T(ds_l/dT)_\mu \ , \ c_{\mu s} = T(ds_s/dT)_\mu \ . \quad (3.9)$$

If the second term of eq. (3.8) is brought to the right hand side and dm_t is replaced by $dm_l + dm_s$, equation (3.8) yields:

$$dQ/dT = m_l c_{\mu l} + m_s c_{\mu s} + W_c - l_\mu dm_s/dT \ . \quad (3.10)$$

The effective heat capacity is simply the sum of the heat capacities along the melting curve and a term originating from the heat of melting of a certain amount of solid dm_s. This amount consists of a contribution from the liquid within the calorimeter caused by the thermal expansion of the solid and the liquid, and of a contribution dm_t from the escaping liquid. These contributions have been separated in eq. (3.8) because the amount of liquid that escapes is measured independently.

During the measurements of the heat capacity with solid helium in the calorimeter, the filling capillary is blocked by the solid. Consequently the process is a closed one and dm_t equals zero. The specific heat of the solid along the melting curve can now be calculated from the effective heat capacity dQ/dT when the amounts of liquid and solid are known:

$$c_{\mu s} = \frac{1}{m_s}\left[\frac{dQ}{dT} - m_l c_{\mu l} - W_c - W_{melt} \right] \ . \quad (3.11)$$

Here W_{melt} denotes the correction due to the melting within the calorimeter:

$$W_{melt} = - l_\mu \frac{dm_s}{dT} = - T \frac{s_l - s_s}{v_l - v_s}\left[m_l \left(\frac{dv_l}{dT}\right)_\mu + m_s \left(\frac{dv_s}{dT}\right)_\mu \right] \ . \quad (3.12)$$

Its calculation requires a knowledge of the specific entropy of the solid s_s which may be found from provisional results of the present measurements. The specific heat $c_{\mu l}$ of the liquid along the melting curve can be found from the specific heat at constant pressure c_{pl} by:

$$c_{\mu l} = c_{pl} + T \frac{s_l - s_s}{v_l - v_s} \left(\frac{\partial s_l}{\partial p}\right)_T \quad . \tag{3.13}$$

Clapeyron's equation has been used to eliminate the slope of the melting curve here:

$$(dp/dT)_\mu = (s_l - s_s) / (v_l - v_s) \quad . \tag{3.14}$$

These corrections will be evaluated in sec. 3-4,e.

In the expansion experiments the heat leak can be eliminated so that dQ equals zero. Then the temperature change dT is such as would occur in an adiabatic expansion when an amount of liquid dm_t is released. Writing W_t for the total heat capacity $m_l c_{\mu l} + m_s c_{\mu s} + W_c$ at the actual masses of solid and liquid, one may calculate the slope of the melting curve from:

$$\left(\frac{dp}{dT}\right)_\mu = \frac{W_t}{T}\left[v_l \frac{dm_t}{dT} + m_l \left(\frac{dv_l}{dT}\right)_\mu + m_s \left(\frac{dv_s}{dT}\right)_\mu \right]^{-1} \quad . \tag{3.15}$$

As an alternative to the measurement of this differential effect upon the release of small amounts of helium, it is also possible to measure the integral temperature effect by the melting of the total amount of solid. Let the calorimeter be filled entirely with the solid at the melting pressure and subsequently adiabatically expanded until it is left just filled with the liquid. The entropy of the solid may then be calculated from the known entropies of the liquid and of the calorimeter. Writing indices i and f for the initial and final values of the quantities involved and integrating the third of eqs. (3.7) one gets (dQ = 0):

$$S_{tf} - S_{ti} = \int_{m_{ti}}^{m_{tf}} s_l \, dm_t \quad . \tag{3.16}$$

From eqs. (3.6) it follows that:

$$m_{ti} = V_t / v_{si} \quad , \quad m_{tf} = V_t / v_{lf} \quad ,$$

$$S_{ti} = S_{ci} + V_t s_{si}/v_{si} \ , \quad S_{tf} = S_{cf} + V_t s_{lf}/v_{lf} \ , \tag{3.17}$$

yielding upon substitution into eq. (3.16):

$$s_{si} = \frac{v_{si}}{v_{lf}} s_{lf} + \frac{S_{cf} - S_{ci}}{V_t/v_{si}} - \frac{v_{si}}{V_t} \int_{T_i}^{T_f} s_l \frac{dm_t}{dT} dT \ . \tag{3.18}$$

The contribution of the integral originating from the liquid that has escaped is small. It is determined by the course of the temperature during the process which must therefore be measured. An approximating evaluation will be given in sec. 3-4,f.

c. L i q u i d a n d g a s . The heat capacity of the calorimeter is determined from measurements of the effective heat capacity with a small amount of liquid. Consequently, the larger part of the calorimeter volume is occupied by the gas phase under the saturated vapour pressure at the actual temperature. In this case some of the gas may escape from the calorimeter system. An equation entirely analogous to eq. (3.8) will hold:

$$dQ + T \frac{s_g - s_l}{v_g - v_l} v_g dm_t = [m_g T(\frac{ds_g}{dT})_\sigma + m_l T(\frac{ds_l}{dT})_\sigma + W_c -$$

$$- T \frac{s_g - s_l}{v_g - v_l} \{m_g(\frac{dv_g}{dT})_\sigma + m_l(\frac{dv_l}{dT})_\sigma\}] dT \ . \tag{3.19}$$

Similarly the specific heat along the vapour pressure curve will be introduced:

$$c_{\sigma l} = T \ (ds_l/dT)_\sigma \ , \tag{3.20}$$

but Clapeyron's equation will be used here to eliminate the specific entropy of the vapour by means of the slope of the vapour pressure curve:

$$(dp/dT)_\sigma = (s_g - s_l)/(v_g - v_l) \ . \tag{3.21}$$

The heat capacity of the calorimeter may now be calculated from:

$$W_c = \frac{dQ}{dT} - m_1\left[c_{\sigma 1} - T \left(\frac{dp}{dT}\right)_\sigma \left(\frac{dv_1}{dT}\right)_\sigma \right] - W_{vap} - W'_{vap} , \qquad (3.22)$$

where W_{vap} and W'_{vap} are abbreviations for the vapour contributions:

$$W_{vap} = m_g\left[T \left(\frac{ds_g}{dT}\right)_\sigma - T \left(\frac{dp}{dT}\right)_\sigma \left(\frac{dv_g}{dT}\right)_\sigma \right] , \text{ and} \qquad (3.23)$$

$$W'_{vap} = - T \left(\frac{dp}{dT}\right)_\sigma v_g \frac{dm_t}{dT} . \qquad (3.24)$$

The former, W_{vap}, includes both the heat capacity of the vapour along the vapour pressure curve and a contribution due to the vaporization required for maintaining the pressure at its saturation value. The latter, W'_{vap}, originates from the heat of vaporization of the amount of helium dm_t that escapes from the calorimeter. Writing out the derivatives:

$$\left(\frac{d}{dT}\right)_\sigma = \left(\frac{\partial}{\partial T}\right)_p + \left(\frac{dp}{dT}\right)_\sigma \left(\frac{\partial}{\partial p}\right)_T , \qquad (3.25)$$

and using one of Maxwell's relations, one obtains for W_{vap}:

$$W_{vap} = m_g\left[c_{pg} - 2\,T \left(\frac{dp}{dT}\right)_\sigma \left(\frac{\partial v_g}{\partial T}\right)_p - T \left(\frac{dp}{dT}\right)^2_\sigma \left(\frac{\partial v_g}{\partial p}\right)_T \right] . \qquad (3.26)$$

A further calculation of these corrections will be given in sec. 3-4,g.

3-3. Data from other experiments

Use is made of existing data on (a) the vapour pressure curve, (b) the equation of state of ^{4}He, and (c) the specific heat of the liquid along the vapour pressure curve.

a. The vapour pressure curve. The 1958 scale of temperatures[3,3]), based on the vapour pressure curve of ^{4}He, is used for the calibrations of the thermometer. It is employed also to compute the contribution of the vapour in the measurements on the heat capacity of the almost empty calorimeter.

b. The density near absolute zero. The density of the liquid at 0 K as a function of the pressure was obtained from the data of Keesom and Miss Keesom[3,4]) on the isopycnals at temperatures above 1.1 K. However, as the values of these authors for the densities are 0.3 to 0.7 % lower than other comparable data[3,5-12]), a positive correction of 0.6 % has been applied to all of their densities (see also Lounasmaa[3,10]) on this subject). At temperatures of 1.00, 1.25, 1.50, 1.75 and 2.00 K, corrected for the difference between the 1932 and 1958 scales, the pressures were read from the isopycnals and plotted as a function of the corrected densities. The values for the densities along the isotherm at 1.75 K thus found agree within 0.0001 g/cm^3 with those obtained by Lounasmaa at that temperature. From this diagram the values of the density at 0 K can be found by extrapolation within an accuracy of 0.0001 g/cm^3, except near the end points at pressures of 0 and 25 atm. The values of 0.1451 and 0.1733 g/cm^3 found at these points, respectively, are less certain. Moreover, diverging values are found by various authors, e.g. 0.1452 g/cm^3 [3,5]) and 0.1455 g/cm^3 [3,7]) at saturated vapour pressure, and 0.1722 g/cm^3 [3,13]) and 0.1730 g/cm^3 [3,14]) at the melting curve. Consequently, no improvement for the densities at evaporation or at solidification can be obtained from those data.

The reliability of the values for the density ρ_1 may be improved, however, by the use of data on the velocity of sound u:

$$u = (\partial p/\partial \rho_1)_{s_1}^{\frac{1}{2}} . \qquad (3.27)$$

In particular, the slope of the isotherm at 0 K is found simply as follows:

$$\lim_{T\to 0} u^2 = \lim_{T\to 0} (\partial p/\partial \rho_1)_{s_1} = \lim_{T\to 0} (\partial p/\partial \rho_1)_T = [dp/d\rho_1]_{T=0\,K} . \qquad (3.28)$$

For this purpose, the data of Atkins and Stasior[3,15]) on the

velocity of sound were extrapolated to absolute zero. It appeared that the square root of the velocities obtained in this way could be represented very well by a linear function of the density. Hence the velocity of sound u, the density ρ_1, and the pressure p at the absolute zero of temperature depend on each other according to the empirical relations:

$$u^{\frac{1}{2}} = a\,(\rho_1 - \rho) = [\,5\,a\,(p + P)\,]^{\frac{1}{5}} . \qquad (3.29)$$

The constants a, ρ, and P are found to be:

$$a = 135.4\ (m/s)^{\frac{1}{2}} / (g/cm^3) = 13720\ (m/s)^{\frac{5}{2}} / \text{atm} ,$$

$$\rho = 0.0312\ g/cm^3 \quad , \text{ and } \quad P = 12.90\ \text{atm} .$$

Table 3,I. The absolute zero isotherm of liquid ^{4}He.

pressure p atm	density ρ_1 g/cm^3	velocity of first sound $u = (dp/d\rho_1)^{\frac{1}{2}}$ m/s	compressibility $\kappa_T = \rho_1^{-1}\, d\rho_1/dp$ 10^{-3}/atm
0.0	0.1455	239	12.2
2.5	0.1496	257	10.3
5.0	0.1532	273	8.9
10.0	0.1594	301	7.0
15.0	0.1645	326	5.8
20.0	0.1690	348	5.0
25.0	0.1729	368	4.3
error	± 0.0002	± 2	± 0.1

With these relations the values of p, ρ_1, and u as given in table 3,I have been computed. The densities obtained in this way are believed to be correct within 0.0002 g/cm^3 and the velocities within 2 m/s. The compressibility κ_T, equal to $\rho_1^{-1} d\rho_1/dp$, is

also given in the table. It differs less than 4 % from the values of the isothermal compressibility $\varkappa_T$ at a temperature of 1.6 K as measured by Grilly[3,16]).

The density ρ_s of the solid at the melting curve at absolute zero was derived from that of the liquid with the use of Swenson's value for the difference of the molar volumes at melting. According to the measurements of Swenson[3,13]), the extrapolated melting pressure at a temperature of 0 K is 25.00 atm; according to table 3,I the corresponding density of the liquid is 0.1729 g/cm^3 (v_l = 5.783 cm^3/g). The difference between the molar volumes amounts to 2.07 cm^3/mole ($v_l - v_s$ = 0.517 cm^3/g), yielding 0.1899 g/cm^3 for the density of the solid (v_s = 5.266 cm^3/g). These values for the densities are employed in the present investigation; both are 0.4 % larger than the ones used by Swenson.

Table 3,II. The relative change of the specific volume of liquid ^{4}He along the melting curve.

T (K)	0.9	1.0	1.1	1.2	1.3	1.4
$-[(v_l/v_{lo}) - 1]_\mu$ (10^{-3})	0.1	0.3	0.8	1.6	3.1	6

c. Thermal expansion along the melting curve. According to Swenson's measurements along the melting curve[3,13]), the difference between the molar volumes of the liquid and the solid is a constant at temperatures up to 1.3 K. Hence, within the required accuracy the temperature derivatives $(dv_s/dT)_\mu$ and $(dv_l/dT)_\mu$ may be set equal in the range of temperatures considered. The relative difference of the specific volume of the liquid with its value v_{lo} at low temperatures, calculated from Swenson's data, is given in table 3,II.

d. The specific heat of the liquid at saturated vapour pressure. This specific heat was used to correct for the contribution of the liquid to the heat capacity when the calorimeter was only partially filled. The values are composed from the data on the specific heat by Kramers, Wasscher, and Gorter[3,17]) (at temperatures between 0.2 and 1.8 K) and those of Wiebes, Niels-Hakkenberg, and Kramers[3,18]) (between 0.2 and 0.7 K). At temperatures below 0.6 K, the former measurements yield a phonon specific heat which is approximately 15 % larger than the value of $20.5\ T^3$ mJ/g K^4, as calculated from the extrapolated velocity of sound of 239 m/s[3,19]) (see chapter VI). This is due to a systematic error introduced by the manner in which the heat capacity of the salt has been eliminated, i.e. by extrapolation of its values at low temperatures according to a T^{-2} law (see also [3,20]) and [3,21])). In order to remove this discrepancy the latter experiments were performed. By variation of the amount of helium they allowed for a direct determination of the heat capacities involved. The calculated value was established within 2 %; consequently, it is taken as the contribution of the phonons to the specific heat.

If the phonon contribution is subtracted, the remaining specific heat can be represented at temperatures up to about 1.3 K by:

$$[\text{a constant}] \cdot \left[1 + (kT/\Delta) + \frac{3}{4}(kT/\Delta)^2\right] T^{-3/2}\, e^{-\Delta/kT}\ , \quad (3.30)$$

where Δ is an effective value for the minimum energy of the rotons (see chapter VI). This formula has been employed to connect the specific heat of Kramers et al. at temperatures above 0.8 K to the phonon specific heat below 0.5 K (below 0.5 K the roton contribution constitutes less than 1 % of the total specific heat).

From the values of the specific heat $c_{\sigma l}$ thus found, the specific entropy s_l of the liquid at saturated vapour pressure has been calculated. Both $c_{\sigma l}$ and s_l are given in table 3,III.

Table 3,III. Specific heat and entropy of liquid ^{4}He under its saturated vapour pressure at temperatures below 1 K.

T K	$c_{\sigma l}$ mJ/g K	s_l mJ/g K	T K	$c_{\sigma l}$ mJ/g K	s_l mJ/g K
0.05	0.00256	0.000853	0.55	3.54	1.145
0.10	0.0205	0.00683	0.60	4.89	1.507
0.15	0.0692	0.0231	0.65	6.91	1.972
0.20	0.1640	0.0547	0.70	10.09	2.59
0.25	0.320	0.1068	0.75	15.12	3.45
0.30	0.554	0.1845	0.80	22.9	4.66
0.35	0.879	0.293	0.85	34.5	6.37
0.40	1.313	0.437	0.90	51.2	8.79
0.45	1.873	0.623	0.95	74.1	12.14
0.50	2.59	0.856	1.00	104.3	16.67

3-4. Method of calculation and correction

The way in which the results are obtained from the directly measured quantities, will be presented in this section. This is done by distinguishing two main parts in the evaluation, one concerning the calculations of the temperature T, the total amount of helium m_t, and their changes ΔT and Δm_t (secs. 3-4,a and b), and one concerning the various corrections (secs. 3-4,c,d,e,f and g). The heat capacity of the calorimeter will not be considered as a mere correction to the measurements. It plays an important role in the results at low temperatures and hence will be treated as a separate measurement in sec. 4-2 of chapter IV.

a. C a l c u l a t i o n o f t e m p e r a t u r e s . For all measuring points the temperature T and its change ΔT have to be determined. For that purpose the mutual-inductance compensator is read as a function of time. This is done both before and after the period of actual heating or blowing-off. The time t_i at the beginning of this period and its duration Δt are also determined.

In fig. 3,1 the evaluation of the temperature is schematically shown. The case presented is ideal in the sense that the fore- and afterdrifts can be regarded as linear. This is found in the vast majority of the measuring points. Equilibrium of temperature within the calorimeter was attained well within the time needed for the measurement of temperature (of the order of 1 s).

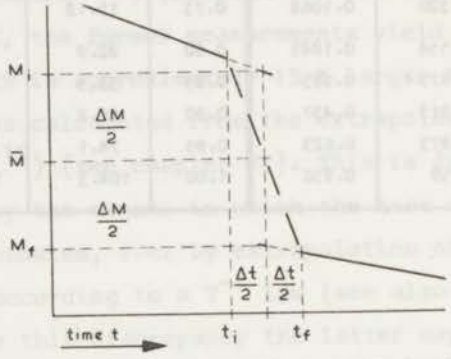

Fig. 3,1. Determination of temperature from mutual inductance: $T = C / (M - M_\infty)$;
——— : M measured as a function of time;
- - - : construction yielding $\bar{M}$ and ΔM.

A correction has to be applied for the amount of heat that leaks into the calorimeter during the period of heating or blowing-off. It can be determined from the fore- and afterdrifts of the temperature and is eliminated in the usual manner as follows. The drifts in the fore- and afterperiods are extrapolated to the centre of the measuring period, yielding values of M_i and M_f for the mutual inductance respectively. The temperature T of the measuring point is defined by the mean value $\bar{M}$ of M_i and M_f (see eq. (2.4)):

$$T = C / (\bar{M} - M_\infty) \cdot \qquad (3.31)$$

Its accuracy is estimated to be 0.2 % over the whole range of temperatures.

An approximate value ΔT for the finite change of temperature is calculated from the difference ΔM of M_i and M_f:

$$\Delta T = - C \, \Delta M \, / \, (\overline{M} - M_\infty)^2 \, . \qquad (3.32)$$

Its accuracy is determined mainly by the accuracy with which ΔM can be found from the extrapolations. In all measurements the error is of the order of 2 %.

In those cases where the calibration $T(M)$ depends on the pressure, the values of $\overline{M}$ and ΔM must be chosen as:

$$\overline{M} = \tfrac{1}{2} \left[M_f - M_\infty(p_f) + M_i - M_\infty(p_i) \right] , \text{ and}$$
$$\Delta M = M_f - M_\infty(p_f) - M_i + M_\infty(p_i) \, . \qquad (3.33)$$

Here $M_\infty(p_i)$ and $M_\infty(p_f)$ are the values of the calibration constant M_∞ at the initial and final pressures, respectively p_i and p_f. This was the case with the experiments on the adiabatic expansion of the liquid. The Curie constant was found to be independent of the pressure (see also chapter IV).

b. D e t e r m i n a t i o n o f t h e a m o u n t s o f h e l i u m . In all two-phase experiments an additional determination of the total amount of helium is required. In the liquid-vapour system this is done by simply collecting the helium and measuring its pressure in a known volume at room temperature, the amount being of the order of 0.6 g. At temperatures up to 1.1 K the remaining gas volume within the calorimeter (of the order of 12 cm^3) contains no more than 0.0002 g of vapour. At these low vapour densities the mass of the liquid need not be corrected for the amount of evaporating liquid.

In the liquid-solid system, however, the densities differ by about 10 % only. The masses of the liquid and the solid must now be deduced from the amount of helium m_{melt} that has to be released in order to melt all of the solid present, whereupon the calorimeter is left completely filled with the liquid under its melting

pressure; the actual temperature will be called T_2. Then the total mass of helium was equal to:

$$m_t = m_{melt} + V_t / v_{12} \; ; \tag{3.34}$$

the subscript 2 refers to quantities under the melting pressure at the temperature T_2. The corresponding amounts of liquid and solid at the temperature T_2, according to eqs. (3.6), would have been:

$$m_{l2} = \frac{V_t - v_{s2} m_t}{v_l - v_s} = \frac{V_t}{v_{12}} - \frac{v_{s2} m_{melt}}{v_l - v_s} \; , \tag{3.35}$$

$$m_{s2} = \frac{v_{12} m_t - V_t}{v_l - v_s} = \frac{v_{12} m_{melt}}{v_l - v_s} \; .$$

Use is made of Swenson's data [3,13]) giving a constant value for $v_l - v_s$ at temperatures below 1.3 K. Due to the thermal expansion the actual amounts at a temperature T different from T_2 are slightly different from m_{l2} and m_{s2}:

$$m_l = m_{l2} - m_{cor} \; , \; m_s = m_{s2} + m_{cor} \; , \; m_{cor} = \frac{v_l - v_{12}}{v_l - v_s} m_t \; . \tag{3.36}$$

Here v_l is the specific volume of the liquid at the temperature T. The correction m_{cor} is of the order of 0.01 g in the range of temperatures considered, with m_t varying between 2.7 and 3.0 g.

c. Correction for finite steps. In a measurement of heat capacity a finite amount of heat Q is added. From the finite change of temperature ΔT according to eq. (3.32), a provisional value is calculated for the heat capacity:

$$W_{prov} = Q / \Delta T \; . \tag{3.37}$$

It differs from the effective heat capacity W at the temperature T. The appropriate correction depends on the behaviour of W as a function of T according to:

$$W = W_{prov} \left[1 - \frac{1}{24} (n + 2)(n + 3) (\Delta T / T)^2 + \ldots\right] . \qquad (3.38)$$

Here n, being equal to $d(\log W)/d(\log T)$, is found as the slope of the double-logarithmic plot of W as a function of T. This negative correction (which does not surpass 1 % in most cases) has been applied to all measurements of the heat capacity.

d. Corrections for the thermal expansion of the liquid. Before the actual measurements of the heat capacity of the liquid (first cooling vessel), the pressure is adjusted to the desired value p_o at the lowest temperature T_o of about 0.3 K. During the measurements up to 1.1 K, this value does not change within the measuring accuracy of 0.05 atm. Towards higher temperatures, however, the pressure shows a gradual decrease causing at 1.5 K a reduction of about 1.5 % of the original value.

This effect is due to the increase of the density ρ_l of the liquid from 1.15 K up to the lambda point[3,4]. It is found to be smaller than the drop of pressure $[p - p_o]_{\rho_{lo}}$ along the isopycnal of the original density ρ_{lo}. This can be explained by the presence of a buffering volume of about 18 cm^3 in the vessel containing the cooling salt; the temperature of this vessel being approximately 0.3 K lower than that of the calorimeter in the higher temperature region. Introducing a factor $f < 1$, one may express the actual changes of the density and the pressure:

$$\rho_l - \rho_{lo} = (1 - f) [\rho_l - \rho_{lo}]_{p_o} \quad \text{and}$$

$$p - p_o = f [p - p_o]_{\rho_{lo}} \qquad (3.39)$$

in the changes of the density along the isobar and of the pressure along the isopycnal:

$$[\rho_l - \rho_{lo}]_{p_o} = - \rho_{lo} \int_{T_o}^{T} \alpha_{pl} \, dT \quad \text{and}$$

$$[p - p_o]_{\rho_{lo}} = -\frac{1}{\rho_{lo}\kappa_T}[\rho_l - \rho_{lo}]_{p_o} . \qquad (3.40)$$

The factor f is calculated to be 0.6 which is in agreement with the values observed.

The correction connected with the thermal expansion is evaluated in the following manner. If the effective heat capacity W and the density $\rho_l(p,T)$ are introduced, eq. (3.4) can be written in the form:

$$c_{pl}(p,T) = \frac{W - W_c}{\rho_l(p,T)\, V_t} + \frac{T\,\alpha_{pl}}{\rho_l}\,\frac{dp}{dT} . \qquad (3.41)$$

A provisional value of the specific heat of the liquid is calculated according to:

$$c_{prov} = (W - W_c) / \rho_{lo} V_t , \qquad (3.42)$$

where ρ_{lo} is written instead of $\rho_l(p_o,T_o)$. The desired value is $c_{pl}(p_o,T)$ at the constant pressure p_o. With the use of eq. (3.39) c_{pl} may now be found from:

$$c_{pl}(p_o,T) = c_{prov} - c_{prov}(1 - f)\,[\frac{\rho_l}{\rho_{lo}} - 1]_{p_o} +$$
$$+ f\,\frac{T}{\rho_{lo}\kappa_T}\,\frac{d^2}{dT^2}\,\frac{1}{2}\,[\frac{\rho_l}{\rho_{lo}} - 1]^2_{p_o} . \qquad (3.43)$$

The correction is calculated from provisional results for the coefficient of thermal expansion. It is positive, approximately proportional to the pressure, and ranges up to 3 % at a temperature of 1.6 K (see fig. 3,2a).

The specific heat at constant volume $c_{vl}(\rho_{lo},T)$ as a function of the density is also needed. It is found from:

$$c_{vl}(\rho_{lo},T) = c_{pl}(p_o,T) - \frac{T}{\rho_{lo}\kappa_T}\,\frac{d^2}{dT^2}\,\frac{1}{2}\,[\frac{\rho_l}{\rho_{lo}} - 1]^2_{p_o} . \qquad (3.44)$$

The similar transformation of the entropy, from a function of the pressure into a function of the density, reads:

$$s_l(\rho_{lo},T) = s_l(p_o,T) - \frac{1}{\rho_{lo}\varkappa_T}\frac{d}{dT}\frac{1}{2}\left[\frac{\rho_l}{\rho_{lo}} - 1\right]^2_{p_o} . \qquad (3.45)$$

For the present purpose the value of the compressibility $\varkappa_T$ may be considered as independent of the temperature[3,16]).

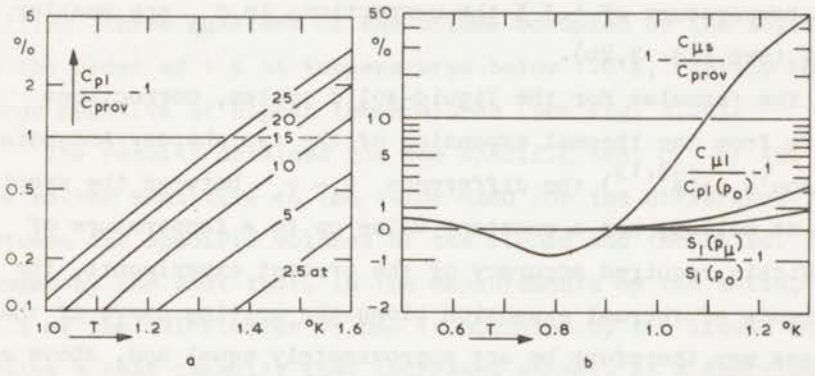

Fig. 3,2. Corrections for thermal expansion;
a. of the liquid; b. along the melting curve.

e. Corrections along the melting curve. From the measurements on the liquid-solid system, the quantities for the solid are calculated from those of the liquid along the melting curve. The latter are found from the quantities of the liquid at the constant pressure p_o equal to 25.0 atm, which coincides with the melting pressure at absolute zero. The appropriate corrections may be computed from provisional results of the present measurements, in particular from the difference $p_\mu(T) - p_o$, where $p_\mu(T)$ is the melting pressure and p_o has been written instead of $p_\mu(0\ K)$. Writing ρ_{lo} for the density of the liquid at low temperatures, one has the following relations for the liquid along the melting curve:

$$\frac{\rho_l(p_\mu,T)}{\rho_{lo}} - 1 = -\int_0^T \alpha_{pl}\, dT + (p_\mu - p_o)\,\kappa_T ,$$

$$s_l(p_\mu,T) = s_l(p_o,T) - (p_\mu - p_o)\,\alpha_{pl} / \rho_l , \quad \text{and}$$

$$c_{\mu l}(T) = c_{pl}(p_o,T) - T\frac{d}{dT}(p_\mu - p_o)\,\alpha_{pl} / \rho_l . \qquad (3.46)$$

Up to a temperature of 1.3 K the corrections in $c_{\mu l}$ are smaller than 2 % (see fig. 3,2b).

In the formulae for the liquid-solid system, corrections originate from the thermal expansion of the two phases. According to Swenson's data[3.13]) the difference $v_l - v_s$ between the specific volumes at melting has a constant value op to a temperature of 1.3 K. Within required accuracy of the present experiments, the coefficients of thermal expansion along the melting curve of the two phases may therefore be set approximately equal and, above a temperature of 0.7 K, both be taken negative. Since the liquid has the larger specific volume, melting occurs in a closed system that is being warmed up above 0.7 K; the value of m_{cor} in eq. (3.36) is positive for temperatures below T_2 as defined in sec. 3-4,b.

In the measurements of the heat capacity, a correction due to this effect is easily found. A provisional value c_{prov} for the specific heat of the solid is calculated from the effective heat capacity W according to:

$$c_{prov} = \frac{1}{m_{s2}}\left[W - m_{l2}c_{\mu l} - W_c\right] . \qquad (3.47)$$

The masses have only approximate values as given in eqs. (3.35) and, as compared with eq. (3.11), the term W_{melt} has been omitted. The correction can be expressed in the following form:

$$c_{\mu s} - c_{prov} = T\frac{d}{dT}\left[(s_l - s_s)\left(\frac{m_s}{m_{s2}} - 1\right)\right] . \qquad (3.48)$$

This equation simply demonstrates the heat effect of the change of

entropy at melting due to the thermal expansion. By eq. (3.35) it is transformed into:

$$c_{\mu s} = c_{prov} + \frac{m_t}{m_{melt}} T \frac{d}{dT} [(s_l - s_s) (\frac{v_l}{v_{12}} - 1)] . \qquad (3.49)$$

The correction has been evaluated with provisional values for the entropy of the solid taken from this experiment. At the usual filling (three quarters of the volume occupied by the solid) it is of the order of 1 % at temperatures below 1.0 K, rapidly becoming large negative at higher temperatures (see fig. 3,2b).

The results obtained for the specific heat $c_{\mu s}$ of the solid are rather sensitive to the value used for the difference $v_l - v_s$ between the specific volumes of the liquid and the solid. This is caused by the fact that, in the measurements on the solid, roughly 25 % of the calorimeter volume is occupied by the liquid contributing a heat capacity that increases steeply as a function of temperature. A systematic error, produced by a value for $v_l - v_s$ which is too low by 1 %, can be estimated from the following expression:

$$c_{prov} = c_{\mu l} + \frac{v_l - v_s}{v_{12} m_{melt}} (W - W_c - m_t c_{\mu l}) . \qquad (3.50)$$

At low temperatures where ($c_{prov} \approx$) $c_{\mu s} > c_{\mu l}$, the specific heat of the solid would also be too low by the order of 1 %. At roughly 0.6 K where the two specific heats are equal $c_{\mu s}$ would not be affected. In the higher region of temperatures where $c_{\mu l}$ dominates $c_{\mu s}$, a value for $c_{\mu s}$ would result that is too high by e.g. 2 % at 0.8 K and by 4 % at 1.0 K. However, from an erroneous value for $v_l - v_s$, no systematic error would result in the melting pressures as calculated from the specific heats. This can be seen from the following expression in which eq. (3.50) is used to eliminate the specific heat of the solid:

$$\frac{dp_\mu}{dT} = \frac{s_l - s_s}{v_l - v_s} = \frac{1}{v_l - v_s} \int_0^T \frac{c_{\mu l} - c_{\mu s}}{T}\, dT$$

$$\approx -\frac{1}{v_{12} m_{melt}} \int_0^T \frac{W - W_c - m_t c_{\mu l}}{T}\, dT \,. \qquad (3.51)$$

In this final result the difference $v_l - v_s$ has dropped out.

In the melting experiments, according to eq. (3.15), the following correction for the thermal expansion is applied to the measured quantity dm_t/dT :

$$\frac{1}{v_l}\left[m_l\left(\frac{dv_l}{dT}\right)_\mu + m_s\left(\frac{dv_s}{dT}\right)_\mu\right] \approx \frac{m_t}{v_l}\left(\frac{dv_l}{dT}\right)_\mu \,. \qquad (3.52)$$

It is negative with a steeply increasing magnitude for increasing temperatures, but its value is only -0.02 g/K at a temperature of 1.1 K. It must be compared with the amounts of 1 to 3 cm^3 of solid that are usually melted in a measuring point, yielding an escaped amount Δm_t of 0.02 to 0.05 g. As the temperature effects ΔT are smaller than 0.05 K, the values of $\Delta m_t/\Delta T$ always exceed 0.4 g/K showing that the correction is of the order of a few percent at a temperature of 1.1 K. Writing the corrected value as:

$$\left(\frac{\Delta m_t}{\Delta T}\right)_{cor} = \frac{\Delta m_t}{\Delta T} + \frac{m_t}{v_l}\left(\frac{dv_l}{dT}\right)_\mu \,, \qquad (3.53)$$

one obtains from eq. (3.15) for the difference of the entropies:

$$s_l - s_s = (\rho_s - \rho_l)\, W_t \,/\, \rho_s\, T\, (\Delta m_t/\Delta T)_{cor} \,. \qquad (3.54)$$

No corrections have been introduced for the finiteness of the temperature steps ΔT in this case or for the thermal expansion in the calculation of the total heat capacity W_t. The latter has been determined from the average amounts of liquid and solid, and the specific heats at the average temperature during the actual process

of melting. From an erroneous value used for the difference $\rho_s - \rho_l$ between the densities of the solid and the liquid, the same error would result in the difference between the entropies. Again, no systematic error would result in the calculated melting pressures.

f. T e m p e r a t u r e e f f e c t o f i n t e g r a l m e l t i n g . In eq. (3.18) for the entropy of the solid at the initial temperature of melting, an integral occurs. Its value depends on the way in which the temperature changes as a function of the amount of escaping liquid. As a first approximation, T varies linearly with this amount yielding for the integral abbreviated by I:

$$I = \int_{T_i}^{T_f} s_l \frac{dm_t}{dT} \frac{dT}{m_{tf} - m_{ti}} \approx \int_{T_i}^{T_f} s_l \frac{dT}{T_f - T_i} , \qquad (3.55)$$

i.e. the entropy of the liquid averaged over the temperature interval. If the densities are introduced into eq. (3.18) and the thermal expansion is neglected, the expression for the initial entropy of the solid becomes:

$$s_{si} = \frac{\rho_l}{\rho_s} s_{lf} + \frac{S_{cf} - S_{ci}}{\rho_s V_t} + \frac{\rho_s - \rho_l}{\rho_s} I . \qquad (3.56)$$

The last term, originating from the escaped liquid, forms a positive correction of the order of 10 % of the initial entropy of the solid. Hence the approximation is justified.

g. C o r r e c t i o n f o r t h e v a p o u r . In the determination of the heat capacity of the calorimeter (second cooling arrangement), the calorimeter is only partly filled with the liquid. The remaining volume is occupied by the vapour under its saturation pressure. During the measurements, the temperature rises and some of the gas may escape from the calorimeter. To maintain the pressure at its saturation value, some of the liquid evaporates contributing its heat of vaporization to the effective heat capacity W.

The correction W_{vap} for the contribution of the vapour within the calorimeter volume is given by eq. (3.26). If the vapour is considered as an ideal gas, the expression becomes:

$$W_{vap} = V_g \frac{p}{T} \left[\frac{5}{2} - 2 \left\{ \frac{T}{p} \left(\frac{dp}{dT} \right)_\sigma \right\} + \left\{ \frac{T}{p} \left(\frac{dp}{dT} \right)_\sigma \right\}^2 \right] . \qquad (3.57)$$

It can be evaluated directly from the data on the vapour pressure curve. In fig. 3,3 an effective vapour density ρ_{eff} is shown as a function of temperature. It is defined by m_{eq}/V_g ; here m_{eq} is the mass of liquid that would contribute the same amount to the effective heat capacity as does the saturated vapour within a volume V_g. In this respect the amount of liquid is the equivalent of the amount of vapour. It is calculated by dividing W_{vap} by both V_g and $c_{\sigma 1}$, and is of the order of 0.01 g of equivalent liquid per cm^3 of saturated vapour at temperatures between 0.8 and 2.0 K. As V_g is approximately 10 cm^3, it follows that m_{eq} is of the order of 0.1 g and that the correction is of the order of 20 % of the total heat capacity. It must be mentioned that the actual amount of liquid is not noticeably affected by the varying amount of vapour. At temperatures up to 1.1 K, the latter never exceeds 0.0002 g.

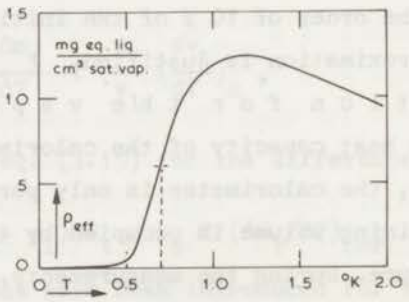

Fig. 3,3. Ratio ρ_{eff} of volume of saturated vapour and equivalent mass of liquid, giving the same effective contribution to the heat capacity, as a function of temperature.

The other correction, W_{vap}, is due to the gas that escapes from the calorimeter into a volume V'_g. This volume is formed by the part of the filling capillary that is immersed in the bath; it is approximately 0.7 cm^3 and remains under a variable pressure p' at the lowest bath temperature T_1 of about 1.1 K. The remaining part of the filling capillary is at room temperature so that its effective volume may be neglected by virtue of the low density of its helium content. If ideal-gas conditions are inserted, eq. (3.24) reads:

$$W'_{vap} = V'_g \frac{p}{T_1} \left\{\frac{T}{p} \left(\frac{dp}{dT}\right)_\sigma\right\}^2 \frac{dp'}{dp} . \qquad (3.58)$$

Instead of the amount of gas escaped from the calorimeter, the change of pressure dp' in the volume V'_g has been introduced here.

This contribution can be estimated by comparison with the last and dominating term of eq. (3.56). The first important difference is the volume V'_g which is about 15 times smaller than V_g. Secondly, a factor dp'/dp has been added which represents the rise dp' during the actual heating, divided by the instantaneous rise dp of the pressure within the calorimeter. A long and gradual rise of the pressure p' contributes only to the effective heat leak which can be eliminated as shown in sec. 3-4,a. A more rapid change of p' could be expected during heating periods only. However, the pressure in the capillary is determined mainly by the saturation value at the temperature of the cooling vessel (second arrangement) which forms the coldest place in the apparatus. It is situated between the calorimeter and almost all of the volume V'_g. Owing to its large heat capacity, its temperature will change only slightly when the calorimeter is heated. Hence dp'/dp will be much smaller than 1, perhaps of the order of 0.1. Therefore, the correction W'_{vap} will be of the order of 1 % of W_{vap} and consequently has been omitted.

REFERENCES

3,1) see e.g. R.Haase, Thermodynamik der Mischphasen(Springer Verlag,Berlin 1956).

3,2) H.J.Hoge, J.Res.Nat.Bur.Stand.36(1946)111.

3,3) F.G.Brickwedde, H.van Dijk, M.Durieux, J.R.Clement and J.K.Logan, J.Res.Nat.Bur. Stand.64A(1960)1.

3,4) W.H.Keesom and A.P.Keesom, Commun.Kamerlingh Onnes Lab.,Leiden No.224d,e; Proc. roy.Acad.Amsterdam 36(1933)482,612.

3,5) H.Kamerlingh Onnes and J.D.A.Boks, Commun.Leiden No.170(1924).

3,6) K.R.Atkins and M.H.Edwards, Phys.Rev.97(1955)1429.

3,7) E.C.Kerr, J.chem.Phys.26(1957)511.

3,8) F.J.Edeskuty and R.H.Sherman, Proc.Vth intern.Conf.on Low Temp.Phys.and Chem. (Madison 1958)p.102.

3,9) M.H.Edwards, Canad.J.Phys.36(1958)884.

3,10) O.V.Lounasmaa, Cryogenics 1(1961)212.

3,11) E.C.Kerr and R.D.Taylor, Ann.Phys.(NY)26(1964)292.

3,12) Z.E.H.A.El Hadi, M.Durieux and H.van Dijk, Commun.Leiden No.364; Physica 41 (1969)289.

3,13) C.A.Swenson, Phys.Rev.79(1950)626.

3,14) E.R.Grilly and R.L.Mills, Ann.Phys.(NY)18(1962)250.

3,15) K.R.Atkins and R.A.Stasior, Canad.J.Phys.31(1953)1156.

3,16) R.Grilly, Phys.Rev.149(1966)97.

3,17) H.C.Kramers, J.D.Wasscher and C.J.Gorter, Commun.Leiden No.288c; Physica 18 (1952)329.

3,18) J.Wiebes, C.G.Niels-Hakkenberg and H.C.Kramers, Commun.Leiden No.308a; Physica 23(1957)625.

3,19) C.E.Chase, Proc.roy.Soc.,London A220(1953)116.

3,20) H.C.Kramers, Progress in Low Temp.Phys., ed.C.J.Gorter(North-Holland Publishing Co., Amsterdam 1957)Vol.II,p.65.

3,21) G.J.C.Bots and C.J.Gorter, Commun.No.320a; Physica 26(1960)337.

CHAPTER IV

THE LIQUID

4-1. Introduction

The separate determination of the heat capacity of the calorimeter, being of great importance to all of the results in the temperature region below 0.5 K, is treated in sec. 4-2. The remainder of this chapter is devoted to the experiments on the liquid. They consist of the measurements of the heat capacity under various pressures and of the expansion experiments. These are treated in secs. 4-3 and 4-4 respectively.

4-2. The heat capacity of the calorimeter

a. E x p e r i m e n t a l . The heat capacity of the calorimeter has been measured at temperatures between 0.28 and 1.1 K. The closed cooling vessel with the filling capillary wound around it (second cooling arrangement) was used in order to reduce the dead volume outside the calorimeter. Three runs, with different amounts of helium, have been performed.

Table 4,I. Helium contents in the partly filled calorimeter.

m_t g	V_l cm^3	V_g cm^3	m_{eq}(0.7 K) g
0.39	2.7	13.1	0.08
0.66	4.5	11.3	0.07
0.85	5.8	10.0	0.06

b. R e s u l t s . In table 4,I the three different amounts of helium m_t, the volumes V_l of the liquid and V_g of the vapour,

and the mass m_{eq} of liquid equivalent to the amount of vapour at 0.7 K (see sec. 3-4,g) are given. Figure 4,1 shows the effective heat capacity W measured as a function of temperature in the three cases. For the lowest content the contributions for the liquid W_{liq} and the vapour W_{vap} (see secs. 3-2,c and 3-4,g), the total helium contribution W_{He}, and the heat capacity of the calorimeter W_c are shown. Part of this run is tabulated in table 4,II also giving the values of W_c/T.

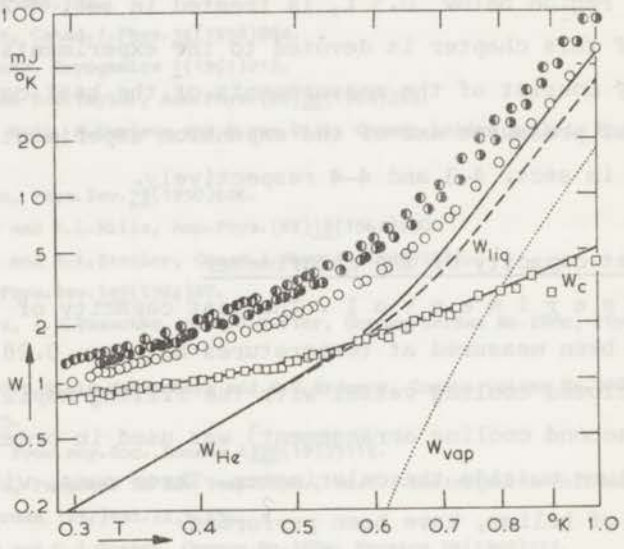

Fig. 4,1. Heat capacities as functions of temperature;
○ ◑ ◐ : calorimeter containing 0.39, 0.66, and 0.85 g of helium;
□ : empty calorimeter, W_c, as calculated from the first by subtracting the contribution W_{He} of 0.39 g of helium equal to $W_{liq} + W_{vap}$.

The results are analysed under the assumption that a cubic lattice term $a T^3$, a linear electronic term $b T$ from the metals, and an inverse square term $c T^{-2}$ due to a Schottky type anomaly contribute to the heat capacity. For this purpose W_c, divided by T, is plotted as a function of T^2 (see fig. 4,2). In the higher region of temperatures the part $a T^2 + b$ dominates; towards lower

Table 4,II. Calculation of the heat capacity of the calorimeter.

part of run with 0.39 g of helium both liquid and vapour								smoothed values		
T K	W_{He} mJ/K	W_c mJ/K	W_c/T mJ/K^2	T K	W_{He} mJ/K	W_c mJ/K	W_c/T mJ/K^2	T K	W_c mJ/K	W_c/T mJ/K^2
299	0.21	0.80	2.68	445	0.71	1.12	2.52	0.30	0.85	2.83
311	0.24	0.84	2.70	457	0.77	1.16	2.54	0.35	0.93	2.64
316	0.25	0.89	2.82	468	0.83	1.13	2.42	0.40	1.01	2.53
321	0.26	0.88	2.74	477	0.87	1.17	2.45	0.45	1.13	2.52
326	0.28	0.86	2.64	485	0.92	1.16	2.39	0.50	1.29	2.58
333	0.30	0.89	2.67	489	0.94	1.27	2.60	0.55	1.49	2.71
339	0.31	0.91	2.69	491	0.96	1.30	2.65	0.60	1.72	2.86
344	0.33	0.95	2.76	503	1.03	1.29	2.57	0.65	1.99	3.06
349	0.34	0.93	2.67	514	1.11	1.31	2.55	0.70	2.29	3.27
354	0.36	0.94	2.66	519	1.15	1.33	2.56	0.80	3.0	3.8
362	0.38	0.94	2.60	534	1.26	1.40	2.62	0.90	3.9	4.3
371	0.41	0.98	2.64	535	1.27	1.32	2.47	1.00	5.0	5.0
379	0.44	0.97	2.56	551	1.41	1.43	2.60	1.10	6.4	5.8
394	0.49	1.01	2.56	577	1.68	1.62	2.81	1.20	7.9	6.6
403	0.52	1.03	2.56	587	1.81	1.65	2.81	1.30	10	7.5
418	0.58	1.03	2.46	610	2.15	1.74	2.86	1.40	12	8.5
419	0.59	1.05	2.51	616	2.25	1.72	2.80	1.50	14	9.5
430	0.64	1.08	2.51	644	2.85	1.87	2.90	1.60	17	10.6

temperatures the lattice term becomes small and the magnitude is governed by the terms $b + c\,T^{-3}$. A minimum value of 2.51 mJ/K^2 is found for W_c/T at a temperature of 0.43 K. In the temperature region below 0.35 K, the term $c\,T^{-3}$ yields a steeper curve than the measurements would indicate. Consequently no analytic form is tried there. Thus in the measuring range, as shown in fig. 4,1, the heat capacity of the calorimeter is an increasing function of the temperature. At temperatures above 0.35 K it is represented well by the expression $a\,T^3 + b\,T + c\,T^{-2}$. In table 4,III the values found for the constants a, b, and c are collected. Also the known contributions of the copper, the niobium, the quartz, and the salt are given. Approximately 30 % of the heat capacity of the

Table 4,III. Composition of the heat capacity of the calorimeter.

$W_c = a\,T^3 + b\,T + c\,T^{-2}$	a mJ K^{-4}	b mJ K^{-2}	c mJ K
measured	3.60	1.40	0.035
154 g copper [4,1]	0.116	1.68	
3.3 g niobium [4,2]	0.003		
18.5 g quartz [4,3]	0.017		
0.016 mole CeMg nitrate [4,4]	0.030		0.001

calorimeter is not accounted for by the sum of the contributions specified (see fig. 4,2). From the contributions of 20.8 g of Perspex and the Amphenol seals, not taken into account, the latter may be responsible for the discrepancy since they are found to be ferro-magnetic.

c. C o n c l u s i o n s . The determination of the heat capacity of the calorimeter forms an essential part in the measurement of the heat capacity of the liquid at low temperatures. Below a temperature of 0.5 K it is of the order of the estimated heat capacities of the liquid to be measured; it is determined with an error of 2 % in this temperature region. Above a temperature of 0.6 K its significance for the determination of the heat capacities diminishes rapidly with increasing temperatures.

The presence of an unknown part in the heat capacity of the calorimeter, though suspected since earlier measurements[4,5)4,6)], was not directly measured before January 1966. It affects the preliminary results as presented during the meeting of the Ninth Conference on Low Temperature Physics held in Columbus, Ohio in September 1964. Data were shown obtained with the calorimeter when it was filled with liquid or solid helium, which at sufficiently low temperatures contributes only a phonon cubic term in the temperature to the heat capacity. It was assumed that the heat

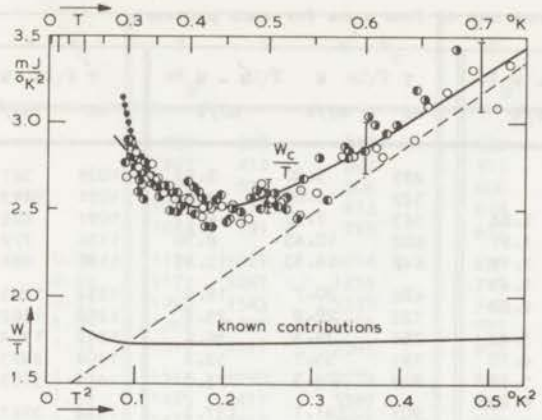

Fig. 4,2. Heat capacities divided by T, as functions of T^2;
○◑● : empty calorimeter, W_c/T, as calculated from three measuring runs;
- - - : $(1.4 + 3.6\ T^2)$ mJ/K²; -•-•- : $(1.4 + 3.6\ T^2 + 0.035\ T^{-3})$ mJ/K²;
——— : sum of known contributions of component parts.

capacity of the calorimeter consisted only of a linear and a cubic term in the temperature. Consequently the constants were calculated from a straight line as found in a diagram of the total heat capacity, divided by T, versus T^2. Clearly systematic errors are introduced by this method if terms other than those mentioned dominate the course of W_c as a function of temperature.

4-3. The heat capacity of the liquid

a. E x p e r i m e n t a l . Measurements of the heat capacity have been made when the calorimeter contained liquid helium under various pressures between the saturated vapour pressure and the melting pressure. The cooling vessel, containing the cooling salt and 18 cm^3 of liquid helium under the same pressure as the helium in the calorimeter (first arrangement), was also used as a thermal buffer. At each of the approximate pressures of 0.1, 2.5, 5, 10, 15, 20, and 25 atm, four runs were performed.

Table 4,IV. Measurements of the heat capacity of liquid helium; one out of four runs for each pressure.

T mK	W mJ/K	W - W_c mJ/K
P_o = 0.07 atm		
341	2.76	1.84
348	2.90	1.97
359	3.13	2.19
373	3.38	2.41
395	3.82	2.82
418	4.49	3.44
448	5.22	4.10
481	6.40	5.18
526	8.22	6.83
568	10.60	9.03
594	12.60	10.91
617	14.15	12.34
638	16.23	14.31
665	19.89	17.82
697	25.2	22.9
730	32.7	30.2
762	42.6	39.9
793	53.7	50.7
825	68.4	65.2
850	82.5	79.1
896	121.3	117.5
924	147.0	142.8
945	171.1	166.7
962	199.2	194.6
982	229	224
1003	258	253
1019	275	270
1041	332	326
1071	399	393
1097	467	461
1126	549	542
1160	659	652
1201	790	782
1247	971	962
1289	1188	1178
1333	1364	1354
1377	1667	1656
1425	2007	1995
1480	2469	2455
1543	2964	2949
1595	3513	3496
P_o = 5.0 atm		
375	2.48	1.51
384	2.71	1.73
412	3.20	2.17
438	3.72	2.62
473	4.46	3.24
499	5.20	3.92
529	6.09	4.69
563	7.67	6.12
602	10.43	8.70
648	14.83	12.85
686	20.7	18.5
722	28.2	25.8
756	39.3	36.6
791	55.7	52.8
829	76.3	73.0
901	141.1	137.2
929	169.3	165.1
959	213	208
991	260	255
1033	344	339
1072	436	430
1114	553	546
1159	714	707
1212	928	920
1255	1140	1130
1293	1387	1377
1332	1596	1586
1371	1863	1852
1405	2127	2115
1444	2386	2373
1493	2927	2913
1558	3530	3514
1622	4460	4442
P_o = 10.1 atm		
347	1.86	0.93
353	1.91	0.97
361	2.05	1.10
375	2.11	1.14
395	2.40	1.40
416	2.76	1.72
441	3.23	2.13
474	3.91	2.71
511	4.78	3.45
549	6.78	5.30
588	9.09	7.42
630	13.03	11.15
673	22.2	20.1
715	31.9	29.5
762	48.9	46.2
812	82.1	79.0
859	125.0	121.5
898	162.3	158.4
933	225	221
972	296	291
1009	367	362
1051	473	467
1091	603	597
1136	779	772
1186	988	980
1232	1245	1236
1288	1562	1552
1342	1974	1963
1404	2475	2463
1471	3105	3091
1534	3765	3750
1590	4535	4518
1655	5470	5451
P_o = 15.15 atm		
351	1.74	0.81
358	1.80	0.86
366	1.92	0.97
379	2.00	1.02
396	2.19	1.19
411	2.39	1.36
430	2.67	1.59
452	2.99	1.86
470	3.30	2.11
495	4.08	2.81
526	5.29	3.90
559	7.09	5.56
595	10.27	8.57
637	15.76	13.85
733	44.6	42.1
784	73.0	70.1
820	105.9	102.7
859	157.6	154.1
894	205	201
926	250	245
965	337	332
1022	431	426
1038	542	536
1075	653	647
1117	834	827
1162	1077	1070
1204	1254	1246
1245	1508	1499
1286	1746	1736
1332	2017	2007
1380	2475	2464
1437	3095	3082
1493	3782	3768
1551	4572	4556

Table 4,IV (continued).

T mK	W mJ/K	W - W_c mJ/K
p_o = 20.25 atm		
370	1.75	0.79
378	1.89	0.92
387	1.96	0.97
400	2.10	1.09
417	2.37	1.33
433	2.53	1.45
446	2.76	1.64
459	2.97	1.82
472	3.13	1.94
506	4.45	3.14
524	5.39	4.01
546	6.83	5.36
572	9.16	7.57
601	12.87	11.14
628	17.82	15.96
658	25.1	23.1
689	36.2	34.0
717	49.4	47.0
742	63.8	61.2
766	79.1	76.3
791	103.9	100.9
817	129.7	126.6
845	162.4	159.0
873	203	199
901	250	246
932	322	318
967	412	407
1004	511	506
1041	619	613
1084	791	785
1132	1021	1014
1177	1267	1259
1220	1543	1535
1266	1862	1853
1313	2317	2307
1367	2790	2779
1425	3411	3399
1473	3919	3905
1514	4611	4596
1565	5510	5496
1605	6710	6693
p_o = 24.9 atm		
334	1.41	0.51
335	1.45	0.55
340	1.44	0.53
349	1.55	0.62
368	1.63	0.67
398	1.97	0.96
426	2.38	1.31
449	2.73	1.60
473	3.34	2.14
505	4.59	2.29
526	5.80	4.41
575	10.60	9.00
600	14.20	12.48
628	21.0	19.14
657	30.2	28.2
691	45.1	42.9
717	60.7	58.3
747	83.3	80.7
775	110.0	107.2
803	138.0	135.0
832	180.5	177.2
862	222	218
889	264	260
920	350	346
955	448	443
990	558	553
1029	698	693
1070	868	862
1117	1108	1101
1160	1366	1360
1203	1670	1662
1248	1990	1981
1293	2380	2370
1344	2920	2909
1400	3630	3618
1445	4390	4377
1484	5060	5046
1516	5420	5405
1574	6480	6464

b. M e a s u r e m e n t s . For each pressure one measuring run is given in table 4,IV. It shows the effective heat capacity W and the heat capacity W - W_c of the liquid. The scatter in the effective heat capacity is of the order of 4 % producing an estimated error in its mean value of 1 to 2 %. The error in the resulting heat capacity of the liquid may now be specified as 2 to 5 % for temperatures below roughly 0.5 K where the calorimeter and the liquid have heat capacities of comparable orders of magnitude. Above that temperature the correction for the calorimeter is relatively small so that the error amounts to 2 %. All values

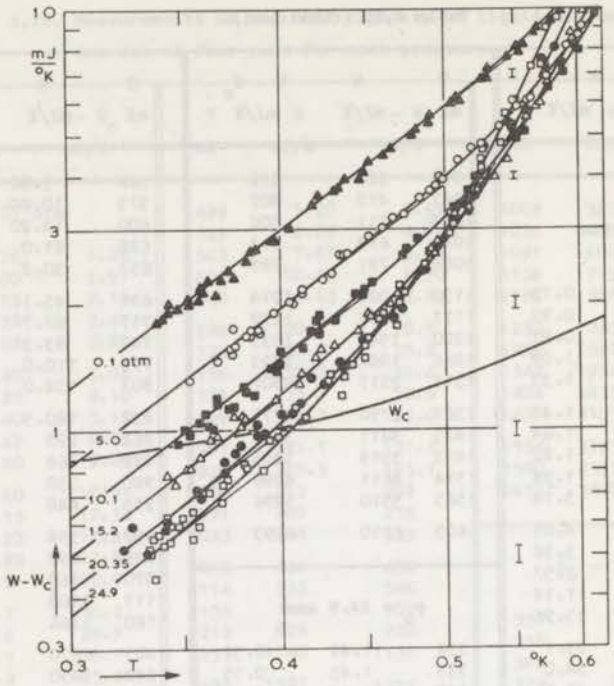

Fig. 4,3. Heat capacities of 15.8 cm^3 of liquid helium at temperatures between 0.3 and 0.6 K; heat capacity W_c of the empty calorimeter;
▲ : 0.1 atm; ○ : 5.0 atm; ■ : 10.1 atm;
△ : 15.2 atm; ● : 20.35 atm; □ : 24.9 atm.

obtained for the heat capacity of the liquid below 0.6 K are given in fig. 4,3. Also the contribution W_c of the calorimeter and the estimated error for several values of $W - W_c$ in that temperature region have been indicated. The pressures indicated are the averages of the adjusted values p_o at the lowest temperatures, differing by less than 0.1 atm from the values in the actual runs. No systematic deviations have been found between different runs at the same pressure. In fig. 4,4 one run between temperatures of 0.4 and 1.6 K is given for each pressure.

c. D i s c u s s i o n . A direct conclusion from the measurements is the establishment of a phonon type of heat capacity in the

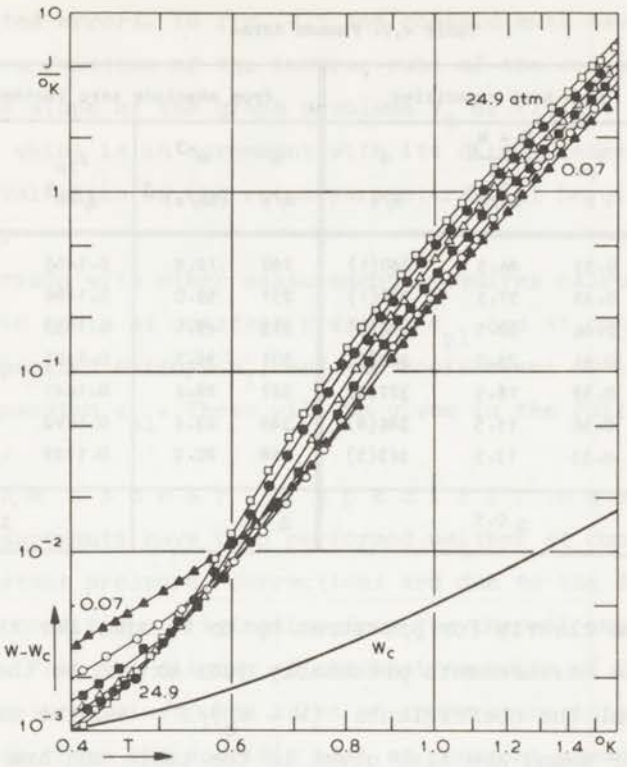

Fig. 4,4. Heat capacities of 15.8 cm^3 of liquid helium at temperatures between 0.4 and 1.6 K; heat capacity W_c of the empty calorimeter;
▲ : 0.07 atm; ○ : 5.0 atm; ■ : 10.1 atm;
△ : 15.15 atm; ● : 20.25 atm; □ : 24.9 atm.

region of low temperatures. This has been indicated by the extended straight lines in the double-logarithmic graph of fig. 4,3, drawn with a slope of 3 through the points at low temperatures. In table 4,V the approximate temperatures T_{ph} are given up to which the phonon formula mentioned in table 6,I of sec. 6-2 is found to be valid. The roton contribution to the specific heat which is dominant at higher temperatures falls off rapidly towards low temperatures. At the temperature T_{ph} it has become of the order of the experimental error. Consequently, at temperatures lower than T_{ph} the specific heat varies as the third power of the temperature.

Table 4,V. Phonon data.

p_o atm	from heat capacities: T_{ph} K	$\frac{W - W_c}{T^3}$ mJ/K^4	u m/s	from absolute zero isotherm: u m/s	u^{-3} (km/s)$^{-3}$	ρ_{lo} g/cm^3	m_t g
0.1	0.53	46.5	240(1)	240	72.4	0.1455	2.30
2.5	0.49	37.5	258(1)	257	59.0	0.1496	2.36
5.0	0.46	30.5	276(2)	273	49.1	0.1532	2.42
10.1	0.41	23.0	304(2)	301	36.7	0.1595	2.52
15.2	0.38	18.5	327(3)	327	28.6	0.1647	2.60
20.35	0.36	15.5	346(4)	349	23.6	0.1692	2.67
24.9	0.35	13.5	363(5)	368	20.2	0.1729	2.73
error		± 0.5		± 2			± 0.01

This is shown clearly for pressures up to 15 atm; for the higher pressures the measurements presumably just extend to the pure phonon region. The coefficients $(W - W_c)/T^3$ and the calculated velocities of sound are also given in the table and are compared with the values deduced from the isotherm at absolute zero (mainly Atkins and Stasior[4,7], see sec. 3-3b). The agreement is within

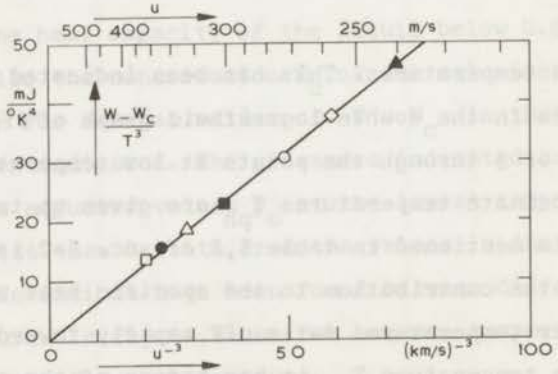

Fig. 4,5. Coefficients of T^3 from phonon heat capacities, as a function of the inverse cube of the velocity of sound.

the estimated errors. In fig. 4,5 the coefficients have been plotted as a function of the inverse cube of the velocity of sound u. From the slope of the graph a volume V_t of $(15.8 \pm 0.1)cm^3$ is calculated which is in agreement with its direct determination. A detailed evaluation of the roton parameters will be given in chapter VI.

Comparison with other measurements requires calculation of the specific heats at constant pressure c_{pl} and at constant volume c_{vl}, the specific entropy s_l, and the coefficient of isobaric thermal expansion α_{pl}. These will be given in the following paragraphs.

d. The isobaric specific heat $c_{pl}(p,T)$. As the measurements have been performed neither at constant volume nor at constant pressure, corrections are due to the deviations from these conditions originating from the thermal expansion of the liquid. From the diagram of the heat capacity of the liquid, $W - W_c$, smoothed values were taken at temperature intervals of 0.05 K. From these the specific heat at constant pressure $c_{pl}(p,T)$ has been calculated as a function of pressure and temperature according to the formulae (3.42) and (3.43). A small correction has been made for the deviations of p_o from smooth values of the pressure. The specific heat data are shown in fig. 4,6 as a function of temperature and as a function of the pressure and are compiled in table 4,VI. The estimated error is 2 %, below 0.5 K towards lower temperatures increasing to 5 %.

The extrapolated value $c_{pl}(0\ atm,T)$ at zero pressure is distinguishable neither from the value $c_{pl}(p_\sigma,T)$ at the saturated vapour pressure p_σ nor from the specific heat $c_{\sigma l}(T)$ along the vapour pressure curve, the differences being smaller than 0.03 % in the range of temperatures considered. Therefore, it may be compared directly with the values of Kramers, Wasscher, and Gorter[4,8]) and with those of Wiebes, Niels-Hakkenberg, and Kramers[4,9]) in the combined form $c_{\sigma l,comb}$ as presented in sec. 3-3,c. In fig. 4,7 the

Table 4,VI. Specific heats of liquid ^{4}He in mJ/g K; at constant pressure, $c_{pl}(p_o,T)$, as a function of the pressure p_o; at constant volume, $c_{vl}(\rho_{lo},T)$, as a function of the density ρ_{lo} corresponding to the pressure p_o at low temperatures.

T	c_{pl}	c_{vl}	c_{pl}	c_{vl}	c_{pl}	c_{vl}	c_{pl}	c_{vl}	c_{pl}	c_{vl}	c_{pl}	c_{vl}	c_{pl}	c_{vl}
K	0.0[1])	0.1455[2])	2.5	0.1496	5.0	0.1532	10.0	0.1594	15.0	0.1645	20.0	0.1690	25.0	0.1729
	atm	g/cm^3	atm	g/cm^3	atm	g/cm^3	atm	g/cm^3	atm	g/cm^3	atm	g/cm^3	atm	g/cm^3
0.30	0.55		0.43		0.34		0.25		0.19		0.16		0.13	
0.35	0.87		0.68		0.54		0.39		0.31		0.25		0.22	
0.40	1.31		1.02		0.81		0.59		0.47		0.39		0.35	
0.45	1.86		1.45		1.16		0.86		0.70		0.62		0.59	
0.50	2.57		2.01		1.64		1.27		1.10		1.05		1.08	
0.55	3.51		2.79		2.36		1.98		1.86		1.95		2.19	
0.60	4.87		4.00		3.55		3.24		3.36		3.82		4.56	
0.65	6.97		6.00		5.59		5.54		6.22		7.43		9.08	
0.70	10.29		9.34		9.09		9.66		11.28		13.82		16.84	
0.75	15.45		14.75		14.86		16.62		19.66		24.2		29.1	
0.80	23.2		23.1		23.8		27.5		32.6		39.8		47.3	
0.85	34.7		35.5		37.0		43.4		51.4		62.0		73.1	
0.90	51.4		53.2		55.9		65.6	65.7	77.5	77.4	92.5	92.4	108.3	108.2
0.95	74.6		77.7		82.2		95.5	95.6	112.9	112.7	132.9	132.6	154.5	154.2
1.00	105.7		110.6		117.4		134.6	134.5	158.4	158.1	184.5	184.0	213	212
1.05	145.8		153.1		162.4		184.4	184.1	215	214	249	248	285	284
1.10	195.9		206		218		246	246	284	283	326	324	372	370
1.15	257		270		285		321	320	366	364	419	416	476	473
1.20	330		346		365		410	408	464	461	528	524	599	594
1.25	416		435		459	458	514	511	579	574	657	650	743	735
1.30	517		540	539	569	568	634	630	712	705	806	795	911	897
1.35	635		663	662	697	695	775	769	868	857	978	961	1107	1085
1.40	772	771	806	804	846	842	939	930	1047	1030	1176	1150	1336	1302
1.45	931	930	972	969	1019	1013	1129	1117	1253	1229	1403	1365	1603	1550
1.50	1115	1113	1165	1160	1220	1212	1350	1331	1490	1455	1665	1609	1915	1833
1.55	1330	1326	1389	1382	1453	1441	1604	1577	1763	1714	1968	1887	2280	2153
1.60	1578	1572	1648	1637	1722	1705	1893	1856	2075	2006	2317	2198	2708	2511

[1])[2]) see text.

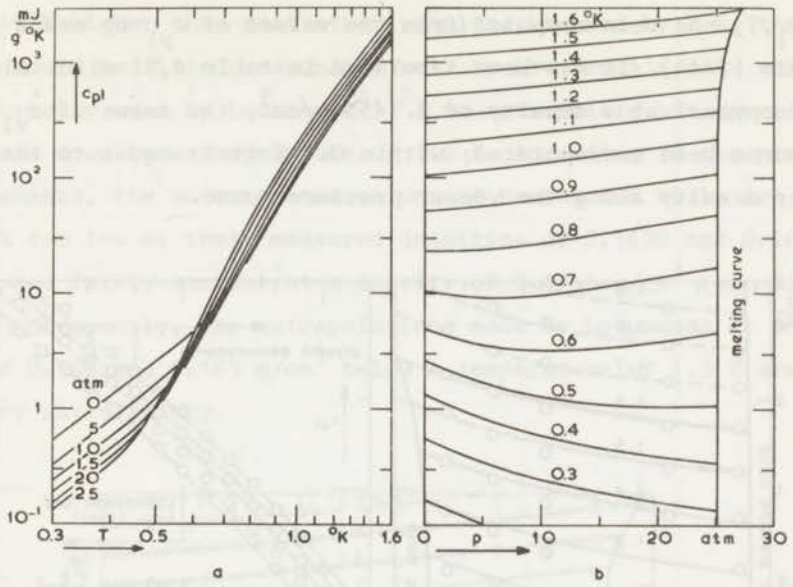

Fig. 4,6. Specific heat at constant pressure c_{pl} of liquid ^{4}He at temperatures below 1.6 K;
a. as a function of temperature; b. as a function of the pressure.

relative deviations plotted as a function of temperature are seen to be of the order of 2 %, i.e. within the limits of the accuracy claimed.

e. The isochoric specific heat $c_{vl}(\rho_l,T)$. At the densities corresponding to the smooth pressure values at low temperatures, the specific heat at constant volume

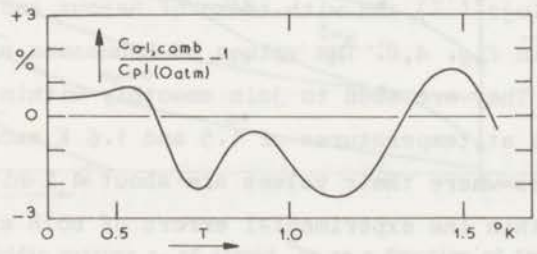

Fig. 4,7. Comparison of the present results for c_{pl}(0 atm) with the combined values $c_{\sigma l,comb}$ of Kramers et al. (1952) and of Wiebes et al. (1957).

$c_{vl}(\rho_l,T)$ has been computed from the values of c_{pl} by means of formula (3.44). It has been tabulated in table 4,VI also. Along the isopycnal at a density of 0.1455 g/cm^3, the value of c_{vl} has of course been extrapolated; within 0.1 % it is equal to the value at the density along the vapour pressure curve.

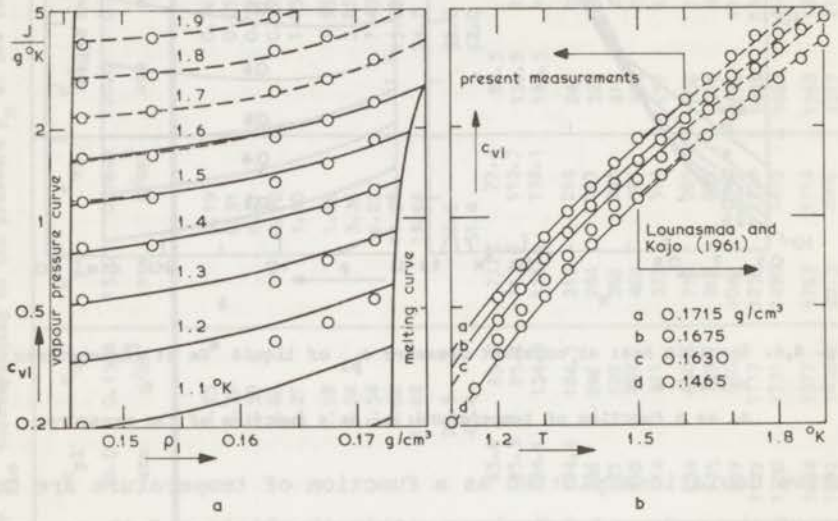

Fig. 4,8. Specific heat at constant volume c_{vl} of liquid ^{4}He;
a. as a function of the density; b. as a function of temperature;
——— : present results; - - - : Lounasmaa and Kojo (1959);
O : Hercus and Wilks (1954) (values decreased by 7 %).

The results may be compared with the earlier measurements of Lounasmaa and Kojo[4,10]) and with those of Hercus and Wilks[4,11]). This is shown in fig. 4,8. The values of Lounasmaa and Kojo extend down to 1.5 K. They are seen to join smoothly within 2 % with the present results at temperatures of 1.5 and 1.6 K except at the lowest densities where their values are about 4 % higher. This discrepancy is within the experimental errors of both experiments, particularly at the extremities of the measured ranges of temperature. The measurements of Hercus and Wilks are known to yield values for the specific heat at saturated vapour pressure that are

about 10 % higher than most other results. Lowered by 7 %, these values could be fitted reasonably well to Lounasmaa's data and were actually used by Lounasmaa[4,12]) to extrapolate his specific heat data down to a temperature of 1.2 K. According to the present measurements, the so corrected values of Hercus and Wilks are up to 12 % too low at their measured densities of 0.1630 and 0.1675 g/cm^3, and fairly correct at a density of 0.1715 g/cm^3 (see fig. 4,8). Consequently, the extrapolations made by Lounasmaa at densities of 0.160 and 0.165 g/cm^3 below a temperature of 1.5 K are not very satisfactory.

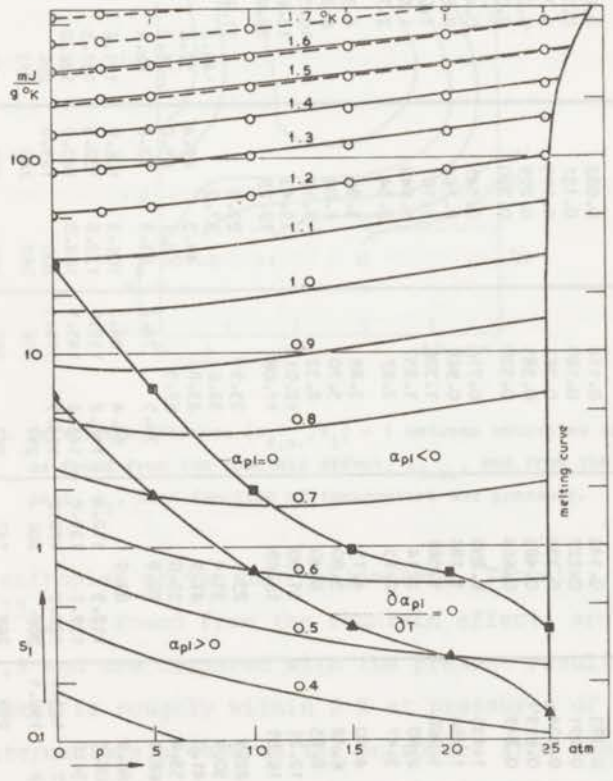

Fig. 4,9. Specific entropy s_1 of liquid ^{4}He as a function of the pressure; loci of zero α_{pl} and $(\partial \alpha_{pl}/\partial T)_p$;
——— : present results; - - - : Lounasmaa and Kojo (1959);
O : van den Meijdenberg et al. (1961) (fountain effect).

Table 4,VII. Specific entropy of liquid ^{4}He in mJ/g K; $s_1(p_o,T)$, as a function of the pressure p_o; $s_1(\rho_{1o},T)$, as a function of the density ρ_{1o} corresponding to the pressure p_o at low temperatures.

T K	0.0[1] atm	0.1455[2] g/cm^3	2.5 atm	0.1496 g/cm^3	5.0 atm	0.1532 g/cm^3	10.0 atm	0.1594 g/cm^3	15.0 atm	0.1645 g/cm^3	20.0 atm	0.1690 g/cm^3	25.0 atm	0.1729 g/cm^3
0.30	0.183		0.143		0.114		0.082		0.064		0.053		0.044	
0.35	0.291		0.227		0.180		0.131		0.103		0.083		0.071	
0.40	0.434		0.339		0.267		0.195		0.154		0.127		0.107	
0.45	0.619		0.483		0.383		0.279		0.221		0.185		0.160	
0.50	0.849		0.664		0.528		0.390		0.313		0.270		0.244	
0.55	1.135		0.892		0.716		0.541		0.449		0.407		0.392	
0.60	1.494		1.186		0.968		0.761		0.668		0.648		0.672	
0.65	1.960		1.581		1.326		1.101		1.039		1.082		1.198	
0.70	2.60		2.14		1.857		1.648		1.670		1.846		2.13	
0.75	3.47		2.95		2.67		2.54		2.71		3.13		3.68	
0.80	4.70		4.15		3.89		3.93		4.37		5.15		6.10	
0.85	6.42		5.90		5.70		6.04		6.88		8.19		9.70	
0.90	8.85		8.40		8.32		9.12		10.54		12.55		14.83	
0.95	12.21		11.90		12.01		13.43		15.66		18.58		21.9	
1.00	16.81		16.69		17.08		19.29		22.6		26.6		31.2	
1.05	22.9		23.1		23.9		27.0		31.6		37.2	37.1	43.3	43.2
1.10	30.9		31.4		32.6		37.0		43.2	43.1	50.5	50.4	58.5	58.4
1.15	41.0		41.9		43.8		49.5	49.4	57.6	57.5	67.0	66.8	77.3	77.1
1.20	53.4		55.0		57.5		65.1	65.0	75.2	75.0	87.1	86.8	100.1	99.7
1.25	68.6		70.8		74.3	74.2	83.8	83.6	96.4	96.1	111.2	110.6	127.4	126.8
1.30	86.9		89.9		94.4	94.3	106.3	106.0	121.6	121.1	139.7	138.8	159.7	158.6
1.35	108.5		112.5	112.4	118.2	118.0	132.8	132.3	151.3	150.4	173.3	171.9	197.6	195.9
1.40	134.0		139.1	139.0	146.2	145.9	164.0	163.2	186.0	184.5	213	211	242	239
1.45	163.7	163.6	170.2	170.0	178.9	178.5	200	199.0	226	224	258	255	293	289
1.50	198.2	198.1	206	206	217	216	242	240	273	270	309	304	352	345
1.55	239	239	248	247	261	260	290	287	326	321	370	363	421	411
1.60	285	285	296	295	311	310	346	342	387	381	438	428	500	485

[1]) The extrapolated value s_1(0 atm,T) at zero pressure equals the value $s_1(p_\sigma,T)$ at saturated vapour pressure within 0.2 %.

[2]) The extrapolated value s_1(0.1455 g/cm^3,T) equals the value $s_1(\rho_{1\sigma},T)$ at the density along the vapour pressure curve within 0.1 %.

f. The specific entropy s_1. If a T^3 dependence is adopted at temperatures below those of the range measured, the specific entropy $s_1(p,T)$ can be found as a function of temperature and pressure from a simple integration of $c_{p1}(p,T)/T$. The resulting specific entropy is given in table 4,VII and is plotted as a function of the pressure in fig. 4,9. The estimated error is of the order of 2 % or 0.005 mJ/g K whichever is greater.

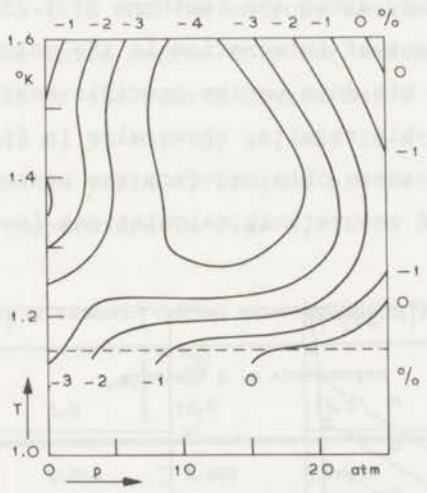

Fig. 4,10. Relative difference $(s_{f.e.}/s_1) - 1$ between entropies of liquid helium, as found from the fountain effect, $s_{f.e.}$, and from the present specific heat, s_1, as a function of temperature and pressure.

The entropies of van den Meijdenberg, Taconis, and de Bruyn Ouboter[4,13]), as found from the fountain effect, are also plotted in fig. 4,9 and are compared with the present results in fig. 4,10. The agreement is roughly within 2 % at pressures of 0 and 25 atm; at the intermediate pressures the entropies from the fountain effect are 2 to 4 % lower than those obtained from the present measurements, with the exception of their lowest temperature of 1.15 K where the agreement is again within 2 %. The differences in the regions of intermediate pressures and higher temperatures are

not significantly larger than the claimed errors would allow. They do have a bearing, however, on the calculated value of the coefficient of isobaric thermal expansion (see the next paragraph).

Another set of comparable entropy data originates from Lounasmaa and Kojo's measurements of the specific heat[4,10]), combined with Lounasmaa's compression data[4,12]) along the isotherm at 1.75 K. From the entropy at saturated vapour pressure according to Kramers et al.[4,8]), and from the entropy of compression, Lounasmaa calculated the entropy along the isotherm at 1.75 K. He used the result as the constant of integration in the calculation of the entropy by means of his data on the specific heat. Within the accuracies claimed, his results, shown also in fig. 4,9, are slightly lower than those obtained from the present measurements.

For purposes of theoretical calculations (see chapter VI),

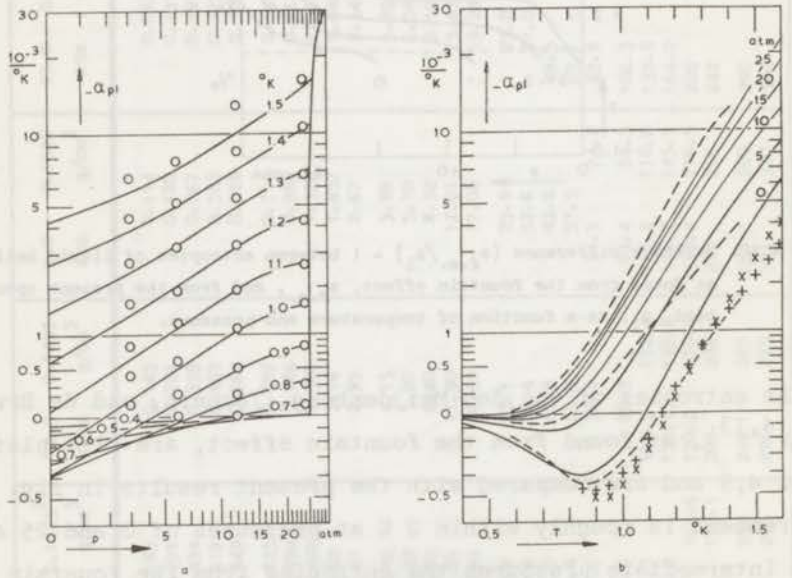

Fig. 4,11. Coefficient of isobaric thermal expansion $\alpha_{pl}(p,T)$ of liquid ^{4}He;
a. as a function of the pressure; b. as a function of temperature;
—— : present results; O : Mills and Sydoriak (1965), at 3, 6, 12 and 24 atm;
- - - : Boghosian and Meyer (1966), at 0, 5 and 25 atm;
+ : Atkins and Edwards (1955), at SVP; X : Kerr and Taylor (1964), at SVP.

the entropy $s_1(\rho_1,T)$ has been tabulated also as a function of density and temperature (table 4,VII). Again the densities corresponding to the smooth values of the pressure at low temperatures have been chosen.

g. The coefficient of isobaric thermal expansion α_{p1}. From the entropy as a function of the pressure, the coefficient of isobaric thermal expansion $\alpha_{p1}(p,T)$ equal to $-\rho_1(\partial s_1/\partial p)_T$, can be found by simple differentiation. To this end the entropy has been approximated by a polynomial of the third degree in p for temperatures above 0.9 K, and by a polynomial of the fourth degree below that temperature using the values at 0, 5, 10, 15, 20, and 25 atm. The calculated values are compiled in table 4,VIII and plotted as functions of the pressure and the temperature in fig. 4,11. In fig. 4,9 the loci of

Table 4,VIII. Coefficient of isobaric thermal expansion $\alpha_{p1}(p,T)$ of liquid ^{4}He in 10^{-3}/K.

T	pressure p in atmospheres					
K	0.0[1])	5.0	10.0	15.0	20.0	25.0
0.3	0.029	0.014	0.007	0.005	0.004	0.002
0.4	0.069	0.033	0.016	0.010	0.009	0.004
0.5	0.132	0.063	0.028	0.016	0.014	+ 0.003
0.6	0.222	0.102	0.038	+ 0.013	+ 0.003	- 0.015
0.7	0.326	0.126	+ 0.016	- 0.039	- 0.070	- 0.120
0.8	0.396	+ 0.089	- 0.10	- 0.22	- 0.28	- 0.37
0.9	0.385	- 0.060	- 0.37	- 0.60	- 0.72	- 0.83
1.0	+ 0.255	- 0.38	- 0.87	- 1.25	- 1.45	- 1.59
1.1	- 0.052	- 0.94	- 1.67	- 2.25	- 2.56	- 2.77
1.2	- 0.59	- 1.79	- 2.83	- 3.66	- 4.16	- 4.52
1.3	- 1.43	- 3.00	- 4.42	- 5.57	- 6.38	- 7.07
1.4	- 2.63	- 4.60	- 6.49	- 8.08	- 9.38	- 10.7
1.5	- 4.23	- 6.61	- 9.08	- 11.3	- 13.4	- 15.8
1.6	- 6.25	- 9.05	- 12.2	- 15.3	- 18.7	- 22.8

[1]) The extrapolated value $\alpha_{p1}(0\text{ atm},T)$ at zero pressure equals the value $\alpha_{p1}(p_\sigma,T)$ at saturated vapour pressure p_σ within 0.1 %.

the minimum values of s_l as a function of the pressure, i.e. α_{pl} equal to zero, and the loci of the maximum value of α_{pl} as a function of temperature, have been indicated. In fig. 4,12 the loci mentioned are shown in the diagram of state. It is clear that no great precision can be claimed for the present values of α_{pl}. In fact, a 2 % error in the entropy will certainly allow for no better accuracy than 10 % in α_{pl} and still larger errors are possible in the values at 0 and 25 atm at the ends of the range of pressure measured.

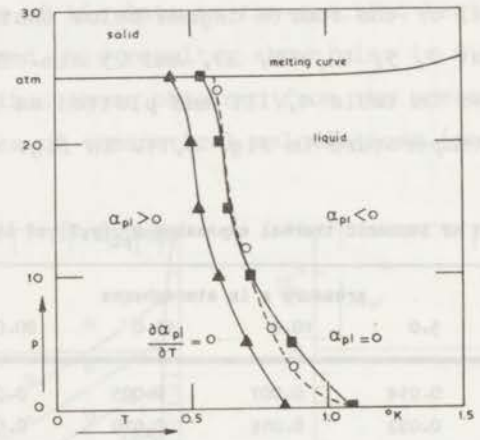

Fig. 4,12. Diagram of state of ^{4}He;
—■— : locus of zero α_{pl}; —▲— : locus of zero $(\partial\alpha_{pl}/\partial T)_p$;
- - - : Boghosian and Meyer (1966); O : Mills and Sydoriak (1965).

Compared with the measurements of Atkins and Edwards[4,14]) and with those of Kerr and Taylor[4,15]) at saturated vapour pressure, as shown in fig. 4,11b, the present results are systematically higher by roughly 20 % for temperatures above 0.8 K. A comparison over the whole range of pressures is possible with the measurements of Boghosian and Meyer[4,16]) (see also fig. 4,11b). At zero pressure deviations similar to the ones mentioned are found. At the maximum of α_{pl}(0 atm), however, all measurements diverge by 10 to 20 %. The present results at 25 atm, on the other hand, are about 20 % lower

than those of Boghosian and Meyer at that pressure, and nearly coincide with their values at 20 atm. At the intermediate pressures the deviations are of the order of 10 % which is within the estimated errors. It may be concluded that the present results at 0 and 25 atm deviate in such a manner as if the present values for the entropy at these pressures were 1 to 2 % too low. This is the same trend as was found in the discussion of the preceeding paragraph where the present entropies appeared to be somewhat higher than other values at the intermediate pressures.

Direct results on α_{pl} have been obtained by Mills and Sydoriak [4,17]) from experiments on adiabatic expansion (see fig. 4,11a). They find a disturbing scatter in α_{pl} as a function of the pressure so that they had to use an unsatisfactory procedure of smoothing according to their equation 7. Compared with the present results, their values at a pressure of 3 atm would be too high as well as their values at 12 atm in the region of higher temperatures. Conclusions will be postponed to the next section where the present expansion experiments will be discussed.

For purposes of corrections due to the thermal expansion, the values along the isobars and the isopycnals of:

$$\frac{\rho_l(p,T)}{\rho_l(p,0)} - 1 = -\int_0^T \alpha_{pl}\, dT \text{ , and} \qquad (4.1)$$

$$\frac{p(\rho_l,T)}{p(\rho_l,0)} - 1 = \frac{1}{p(\rho_l,0)\ \varkappa_T} \int_0^T \alpha_{pl}\, dT \qquad (4,2)$$

are shown in fig. 4,13. The change of the compressibility:

$$\varkappa_T(T) - \varkappa_T(0) = \frac{\partial}{\partial p} \frac{\rho_l(p,T)}{\rho_l(p,0)} \qquad (4,3)$$

is seen to be smaller than $0.2\ 10^{-3} atm^{-1}$ justifying its neglection in sec. 3-4,d (compare also sec. 3-3,b).

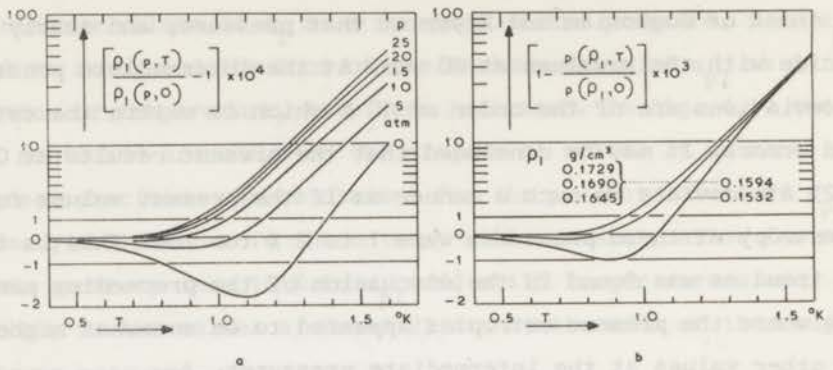

Fig. 4,13. Thermal expansion of liquid ^{4}He; a. relative changes of the density ρ_l along isobars; b. relative changes of the pressure p along isopycnals.

4-4. The adiabatic expansion of the liquid

a. E x p e r i m e n t a l . Expansion experiments have been made with the calorimeter containing liquid helium. Amounts of helium were blown off at several rates, lowering the pressure by steps Δp of about 5 atm at average pressures of approximately 22.5, 17.5, 12.5, 7.5, and 3.0 atm. At several average temperatures between 0.6 and 1.4 K, the related increase ΔT of the temperature has been measured.

The calibration of the magnetic thermometer appeared to depend on the pressure within the calorimeter. At a temperature of 1.0 K and a difference of 5 atm in the pressure, the temperature difference corresponding to the related change in the calibration amounted up to 8 mK on different measuring days. As only the mutual-inductance constant M_∞ was found to be affected by the pressure, an additional calibration as a function of the pressure could be performed at the lowest obtainable bath temperature yielding (see sec. 2-2,d):

$$T = C / [\, M - M_\infty(p) \,] \,. \qquad (4.4)$$

In one of the measuring runs this was done at the pressures between

all subsequent expansions (called: intermediate calibration), and in others after the expansions (called: terminal calibration). The additional calibration data could also be obtained from measurements of the heat capacity between the expansions (called: calibration heat capacity). For this purpose the heat capacities as calculated with a provisional calibration were compared with the known values at the provisional temperatures. The necessary change δM_∞ in the calibration constant was then calculated from the relative deviation $\delta W/W$ in the heat capacity equal to

Table 4,IX. Measurements of adiabatic expansion of liquid helium.

run	calibration	p	- Δp	T	ΔT	W_t	$-\alpha_{pl}$	rate
		atm	atm	mK	mK	mJ/K	10^{-3}/K	mm^3/s
I	intermediate	22.3	5.1	1126	27.8	1090	3.30	3
		17.3	4.9	1122	27.7	910	2.86	9
		12.5	4.6	1118	23.6	760	2.18	16
		7.6	5.3	1115	15.9	630	1.06	9
		2.8	4.3	1107	8.0	510	0.54	19
II	terminal	22.2	3.65	1105	17.8	970	2.68	17
		17.7	5.35	1129	25.6	940	2.49	19
		12.6	4.8	1155	20.6	910	2.12	30
		7.6	5.2	1178	21.7	870	1.92	22
		2.9	4.15	1199	10.3	830	1.08	19
III	terminal	22.2	4.9	1037	23.5	670	1.94	16
		17.4	4.7	1069	23.0	685	1.96	13
		12.5	5.0	1097	20.3	670	1.55	19
		7.5	5.0	1124	13.3	665	0.98	17
		2.9	4.2	1143	5.5	625	0.45	28
IV	terminal	22.2	4.6	868	19.0	214	0.64	10
		17.4	4.8	894	20.3	221	0.65	9
		12.5	5.0	927	17.4	230	0.54	12
		7.6	4.8	979	8.0	276	0.29	15
		3.1	4.3	1022	2.6	310	0.11	14
V	terminal	22.3	5.1	679	24.0	33.9	0.147	14
		17.4	4.65	711	17.5	39.9	0.132	15
		12.5	5.05	754	11.0	51.2	0.093	19
VI	terminal	22.2	4.5	638	21.9	20.7	0.098	14
		17.5	4.9	671	20.7	25.5	0.100	15
		12.6	4.8	703	8.0	30.0	0.044	19
VII	terminal	22.5	4.85	596	30.9	12.3	0.082	16
		17.6	5.1	636	24.0	17.2	0.079	12
		12.5	4.95	666	9.3	20.1	0.035	15
VIII	heat capacity	22.1	4.2	1184	29.0	1410	5.14	7
		17.6	4.8	1239	34.1	1550	5.56	13
		12.7	5.0	1275	34.1	1550	5.18	17
		7.6	5.2	1340	29.9	1740	4.67	15
		3.0	4.1	1389	21.7	1850	4.40	6

$-(n+2)\,T\,\delta M_\infty / C$, where n equals d(logW)/d(logT). The constant $M_\infty(p)$ was found to vary almost linearly with the pressure and was reproducable in different runs on the same measuring day.

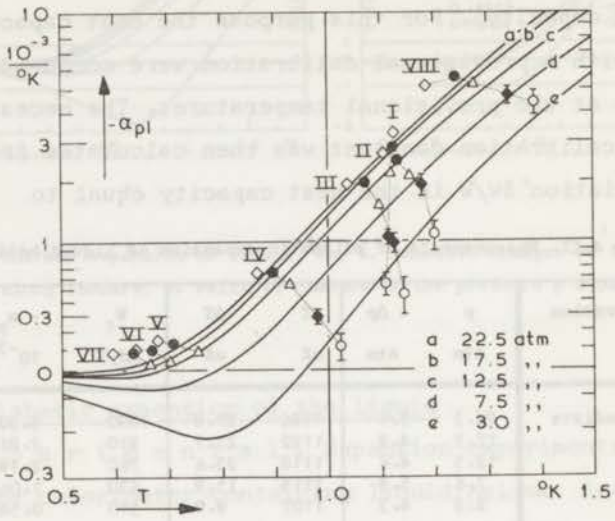

Fig. 4,14. Coefficient of isobaric thermal expansion α_{pl} of liquid ^{4}He; ◇ : 22.5 atm; ● : 17.5 atm; △ : 12.5 atm; ◆ : 7.5 atm; ○ : 3.0 atm, from expansion experiments; —— : as calculated from the entropies.

b. M e a s u r e m e n t s . The results calculated according to eq. (3.5) are given in table 4,IX and are plotted in fig. 4,14 as a function of temperature. The runs numbered V, VI, and VII had to be interrupted owing to the large heat leak at a pressure of about 10 atm and a temperature of approximately 0.7 K. This could perhaps have been overcome by heating the calorimeter to a temperature higher than that of the cooling salt vessel. Since this was not done, no measuring points are available in the region of low pressure and low temperature where the coefficient of thermal expansion is positive. Moreover, no compressions have been performed as the temperature of the entering liquid would have been uncertain. Systematic errors due to irreversibilities are therefore difficult to estimate. Consideration has been given to the

rate of blowing-off expressed in escaping volume of liquid per time. No systematic effect on the temperature increase could be detected. The estimated error amounts to 5 % in the region of higher temperature and pressure; in some of the other points the error has been indicated.

c. D i s c u s s i o n . The calculated values as found in the preceeding section are also shown in fig. 4,14 as fully-drawn lines. The expansion measurements yield values of α_{pl} that agree with the values as computed from the specific entropy within the rather large errors. They seem to agree somewhat better though with the results of Boghosian and Meyer[4,16]). The latter tend to higher high-pressure and to lower low-pressure values than the present computed values would indicate. This tendency is also found in the present expansion experiments.

The results of Mills and Sydoriak[4,17]) at pressures of 3, 6, 12, and 24 atm have been given in fig. 4,11a. These have been obtained in a similar way as the present results. Although both expansions and compressions have been performed and the results averaged, their measurements show an unsatisfactory dependence on the pressure that is not confirmed by the present determination of α_{pl}.

It may be concluded that the present expansion experiments do not significantly deviate from other results. They do not contribute to a better determination of the coefficient of thermal expansion. Indeed, this was not to be expected with the present apparatus which was not at all designed for such measurements.

REFERENCES

4,1) N.E.Phillips, Phys.Rev.134(1964)385.

4,2) B.J.C.van der Hoeven and P.H.Keesom, Phys.Rev.134(1964)1320.

4,3) G.H.S.Jones and A.C.Hollis Hallett, Canad.J.Phys.38(1960)696.

4,4) J.M.Daniels and F.N.H.Robinson, Phil.Mag.44(1953)630.

4,5) J.Wiebes and H.C.Kramers, Phys.Letters 4(1963)298.

4,6) J.Wiebes and H.C.Kramers, Proc.IXth intern.Conf.on Low Temp.Phys.(Columbus 1965)p.258.

4,7) K.R.Atkins and R.A.Stasior, Canad.J.Phys.31(1953)1156.

4,8) H.C.Kramers, J.D.Wasscher and C.J.Gorter, Commun.Kamerlingh Onnes Lab.,Leiden No.288c; Physica 18(1952)329.

4,9) J.Wiebes, C.G.Niels-Hakkenberg and H.C.Kramers, Commun.Leiden No.308a; Physica 23(1957)625.

4,10) O.V.Lounasmaa and E.Kojo, Ann.Acad.Sci.fenn.A VI,No.36(1959).

4,11) G.R.Hercus and J.Wilks, Phil.Mag.45(1954)1163.

4,12) O.V.Lounasmaa, Cryogenics 1(1961)212.

4,13) C.J.N.van den Meijdenberg, K.W.Taconis and R.de Bruyn Ouboter, Commun.Leiden No.326c; Physica 27(1961)197.

4,14) K.R.Atkins and M.H.Edwards, Phys.Rev.97(1955)1429.

4,15) E.C.Kerr and R.D.Taylor, Ann.Phys.(NY)26(1964)292.

4,16) C.Boghosian and H.Meyer, Phys.Rev.152(1966)200.

4,17) R.L.Mills and S.G.Sydoriak, Ann.Phys.(NY)34(1965)276.

CHAPTER V

THE MELTING CURVE

5-1. Introduction

This chapter deals with the experiments on the liquid-solid system. Section 5-2 is devoted to the measurements of the heat capacity from which the entropy of the solid and the melting pressure are calculated. In sec. 5-3 the expansion experiments are presented yielding the temperature derivative of the melting pressure. Both experiments indicate the existence of a shallow minimum in the melting pressure at a temperature of 0.76 K. From the two experiments, respectively, its depth is found to be (0.0073 ± 0.0003) and (0.0085 ± 0.0005) atm below the melting pressure at the absolute zero of temperature. The conclusions are given in sec. 5-4. It is argued that the depth of 0.0073 atm resulting from the heat capacity measurements is probably too low by 10 %.

5-2. The heat capacities at melting

a. E x p e r i m e n t a l . Measurements of the heat capacity have been made when the calorimeter contained about 12 cm^3 of solid and 4 cm^3 of liquid helium. In order to reduce the dead volume

Table 5,I. Amounts of solid and liquid helium at 1.1 K.

m_{melt} g	m_t g	m_{s2} g	m_{12} g	V_{s2} cm^3	V_{12} cm^3
0.191	2.925	2.136	0.789	11.25	4.55
0.205	2.939	2.292	0.647	12.05	3.75
0.198	2.932	2.213	0.719	11.65	4.15

Table 5,II. Measuring run on the heat capacity of the solid.

T mK	W mJ/K	W_c mJ/K	$m_{12}c_{\mu l}$ mJ/K	c_{prov} mJ/g K	T mK	W mJ/K	W_c mJ/K	$m_{12}c_{\mu l}$ mJ/K	c_{prov} mJ/g K
374	4.17	0.97	0.21	1.40	569	14.95	1.58	2.29	5.19
381	4.37	0.98	0.23	1.48	592	17.55	1.68	3.21	5.93
389	4.66	0.99	0.25	1.60	621	21.45	1.83	4.81	6.94
397	4.77	1.01	0.27	1.63	644	25.4	1.95	6.61	7.89
407	5.16	1.03	0.29	1.80	664	29.9	2.06	8.52	9.03
420	5.61	1.05	0.34	1.98	681	32.6	2.2	10.5	9.32
428	5.96	1.07	0.36	2.12	700	37.3	2.3	13.3	10.2
430	6.11	1.08	0.37	2.18	728	44.6	2.5	18.2	11.2
440	6.45	1.10	0.41	2.31	757	57.5	2.7	24.6	14.1
448	6.85	1.12	0.45	2.47	780	66.9	2.9	31.0	15.5
460	7.38	1.16	0.52	2.67	811	84.1	3.1	41.3	18.6
461	7.43	1.16	0.53	2.69	847	106.6	3.4	56.3	22.0
478	8.15	1.21	0.65	2.94	884	138.2	3.8	75.7	27.5
493	9.14	1.26	0.78	3.33	921	173.9	4.1	99.8	32.8
506	9.82	1.31	0.93	3.55	966	225	5	136	39.4
522	11.13	1.37	1.16	4.03	1018	299	5	187	50.1
535	12.10	1.43	1.39	4.34	1059	331	6	237	41.2
543	12.53	1.46	1.56	4.45	1102	452	6	298	69
552	13.51	1.50	1.78	4.79	1148	547	7	375	77

outside the calorimeter the second cooling arrangement was used. The amounts of solid were calculated from the amounts of helium, m_{melt}, that had to be released in order to melt the solid, and from the known densities. For this purpose the solid was melted at the lowest calibration point at a temperature of about 1.1 K. In table 5,I the amounts are given. Three measuring runs have been performed at temperatures between 0.3 and 1.2 K.

In the low-temperature parts of the runs and also during the final melting, one or two small irregular jumps were encountered in the readings of the temperature. They correspond to a few millidegrees at most. It is difficult to observe the jumps while actual heating takes place but they can be expected to occur particularly in the higher region of temperatures where, due to the thermal

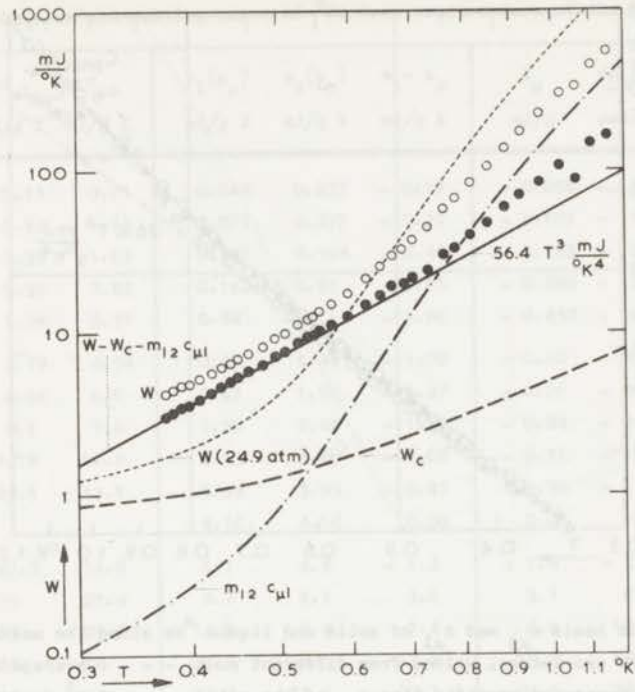

Fig. 5,1. Heat capacities of helium along the melting curve;
O : total heat capacity; ● : provisional contribution of 11.25 cm^3 of solid;
– – – : calorimeter contribution; –·–·– : contribution of 4.55 cm^3 of liquid;
——— : T^3 dependence; .... : total heat capacity with liquid under 24.9 atm.

expansion, small amounts are melted. The effects were found to be smaller if better equilibrium conditions had been maintained during the initial solidification. For this reason the liquid under a pressure of 25 atm was partly solidified by careful compression at the lowest bath temperature under an over-pressure of 0.5 atm at most. The jumps are ascribed to strains in the solid which upon release give rise to small displacements in the thermometer system. As in the case of the pressure dependent calibration (see sec. 4-4,a), only the additional mutual-inductance constant M_∞ is affected. Likewise, the lowest calibration point is measured both before and after the melting. The temperature difference corresponding to the difference found in M_∞ amounts to 1 to 5 mK at

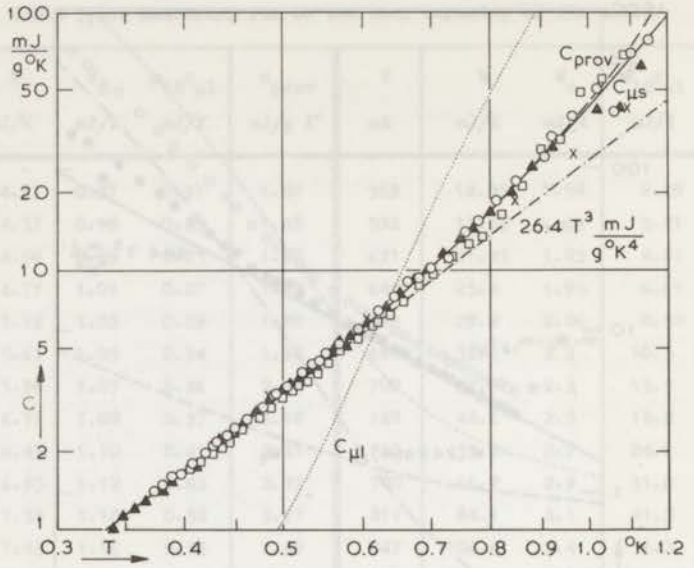

Fig. 5,2. Specific heats $c_{\mu s}$ and $c_{\mu l}$ of solid and liquid ^{4}He along the melting curve;
○ ▲ □ : provisional values from different runs; - - - : average of c_{prov};
—— : corrected specific heat $c_{\mu s}$ of the solid; -·-·- : T^3 dependence;
× : specific heat of the solid at constant volume, Edwards and Pandorf (1965)
···· : specific heat $c_{\mu l}$ of the liquid.

this temperature of about 1.1 K. From the expansion of the solid upon the release of strains, a thermal effect of the order of only - 1 mK may result at this temperature.

b. M e a s u r e m e n t s . One of the three runs has been tabulated in table 5,II and plotted in fig. 5,1. The contributions of the calorimeter and the liquid are given. Also, the heat capacity of the calorimeter when filled with the liquid under a pressure of 24.9 atm has been indicated for comparison (dotted line); the volume heat capacities of the solid and the liquid are apparently equal at a temperature of approximately 0.65 K.

From the present measurements, a provisional melting curve was derived and used in the corrections for the quantities of the liquid at melting (see eqs. (3.46)). In fig. 5,2 the provisional values c_{prov} for the specific heat of the solid as calculated

Table 5,III. Data on the melting curve of ^{4}He from measurements of the heat capacities.

T K	$c_{\mu l}$ mJ/g K	$c_{\mu s}$ mJ/g K	$s_l(p_\mu)$ mJ/g K	$s_s(p_\mu)$ mJ/g K	$s_l - s_s$ mJ/g K	l_μ mJ/g	dp_μ/dT matm/K	$p_\mu - p_o$ matm
0.30	0.13	0.71	0.044	0.237	- 0.19	- 0.058	- 3.7	- 0.28
0.35	0.22	1.13	0.071	0.377	- 0.31	- 0.107	- 5.9	- 0.51
0.40	0.35	1.69	0.107	0.564	- 0.46	- 0.183	- 8.7	- 0.88
0.45	0.59	2.43	0.160	0.81	- 0.65	- 0.290	- 12.3	- 1.40
0.50	1.08	3.37	0.24	1.11	- 0.86	- 0.432	- 16.5	- 2.12
0.55	2.19	4.54	0.39	1.48	- 1.09	- 0.60	- 20.8	- 3.1
0.60	4.56	6.0	0.67	1.94	- 1.27	- 0.76	- 24.2	- 4.2
0.65	9.1	7.8	1.20	2.49	- 1.29	- 0.84	- 24.6	- 5.4
0.70	16.8	10.2	2.13	3.15	- 1.02	- 0.71	- 19.5	- 6.6
0.75	29.1	13.1	3.68	3.95	- 0.27	- 0.20	- 5.2	- 7.3
0.762			4.16	4.16	0.00	0.00	0.0	- 7.3
0.80	47.3	16.8	6.1	4.9	+ 1.2	+ 1.0	+ 23	- 6.9
0.85	73	21.4	9.7	6.1	3.6	3.1	69	- 4.7
0.90	109	27.1	14.8	7.4	7.4	6.6	141	+ 0.5
0.95	155	34	21.9	9.1	12.8	12.2	244	10
1.00	213	43	31.2	11.1	20.1	20.1	386	26
1.05	285	53	43.3	13.4	30	31	573	49
1.10	373	65	58.6	16.1	43	47	812	84
1.15	479	80	77.6	19.3	58	67	1111	132
1.20	606	98	100.6	23.1	78	93	1480	196

according to eq. (3.47) are shown for the three runs. There appears to be a systematic difference of up to 10 % between different runs particularly in the temperature region from 0.5 to 0.9 K. This can be explained in part by changes in the constant M_∞ of the thermometer calibration during the measurements at temperatures above 0.9 K. Accordingly, the large spreading in the points above 0.9 K is ascribed to the jumps in the calibration constant originating from the appreciable effect of the thermal expansion on strains in the solid. Corrections for this effect are difficult to estimate and have not been applied. Care was taken not to heat the calorimeter to a higher temperature than that of the lowest calibration

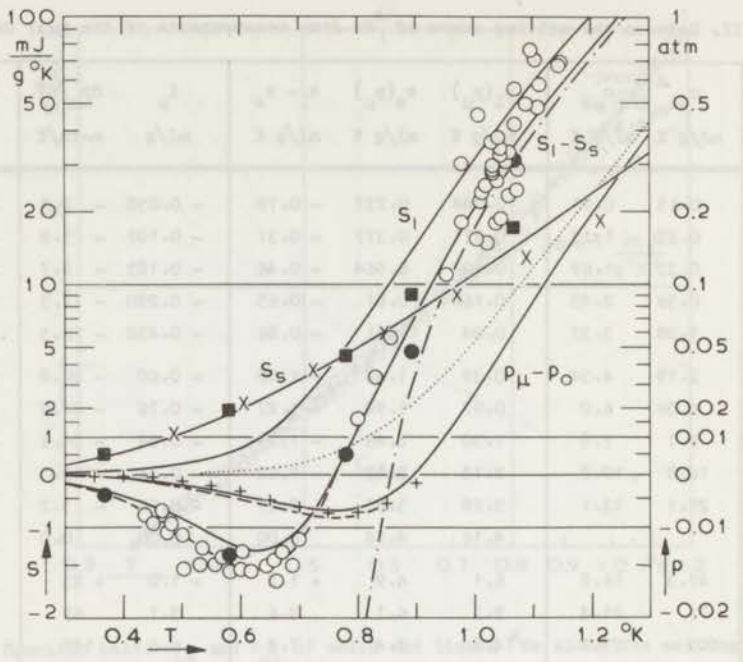

Fig. 5,3. Specific entropies of liquid (s_l) and solid (s_s) ^{4}He at melting, entropy difference ($s_l - s_s$), and difference between melting pressure and its value at absolute zero ($p_\mu - p_o$);
—— : calculated from measurements of the heat capacities;
■ : specific entropy of solid from integral expansion experiments;
● ○ : entropy differences from integral and differential expansion experiments respectively; - - - : average values from expansion experiments;
.... : extrapolated difference of melting pressures, Swenson (1950);
-·-·- : entropy difference, Sydoriak and Mills (1965);
× : specific entropy of solid at melting, Edwards and Pandorf (1965);
++ : difference of melting pressures, Straty and Adams (1966).

point. Systematic errors may arise also from the manner in which the amounts of solid have been determined (see sec. 3-4,b). The collected amounts m_{melt} should originate only from melting within the calorimeter. However, it is not possible to exclude entirely contributions from melting in parts of the capillary outside the vacuum vessel. Consequently, m_{melt} may be a few percents too high.

In the region of higher temperatures a correction due to the thermal expansion is applied yielding $c_{\mu s}$. Up to 0.5 K the specific

heat shows a third power in the temperature with a coefficient of (26.4 ± 0.8) mJ/g K^4. At higher temperatures it shows a steeper rise. Between 0.5 and 0.9 K the error is estimated to 6 % increasing to 10 % above a temperature of 0.9 K. Also $c_{\mu l}$ is shown in fig. 5,2; it is equal to $c_{\mu s}$ at a temperature of 0.63 K. Both specific heats have been tabulated in table 5,III.

From the present results of the specific heats the specific entropies, the entropy difference, the specific heat of melting, the temperature derivative of the melting pressure, and the difference of the melting pressure p_μ with its value p_o at the absolute zero of temperature have all been calculated. They are also given in the table and some are shown in fig. 5,3 as fully-drawn curves. At temperatures below 1.0 K, the entropy of the solid is probably accurate to 4 %. The specific entropies are equal at a temperature of (0.76 ± 0.01) K which therefore is the temperature of the minimum in the melting pressure. The difference of the specific entropies has an error of 4 % or, in the vicinity of the minimum, of about 0.2 mJ/g K. The error in the difference between the melting pressure and its value at absolute zero is estimated to 4 % or, near a temperature of (0.90 ± 0.01) K where this difference is zero, of the order of 0.0003 atm. The depth of the minimum amounts to (0.0073 ± 0.0003) atm.

c. D i s c u s s i o n . In the region of low temperatures no direct measurements of the specific heat of the solid along the melting curve exist for comparison. However, the specific heats at constant volume c_{vs} at several densities of the solid have been measured lately[5,1-3]).

Those of Edwards and Pandorf[5,2]) extend to both low-temperature and low-density regions. They give c_{vs} and s_s as functions of T/θ where the effective Debije temperature θ is given as a function of the density. Their values of c_{vs} have been plotted in fig. 5,2 showing agreement with the present results within 5 % at temperatures below 0.7 K. At higher temperatures their values are

systematically lower than the present measurements would indicate. Part of this discrepancy could be accounted for by a systematic error in the determination of the amounts of solid mentioned before. From their data combined with the compressibility[5,4]) it follows that c_{vs} should be less than 1 % higher than $c_{\mu s}$ in that region. In fig. 5,3 their entropies are compared with the present results showing the same deviations as do the specific heats.[+])

Direct measurements of the melting pressure by Swenson[5,6]) and le Pair et al.[5,7]) are in agreement with the present results within their estimated errors which are appreciably larger than those of the present determination. Swenson's extrapolated value of $P_\mu - P_o$ equal to $0.053\ T^8$ atm K^{-8}, is shown in fig. 5,3 as a dotted curve. The measurements of le Pair indicate the presence of a minimum between 0.6 and 0.9 K. Accurate measurements of the melting pressure by Straty and Adams[5,8]) using a capacitive method show reasonable agreement with the present results. They find a minimum melting pressure at a temperature of 0.775 K differing by 0.0075 atm from the melting pressure at 0.35 K; the present experiment would give 0.0068 atm for that difference. The difference of 10 % cannot arise from errors in the value used for the difference $\rho_s - \rho_l$ (see sec. 3-4,e). It could result partly from values for m_{melt}, used in the determination of the amounts of solid, that are too high.

[+]) Recently accurate measurements at temperatures down to 0.3 K on the molar volumes and the heat capacities at constant volume of the solid, the liquid, and the two-phase system have been made by Hoffer[5,5]). Within the accuracy required here, the densities of the solid and the liquid along the melting curve as found by Hoffer are 0.1908 and 0.1731 g/cm^3 respectively. The resulting difference of 0.0177 g/cm^3 is 4 % larger than the difference used in the present calculations (taken from Swenson, see sec. 3-3b). As discussed in sec. 3-4e, the effect of a systematic error of this magnitude would amount to 16 % at 1.0 K, thus accounting for more than half of the discrepancy between the present results and those of Edwards and Pandorf (Hoffer's results for the specific heat of the solid are consistent with the latter). See also sec. 5-3.

The experiments on the minimum in the melting pressure by Sydoriak and Mills[5,9]) were performed by using adiabatic expansion methods as well as by making direct measurements of the pressure. The discussion of their results will be deferred to the next section where the present expansion experiments will be described.

5-3. The adiabatic expansion at melting.

a. E x p e r i m e n t a l . In the integral expansion experiments, helium was blown off at a constant rate until the pressure had fallen to about 2 atm below the melting pressure. The first cooling arrangement, with a large buffering volume of helium in the cooling vessel, was used. The helium had been solidified under an external pressure of about 28 atm while the surrounding helium bath was cooling down slowly to its lowest temperature. These experiments, together with provisional data on the entropy of the solid and the depth of the minimum in the melting pressure, have been published earlier[5,10]).

Additional measurements have been performed in which the calorimeter contained varying amounts of liquid and solid helium that were expanded differentially. The second cooling arrangement was employed; the helium was solidified at a temperature of about 1.1 K under an over-pressure of no more than 0.5 atm in order to avoid large strains in the solid. Amounts of the order of 30 mg of helium were blown off and collected and the resulting change of temperature was measured at several temperatures between 0.4 and 1.2 K.

b. M e a s u r e m e n t s . The course of the pressure and the temperature in the five integral expansions are shown in fig. 5,4. When the pressure first reaches 25.0 atm melting occurs, but it takes an appreciable time before the temperature within the calorimeter starts to change. This delay is caused by the melting of the solid within the vessel containing the cooling salt. Again, small irregularities were encountered in the course of the

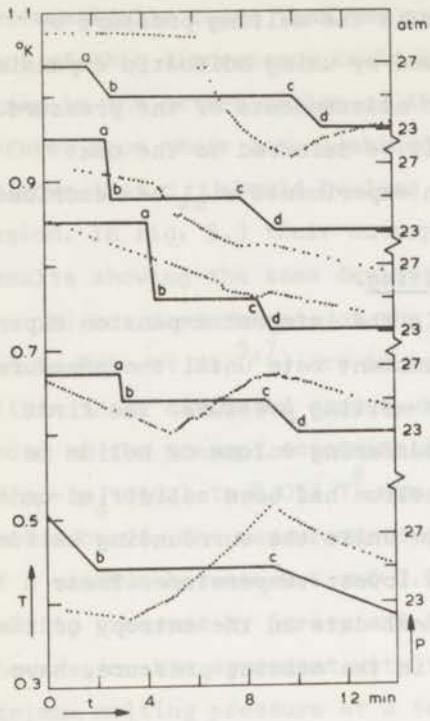

Fig. 5,4. Temperature (....) and pressure (——) within the calorimeter as a function of time during integral expansion of solid helium;
a - d : period of blowing-off;
b - c : period at melting pressure.

temperature, ascribed to sudden changes in the calibration of the thermometer resulting from the release of strains in the solid upon melting (see also sec. 5-2,b). Perhaps a small thermal effect from the expansion of the solid under stress is also included in the temperature changes measured. The initial and final temperatures were found in the usual way by elimination of the heat leak

Table 5,IV. Integral adiabatic expansion of solid helium.

T_i mK	T_f mK	$\frac{\rho_l}{\rho_s} s_{lf}$ mJ/g K	$\frac{S_{cf} - S_{ci}}{\rho_s V_t}$ mJ/g K	$\frac{\rho_s - \rho_l}{\rho_s} I$ mJ/g K	s_{si} mJ/g K	$s_{li} - s_{si}$ mJ/g K
367	547	0.349	0.153	0.017	0.519	- 0.437
580	688	1.70	0.11	0.10	1.91	- 1.37
780	770	4.12	- 0.01	0.40	4.51	+ 0.49
892	842	8.2	- 0.1	1.0	9.1	+ 4.8
1068	912	14.9	- 0.3	2.7	17.3	+ 31.2

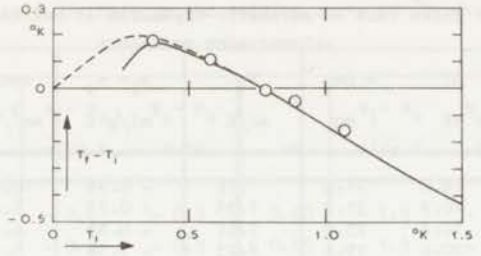

Fig. 5,5. Change of temperature $T_f - T_i$ upon adiabatic melting of solid ^4He, as a function of the initial temperature T_i;
——— : solid helium contained in the calorimeter;
- - - : contained in a calorimeter with negligible heat capacity.

(see sec. 3-4,a); the five resulting changes of temperature are plotted in fig. 5,5 as a function of the initial temperatures. The temperatures and the three component terms of the initial entropy of the solid according to eq. (3.56) are given in table 5,IV. It is assumed that at the beginning of the expansion the calorimeter was entirely filled with the solid under its equilibrium pressure. However, the calorimeter may have contained an amount of liquid of the order of 10 % that could not be detected due to the presence of solid helium in the cooling vessel. This would result in a systematic error of the order of 10 % in the calculated initial entropy of the solid, yielding values too high at temperatures above that of the minimum in the melting curve and too low below that temperature. Both the initial entropy of the solid and the entropy difference have been plotted in fig. 5,3 as solid squares and circles respectively.

For three runs of the differential expansion experiments the temperature, its change ΔT, and the escaped amounts of helium Δm_t are given in table 5,V. The total heat capacity has been calculated from the average amounts of liquid and solid and from the specific heats as found in the preceeding section. The entropy difference was calculated according to eq. (3.52); the rate of outflow of liquid is also indicated. The results of $s_l - s_s$ are

Table 5,V. Three runs on adiabatic expansion at melting.

T	ΔT	$-\Delta m_t$	W_t	$s_l - s_s$	rate
mK	mK	mg	mJ/K	mJ/g K	mm^3/s
450	14.2	21.5	7.16	- 0.94	10.6
464	10.9	21.2	7.35	- 0.73	7.4
480	16.8	25.2	7.61	- 0.95	6.2
503	20.6	19.6	8.25	- 1.54	5.8
529	25.4	26.4	9.25	- 1.51	4.3
556	21.3	24.5	10.8	- 1.51	6.0
581	23.8	29.6	12.8	- 1.58	9.4
602	14.5	24.9	15.5	- 1.34	5.4
618	13.0	21.9	18.2	- 1.57	4.3
799	- 7.2	52.8	105	1.60	12.4
830	- 7.5	37.1	153	3.33	27.2
858	- 6.9	27.3	210	5.55	8.1
1022	- 12.0	26.8	624	25	8.0
1033	- 23.3	35.4	620	36	3.7
1048	- 21.8	33.2	597	34	4.3
1062	- 19.3	28.2	567	33	7.0
1075	- 17.8	33.4	530	24	9.0
1106	- 38.6	23.6	526	71	4.5
1150	- 40.8	26.3	547	69	7.1

shown in fig. 5,3 as open circles. The relative influence of a variation of the calibration constant on the small changes of temperature in the differential expansions is much larger than that on the integral temperature effects. In particular the points at high temperatures show an appreciable spreading. If the helium was not solidified carefully under almost equilibrium conditions the spreading was significantly larger. Those measuring points have been omitted here but they were reported in an earlier communication[5,11]).

The smoothed differences of the entropies and of the melting pressures as calculated from the expansion experiments are indicated by intermittedly drawn curves in fig. 5,3 and tabulated in table 5,VI for temperatures below 0.8 K. The minimum in the melting pressure is found at a temperature of 0.76 K; its depth is (0.0085 ± 0.0005) atm.

c. D i s c u s s i o n . The results of the integral expansion experiments agree with the differential results within the rather

Table 5,VI. Data on the melting curve of ^{4}He from expansion experiments.

T mK	$s_l - s_s$ mJ/g K	$p_\mu - p_o$ matm	T mK	$s_l - s_s$ mJ/g K	$p_\mu - p_o$ matm
0.30	- 0.2	- 0.3	0.60	- 1.5	- 4.9
0.35	- 0.3	- 0.5	0.65	- 1.5	- 6.2
0.40	- 0.5	- 0.9	0.70	- 1.2	- 7.6
0.45	- 0.8	- 1.5	0.75	- 0.4	- 8.4
0.50	- 1.1	- 2.4	0.76	0.0	- 8.5
0.55	- 1.3	- 3.6	0.80	+ 1.3	- 8.0

large experimental error. The two values at the higher temperatures yield specific entropies of the solid that are too high. This can be ascribed to the presence of liquid in the calorimeter as mentioned before.

A survey of available data on the minimum in the melting pressure is given in table 5,VII. As compared with the results from the measurements of the specific heat the expansion experiments yield systematically lower, i.e. larger nagative values for the entropy difference $s_l - s_s$ at temperatures below that of the minimum of the melting curve. In the region of higher temperatures the scatter is large; above 1.05 K the expansion results lie perhaps somewhat higher than those derived from the heat capacities. The scatter may be attributed largely to strains in the solid and related changes of the thermometer calibration. The systematic deviations are such as could have been caused by irreversibilities producing entropy, thus resulting in final temperatures of the measuring points that are too high. Then the rises of temperature in the range of lower temperatures would be too large. Since the calculated differences of the entropies are proportional to the measured changes of temperature, this would explain the direction of the deviations as found. They are not associated, however, with the rate of liquid outflow within the present limits. At very much

Table 5,VII. Data on the minimum in the melting pressure of ^{4}He.

authors	year, ref.	method used	T_{min} K	$p(0) - p_{min}$ matm
Goldstein	1962; 5,16)	calculation	~ 1.0	~ 52
van den Meijdenberg	1961; 5,17)	estimate from entropy	< 0.8	< 40
Wiebes and Kramers	1963; 5,10)	expansion experiments	0.76	8
le Pair et al.	1963; 5,7)	direct measurements	-	8 ± 3
Sydoriak and Mills	1964; 5,9)	expansion experiments	0.857	> 27
		direct measurements	-	-
Zimmerman	1964; 5,13)	expansion experiments	> 0.63	large
le Pair et al.	1965; 5,18)	direct measurements	~ 0.75	8
Wiebes and Kramers	1966; 5,11)	specific heats	0.76	7
		expansion experiments	0.76	9
Straty and Adams	1966; 5,8)	direct measurements	0.775	8.0
Goldstein and Mills	1967; 5,19)	calculations	0.76 - 0.77	8.0
Hoffer	1968; 5,5)	specific heats	0.776	8.04
this work	1969	specific heats	0.76 ± 0.01	7.3 ± 0.3
		expansion experiments	0.76 ± 0.01	8.5 ± 0.5

smaller rates the irreversibilities could possibly have been suppressed.

A way of eliminating these effects would be to perform both expansions and compressions and to average the results under the assumption that the irreversible productions of entropy are equal in both experiments. In the experiments on the liquid by Mills and Sydoriak[5,12]) this was actually done; the two types of experiments yield systematic differences of the order of 15 %. In their experiments on the minimum in the melting pressure[5,9]), however, they used only the expansion technique. The rate of liquid outflow was of the same order of magnitude as that in the present measurements; their measurements do not extend below the temperature of the minimum in the entropy difference (about 0.6 K). Compared with the present expansion results, their entropy difference is substantially lower (larger negative) as shown in fig. 5,3. They find a zero change of temperature upon expansion at 0.857 K which is nearly

0.1 K higher than the present measurements indicate. However, the average deviation of their entropy differences is reported to be 3 mJ/g K which is about twice the depth of the minimum in the entropy difference as found from the present measurements. It will be clear that from these data no better accuracy than several hundredths of a degree can be obtained for the temperature of the zero point in the entropy difference. Also their estimate for the depth of the minimum in the melting pressure, of several tenths of an atmosphere, may be erroneous since their errors are likely to be systematic. Moreover, in the plot of their direct measurements of the melting pressure, a systematic difference occurs with the pressure at temperatures between 0.9 and 1.1 K as calculated from their values of $s_l - s_s$; the direct measurements would indeed indicate a lower value for the temperature of the minimum in the melting curve. The computed depth of the minimum of their melting pressure is an order of magnitude larger than the values of 0.0085 atm from the present expansion experiments, or 0.0073 atm as calculated from the experiments on the heat capacities. Straty and Adams[5,8]) have accurately determined the melting curve (see fig. 5,3) using a capacitive method of measuring the pressure. They find a pressure minimum at a temperature of 0.775 K, with an increase in pressure of 0.0075 atm upon cooling to 0.35 K. Combined with the present value of 0.0005 atm at the latter temperature, the depth of their minimum amounts to 0.0080 atm which is in agreement with the results from the present expansion experiments. Between the two temperatures mentioned, however, their results are probably slightly in error (by 0.001 atm at most) yielding a curvature of the melting curve that is somewhat too large.[+])

[+]) According to Hoffer's measurements[5,5]) mentioned in sec. 5-2, the minimum is located at 0.776 K and has a depth of 8.04 matm. Within the estimated error, the results obtained from the present expansion experiments are consistent with Hoffer's determination but those from the present heat capacities are not. As discussed in sec. 3-4e, discrepancies cannot originate from the value for the difference $\rho_s - \rho_l$ as used in the present calculations.

Warming up during integral expansions has also been reported by Zimmerman[5,13]. His increase of temperature from 0.15 to 0.63 K appears to be too large by a factor of four (compare fig. 5,5). Possibly his rate of releasing the liquid has been too high causing irreversible heating.

5-4. Conclusions

a. The velocities of sound in the solid. The results for the specific heat of the solid at temperatures below 0.5 K may be analysed by means of the Debije temperature θ_o or, alternatively, by the velocities of longitudinal sound u_l and transverse sound u_t according to:

$$c_{vs} = \frac{12\,\pi^4}{5}\,\frac{k}{m}\,\left(\frac{T}{\theta_o}\right)^3 = \frac{2\,\pi^2}{15}\,\frac{k^4}{\hbar^3}\,\frac{1}{\rho_s}\,\left(\frac{1}{u_l^3} + \frac{2}{u_t^3}\right)\,T^3 \,. \qquad (5.1)$$

Here m is the mass of the ^{4}He atom. The resulting constants are given in table 5,VIII. Use is made of the value of 478 m/s for the velocity of longitudinal sound waves as measured by Vignos and Fairbank[5,14]. The result for u_t may be compared with those of Lipschultz and Lee[5,15] who found velocities of 230 and 315 m/s for shear waves, presumably depending on the angle between the directions of propagation and of the crystal axis. Also the corresponding value for the Poisson ratio σ has been given.

b. The minimum in the melting curve. The existence of a minimum in the melting pressure of ^{4}He may be considered as experimentally well verified by caloric measurements,

Table 5,VIII. Resulting data of solid ^{4}He.

$\lim_{T\to 0} c_{vs}/T^3$ mJ/g K^4	θ K	$u_l^{-3} + 2\,u_t^{-3}$ (km/s)$^{-3}$	u_l m/s	u_t m/s	σ
26.4 ± 0.08	26.3 ± 0.3	112 ± 4	478	268 ± 3	0.27 ± 0.01

thermal methods using adiabatic expansion, and direct measurements of the pressure (see table 5,VII). Discrepancies between different expansion experiments may arise from irreversible heating but more trivial sources of error cannot be excluded. The systematic difference between the results of the present expansion experiments and those obtained from the present measurements of the heat capacity may well result from systematic errors that are difficult to avoid with the present apparatus. Compared with the direct measurements by Straty and Adams and with the results from the caloric experiments by Hoffer, the results derived from the present heat capacities are probably too low by 10 %. Apart from difficulties with thermometer calibration, systematic errors may arise also from the manner in which the amounts of solid helium have been determined, i.e. from the amounts of helium to be released in order to melt the solid. The most complete and reliable data on the minimum in the melting pressure at present seem to be those obtained from Hoffer's measurements of the molar volumes and the heat capacities.

REFERENCES

5,1) J.P.Franck, Phys.Letters 11(1964)208.

5,2) D.O.Edwards and R.C.Pandorf, Phys.Rev.140(1965)816.

5,3) G.Ahlers, Phys.Letters 22(1966)404.

5,4) J.S.Dugdale and F.E.Simon, Proc.roy.Soc.A 218(1953)291.

5,5) J.K.Hoffer, Ph.D.Thesis (Berkeley 1968).

5,6) C.A.Swenson, Phys.Rev.79(1950)626.

5,7) C.le Pair, K.W.Taconis, R.de Bruyn Ouboter and P.Das, Physica 29(1963)755.

5,8) G.C.Straty and E.D.Adams, Phys.Rev.Letters 17(1966)290,505.

5,9) S.G.Sydoriak and R.L.Mills, Proc.IXth intern.Conf.on Low Temp.Phys.(Columbus 1965)p.273.

5,10) J.Wiebes and H.C.Kramers, Phys.Letters 4(1963)298.

5,11) J.Wiebes and H.C.Kramers, Proc.Xth intern.Conf.on Low Temp.Phys.(Moscow 1967) Vol.I,p.243.

5,12) R.L.Mills and S.G.Sydoriak, Ann.Phys.(NY)34(1965)276.

5,13) G.O.Zimmerman, Proc.IXth intern.Conf.on Low Temp.Phys.(Columbus 1965)p.240.

5,14) J.H.Vignos and H.A.Fairbank, Phys.Rev.147(1966)185.

5,15) F.P.Lipschultz and D.M.Lee, Phys.Rev.Letters 14(1965)1017; Proc.Xth intern.Conf. on Low Temp.Phys.(Moscow 1967)Vol.I,p.309.

5,16) L.Goldstein, Phys.Rev.128(1962)1520.

5,17) C.J.N.van den Meijdenberg, Proposition VIII accompanying the Ph.D.Thesis (Leiden 1961).

5,18) C.le Pair, R.de Bruyn Ouboter and J.Pit, Commun.Kamerlingh Onnes Lab.,Leiden No.344a; Physica 31(1965)813.

5,19) L.Goldstein and R.L.Mills, Phys.Rev.159(1967)136.

CHAPTER VI

THE DISPERSION CURVES

6-1. Introduction

In this chapter the results obtained for the entropy of the liquid will be analysed in terms of constants relating to the shapes of the dispersion curves for elementary excitations. At temperatures below 1.6 K the original concepts of Landau need only slight refining in order to account for the dependence of the entropy on temperature. In sec. 6-2 the simplest parabolic approximation for rotons will be reviewed. The two refinements concern the symmetric deviation from parabolic behaviour in the roton region and a way to account for the interactions between the excitations. The former, treated in sec. 6-3, has to be estimated from the dispersion curves as obtained from experiments on inelastic neutron scattering. These are available at saturated vapour pressure and at 25.3 atm only; however, a general correction function $\varphi(T)$ can be introduced that seems to be practically independent of pressure. The latter, treated in sec. 6-4, will result in values for the roton minimum energy Δ that depend on temperature. In sec. 6-5 the final results for the roton parameters will be given and discussed.

6-2. The Landau spectrum

The concept of elementary excitations in liquid helium and the relations between their energy ε and momentum of magnitude p was proposed originally by Landau[6,1]). He distinguished between phonons or long-wave excitations (denoted by ph) and rotons with wavelengths of the order of the distance between atoms (denoted by r). The dispersion curves for pressures of 0 and 25.3 atm are shown in fig. 6,1. The dispersion relation for the phonons is:

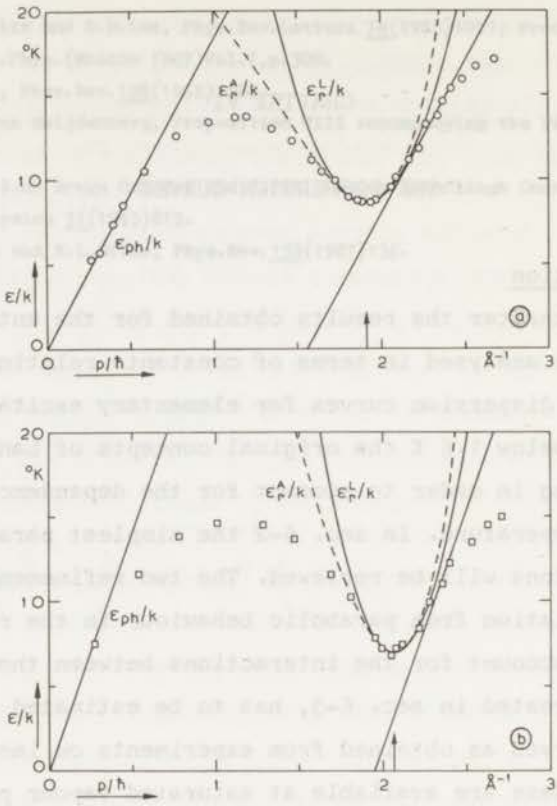

Fig. 6,1. Dispersion curves of liquid helium at 1.1 K; energy ε of elementary excitations as a function of momentum p;
a. at saturated vapour pressure; b. at 25.3 atm;
O □: results of Henshaw and Woods (1961), from neutron scattering;
—— : approximation of Landau (1941, 1947), linear for phonons (ε_{ph}) and parabolic for rotons (ε_r^L); - - - : asymmetric approximation for rotons (ε_r^A).

$$\varepsilon_{ph} = u\, p \ , \tag{6.1}$$

in which u is the velocity of ordinary or first sound. For the rotons a minimum is expected in the dispersion curve which therefore to a first approximation forms a parabola:

$$\varepsilon_r^L = \Delta + (p - p_o)^2 / 2\mu \ . \tag{6.2}$$

Table 6,I. Thermodynamic quantities and phonon contributions.

quantity	formula; $n = [\exp(\frac{\varepsilon}{kT}) - 1]^{-1}$	phonons, $\varepsilon_{ph} = u\,p$
number	$N = \frac{V}{h^3}\int n\, d^3p$	$N_{ph} = \frac{1.202}{\pi^2}\, V\, (\frac{kT}{u\hbar})^3$
free energy	$F = -\frac{V\,kT}{h^3}\int \ln(1+n)\, d^3p$	$F_{ph} = -\frac{\pi^2}{90} V\, u\, \hbar\, (\frac{kT}{u\hbar})^4 = -0.900\, N_{ph}\, kT$
entropy	$S = \frac{V\,k}{h^3}\int [\ln(1+n) + \frac{n\,\varepsilon}{kT}]\, d^3p$	$S_{ph} = \frac{2\pi^2}{45} V\, k\, (\frac{kT}{u\hbar})^3 = 0.900\, N_{ph}\, 4\, k$
heat capacity	$C_v = \frac{V}{h^3 kT^2}\int n\,(1+n)\,\varepsilon^2\, d^3p$	$C_{vph} = \frac{2\pi^2}{15} V\, k\, (\frac{kT}{u\hbar})^3 = 0.900\, N_{ph}\, 12\, k$
normal density	$\rho_n = \frac{1}{3\,h^3 kT}\int n\,(1+n)\,p^2\, d^3p$	$\rho_{nph} = \frac{2\pi^2}{45}\,\frac{\hbar}{u}\,(\frac{kT}{u\hbar})^4 = 0.900\,\frac{N_{ph}}{V}\,\frac{4\,kT}{u^2}$

Here Δ is the minimum energy required to excite a roton. The magnitude of the wave vector in the minimum, $p_o/\hbar$, is of the order of 2π times the inverse of the atomic distance. The parameter μ has the dimension of a mass.

The behaviour of the liquid can be deduced from this model. For the present purpose mainly the thermodynamical properties are of interest. These can be derived under the consideration that at low enough temperatures the excitations behave like a Bose-Einstein gas of weakly interacting particles the number of which, however, is not preserved. Straightforward calculations with the appropriate distribution function and differential in phase space:

$$n(\varepsilon) = [\exp(\frac{\varepsilon}{kT}) - 1]^{-1},\quad V\,h^{-3}d^3p = (6\pi^2)^{-1}\,V\,d(\frac{p}{\hbar})^3\,, \qquad (6.3)$$

yield the thermodynamic quantities. Some of these are shown in table 6,I. Also the phonon contributions are given varying as simple powers of the temperature. At sufficiently low temperatures the thermodynamic quantities are almost exclusively due to the contributions of the low-energetic phonons.

Table 6,II. Roton contributions to thermodynamic quantities.

quantity	Landau spectrum	Asymmetric spectrum
	$\varepsilon_r^L = \Delta + (p - p_*)^2 / 2\mu$	$\varepsilon_r^A = \Delta + a\,[(\frac{p}{\hbar})^3 - (\frac{p_*}{\hbar})^3]^2$ for $\lvert(\frac{p}{\hbar})^3 - (\frac{p_*}{\hbar})^3\rvert \le \frac{b}{2a}$
		$\varepsilon_r^T = (\Delta - \frac{b^2}{4a}) + b\,\lvert(\frac{p}{\hbar})^3 - (\frac{p_*}{\hbar})^3\rvert$ for $\lvert(\frac{p}{\hbar})^3 - (\frac{p_*}{\hbar})^3\rvert \ge \frac{b}{2a}$
	$A = \frac{2}{(2\pi)^{3/2}} \frac{m^{\frac{1}{2}} k^{\frac{1}{2}}}{\hbar} (\frac{p_*}{\hbar})^2 (\frac{\mu}{m})^{\frac{1}{2}}$, $\Theta = \frac{p_*^2}{\mu k}$	$a = \frac{\hbar^6}{18\,\mu\, p_*^4}$, $A = \frac{1}{6\,\pi^{3/2}} \frac{k^{\frac{1}{2}}}{a^{\frac{1}{2}}}$, $\theta = \frac{4\,a\,kT}{b^2}$
number	$N_r^L = A\,V\,T^{\frac{1}{2}}\, e^{-\Delta/kT}\,[1 + \frac{T}{\Theta} + 2^{\frac{1}{2}} \exp(-\frac{\Delta}{kT})]$	$N_r^C = A\,V\,T^{\frac{1}{2}}\, e^{-\Delta/kT}\,[1 + \varphi(\theta)]$
free energy	$F_r^L = - N_r^L\, kT\,[1 - 2^{-3/2} \exp(-\frac{\Delta}{kT})]$	$F_r^C = - N_r^C\, kT$
entropy	$S_r^L = N_r^L \frac{\Delta}{T}\,[1 + \frac{3}{2}\frac{kT}{\Delta} + \frac{kT}{\Delta}\frac{T}{\Theta} - 3\,2^{-5/2}\frac{kT}{\Delta}\exp(-\frac{\Delta}{kT})]$	$S_r^C = N_r^C \frac{\Delta}{T}\,[1 + \frac{3}{2}\frac{kT}{\Delta} + \frac{\theta\,\varphi'}{1+\varphi}\frac{kT}{\Delta}]$
heat capacity	$C_{vr}^L = N_r^L \frac{\Delta^2}{kT^2}\,[1 + \frac{kT}{\Delta} + \frac{3}{4}(\frac{kT}{\Delta})^2 + 2^{-\frac{1}{2}}\exp(-\frac{\Delta}{kT}) + 2\frac{kT}{\Delta}\frac{T}{\Theta}]$	$C_{vr}^C = N_r^C \frac{\Delta^2}{kT^2}\,[1 + \frac{kT}{\Delta} + \frac{3}{4}(\frac{kT}{\Delta})^2 + 2\frac{\theta\,\varphi'}{1+\varphi}\frac{kT}{\Delta}\,(1 + \frac{3}{2}\frac{kT}{\Delta})]$
normal density	$\rho_{nr}^L = \frac{N_r^L}{V}\frac{p_o^2}{3\,kT}\,[1 + 5\frac{T}{\Theta} + 2^{-\frac{1}{2}}\exp(-\frac{\Delta}{kT})]$	$\rho_{nr}^C = \frac{N_r^C}{V}\frac{p_o^2}{3\,kT}\,[1 - \{\frac{kT}{2\,b(p_o/\hbar)^3}\}^2]$

At higher temperatures enough energy becomes available to excite rotons. Their contribution to the thermodynamic quantities have been compiled in the first column of table 6,II. They show a steeply rising exponential factor $e^{-\Delta/kT}$. As a result the contributions of the rotons become dominant at temperatures above 1.0 K. Owing to the various terms within the square brackets, the roton contributions are not of a simple form. However, correction terms containing $\exp(-\Delta/kT)$, originating from the boson nature of the excitations, and those containing $1/\Theta$, arising from the symmetry of the approximation used for the excitation curve, do not exceed 1 % at temperatures below 1.6 K and will be omitted. The remaining correction, containing terms in kT/Δ, is of the order of 10 % at temperatures above 1.0 K.

With reasonable consistency the roton parameters may now be calculated from several thermodynamic quantities. As a result of the approximations made for the dispersion curve, effective values are found depending somewhat on the particular thermodynamic quantity and on the temperature interval used for the evaluation. Differences between values computed from different quantities may originate from the different weighting of the deviations from the actual curve according to the formulae in the first column of table 6,I. In the values obtained for Δ/k, which is of the order of 8 K, these effects may amount to a few tenths of a degree.

Better consistency can be obtained if two kinds of corrections are introduced to the Landau picture in its simplest form as presented above. The first concerns a better approximation to the actual shape of the dispersion curve, the second and more important one originates from the dependence of the curve on temperature. Both corrections have been made possible by a direct determination of the dispersion curves based on the ideas of Cohen and Feynman [6,2]. This was done by experiments on inelastic neutron scattering [6,3-9] yielding the energy and its spread at limited values of the momentum. The measuring points in fig. 6,1 are those of Henshaw

and Woods[6,8]). It was found that at increasing temperatures above 1.0 K the dispersion curve is lowered; consequently, a lower value for the minimum energy results. A further examination of this effect will be given in sec. 6-4 where the appropriate correction will be treated.

6-3. Corrections for the shape of the dispersion curve

The influence of a first correction depending on the actual shape of the curve is more clearly seen in a plot of ε/k as a function of $(p/\hbar)^3$ than in fig. 6,1. This is because the differential in phase space essentially equals $d(p/\hbar)^3$. Plotted in this way, the measuring points from the neutron experiments yield fairly symmetric curves (see fig. 6,2 for the two pressures mentioned). Near the minimum it may be approximated by a parabola in $(p/\hbar)^3$:

$$\varepsilon_r^A = \Delta + a\,[(p/\hbar)^3 - (p_o/\hbar)^3]^2 . \qquad (6.4)$$

In fig 6,1 the corresponding curves have been plotted as dotted lines. The curvature in the minimum of the new curves as a function of $p/\hbar$ should be the same as that in the simple Landau spectrum ε_r^L. To fulfil this condition the coefficient a must have the value $\hbar^6/18\,\mu\,p_o^4$. The new curves are clearly asymmetric in $p/\hbar$; for that reason the energy has been labelled A.

The contributions may now be calculated that would follow from these values ε_r^A. The only difference with the results obtained from ε_r^L is the disappearance of all the correction terms containing $1/\Theta$ except for the one concerning the normal density ρ_{nr}. In the latter the term $+5T/\Theta$ becomes $-T/\Theta$. Clearly the asymmetry is of little importance to the thermodynamic quantities, giving effects of only second order of magnitude.

A further approximation is shown in fig. 6,2. At some distance from the minimum the curves can be well described by tangents to

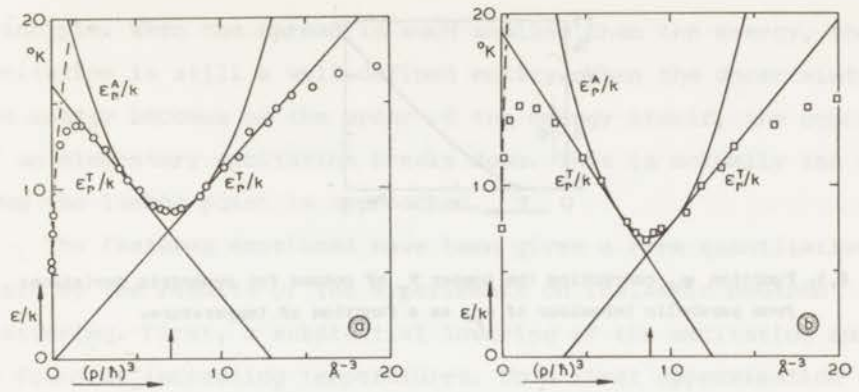

Fig. 6,2. Energy ε of elementary excitations in liquid helium at 1.1 K, as a function of the third power of momentum, p^3;
a. at saturated vapour pressure; b. at 25.3 atm;
○ □ : results of Henshaw and Woods (1961), from neutron scattering;
—— : asymmetric approximation for rotons composed of a parabola (ε_r^A) and its tangents (ε_r^T) in p^3; - - - :phonon branch.

the parabola:

$$\varepsilon_r^T = (\Delta - b^2/4\,a) + b \left|(p/\hbar)^3 - (p_o/\hbar)^3\right| \qquad (6.5)$$

$$\text{for} \quad \left|(p/\hbar)^3 - (p_o/\hbar)^3\right| \geq b / 2\,a\,.$$

Here b is the absolute value of the slope of the tangent, $d\varepsilon_r^T/d(p/\hbar)^3$. Omitting asymmetries in the calculations, b is given the same (averaged) value on both sides of the minimum. The environment of the minimum itself, within the region where $\left|(p/\hbar)^3 - (p_o/\hbar)^3\right|$ is smaller than b/2a, will still be described by the parabola ε_r^A.

The corrected thermodynamic quantities denoted by C, as calculated with this approximation, are given in the second column of table 6,II. A correction $\varphi(\theta)$ applies to the number of rotons and its derivative φ' occurs in the expressions for the entropy and the specific heat. It depends on only one variable θ equal to $4kTa/b^2$ and is equal to the integral:

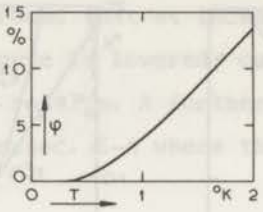

Fig. 6,3. Function φ, correcting the number N_r of rotons for symmetric deviations from parabolic behaviour of ε_r, as a function of temperature.

$$\varphi = \int_{(p_o/\hbar)^3 + b/2a}^{\infty} [e^{-\varepsilon_r^T/kT} - e^{-\varepsilon_r^A/kT}] d(p/\hbar)^3 \Big/ \int_{(p_o/\hbar)^3}^{\infty} e^{-\varepsilon_r^A/kT} d(p/\hbar)^3 \qquad (6.6)$$

This can be shown to reduce to:

$$\varphi(\theta) = \tfrac{1}{2}\, \pi^{-\frac{1}{2}} \int_0^{\theta} x^{-\frac{1}{2}}\, e^{-1/x}\, dx\ . \qquad (6.7)$$

The constant $b^2/4ak$ has been estimated from figs. 6,2a and b and has the approximate value of 0.88 K, being almost independent of the pressure. The correction is given in fig. 6,3 as a function of temperature. The extra corrections to the thermodynamic quantities due to φ are of the order of 10 % at temperatures above 1.0 K.

6-4. The temperature dependence of the dispersion curve

In the treatment given in the previous sections, no attention was paid to the interactions between the excitations. The interactions were supposed to be "weak" meaning that they establish thermal equilibrium without contributing to the energy. However, it must be expected that at temperatures above 1.0 K the boson gas can no longer be regarded as a perfect gas. At increasing excitation density the number of collisions will increase. The energy of the excitations will be affected and their lifetimes decreased causing a finite spread in their energies as a result of the uncertainty

principle. When the spread is much smaller than the energy, the excitation is still a well-defined entity. When the uncertainty in the energy becomes of the order of the energy itself, the concept of an elementary excitation breaks down. This is actually the case when the lambda point is approached.

The features mentioned have been given a firm quantitative basis by the results of the experiments on inelastic neutron scattering. First, a substantial lowering of the excitation curve is found at increasing temperatures. To a first approximation the general form of the curve is conserved and only the value of the parameter Δ is affected, becoming a function of the temperature (see fig. 6,6 for the results of Yarnell et al.[6,7]) and those of Henshaw and Woods[6,9])). The question may be raised whether the lowering of the energies at increasing density is a consequence of the boson nature of the excitations. Secondly, the line widths of the scattered neutrons are found to increase at increasing temperatures and to become of the order of the excitation energies at the lambda point. Consequently, the excitations by no means possess unique energies in that case. However, this effect has not been taken into account in the calculations of the thermodynamic quantities, which have been performed on the assumption of sharp dispersion curves.

From dispersion curves at saturated vapour pressure as measured by Yarnell, Arnold, Bendt, and Kerr[6,7]), the thermodynamic quantities have been computed by Bendt, Cowan, and Yarnell[6,10]). In the case of small interactions there seems to be agreement about the statistical procedures by which the calculations must be performed if the excitation curve depends on temperature[6,10])[6,11]). By a simple argument it can be shown that the expression for the entropy is the same as the one given in the first column of table 6,I; at each temperature the entropy may be computed from the corresponding excitation curve $\varepsilon(T)$. Consequently, the other quantities cannot be calculated according to the formulae mentioned.

They must be computed directly from the entropy, either by differentiation (C_v) or by integration (F).

The calculations of Bendt et al. have been made for several ways of interpolating the values of $\varepsilon(T)$ from those measured at temperatures of 1.1, 1.6, and 1.8 K. The lowering of the energies may be taken proportional either to the number density or to the normal density. Within the accuracy reached the difference between the two is not significant. An agreement of the order of 2 % is claimed between the calculated values and those measured for the entropy, the specific heat, and the normal density at saturated vapour pressure.

Reversing the procedure it must also be possible to calculate the temperature dependent values of the roton minimum energy $\Delta(T)$ from the entropies. This can be done only if the necessary corrections for the shape of the excitation curve can be applied. This analysis is given in the next section. It is based on the form of S_r^C from the second column of table 6,II for the roton entropy.

6-5. Analysis of the results for the entropy

As a first step in the analysis, the values at low temperatures of the measured heat capacities of liquid helium have been divided by T^3 (see sec. 4-3,c, table 4,V, and figs. 4,3 and 4,5). Up to temperatures indicated by T_{ph} there result constant values of $(W - W_c)/T^3$ that are proportional to the inverse cube u^{-3} of the velocity of first sound. Consequently at temperatures below T_{ph}, the heat capacity is due to phonon contributions only.

The second step is the analysing of the roton contributions. This should be done from the specific entropies $s_l(\rho_l, T)$ as has been argued in the previous section. Thus, the phonon contributions s_{lph} (equal to $S_{ph}/V\,\rho_l$) have been subtracted; the remainders are taken as the roton contributions s_{lr}. No corrections have been applied for the dependence of the velocity of sound on the

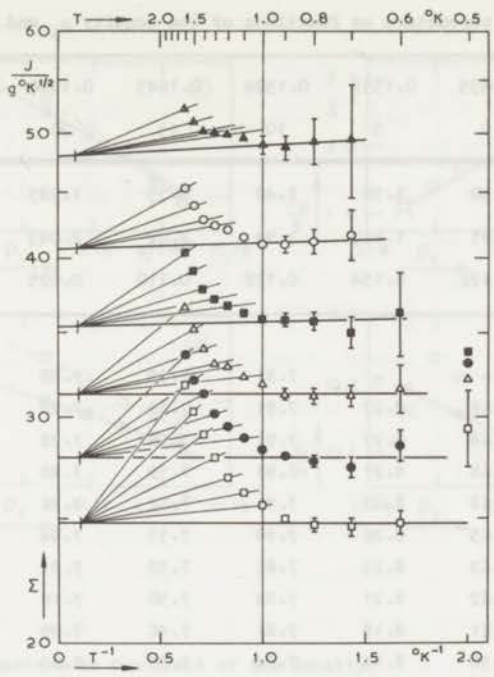

Fig. 6,4. Calculation of roton parameters; modified entropies Σ (see text) at several densities, as functions of the inverse of temperature;
▲: 0.1455 g/cm^3; ○ : 0.1532 g/cm^3; ■ : 0.1594 g/cm^3;
△: 0.1645 g/cm^3; ● : 0.1690 g/cm^3; □ : 0.1729 g/cm^3.

temperature since at temperatures above 1.0 K the phonon contributions are small as compared to those of the rotons; hence the corrections are negligible.

According to the second column of table 6,II, the specific entropy due to the rotons has the following form:

$$s_{1r}(\rho_1,T) = \frac{A\Delta}{\rho_1} T^{-\frac{1}{2}} e^{-\Delta/kT} \left(1 + \frac{3}{2}\frac{kT}{\Delta}\right)\left(1 + \varphi + \frac{\theta\,\varphi'\,kT/\Delta}{1 + \frac{3}{2}\,kT/\Delta}\right) . \quad (6.8)$$

The correction factors may be estimated within the required accuracy from preliminary values for the parameters. In order to avoid steep functions, a large part of the exponential factor was eliminated beforehand. This was done by dividing the entropy by $\exp(-\Delta_a/kT)$ where Δ_a is an approximate value for the roton minimum

Table 6,III. Roton parameters as functions of the density ρ_1 and the temperature.

ρ_1	0.1455	0.1532	0.1594	0.1645	0.1690	0.1729	g/cm^3
pressure at 0 K	0	5	10	15	20	25	atm
$(p_o/\hbar)^2(\mu/m)^{\frac{1}{2}}$	1.60	1.50	1.42	1.35	1.285	1.215	Å^{-2}
$p_o/\hbar$ [1])	1.91	1.955	1.99	2.02	2.045	2.065	Å^{-1}
μ/m	0.192	0.154	0.128	0.110	0.095	0.082	
$\Delta(T)/k$							
T = 0.6 K	–	–	7.91	7.59	7.28	7.00	K
0.7	8.68	8.27	7.91	7.59	7.28	7.00	
0.8	8.68	8.27	7.91	7.59	7.28	7.00	
0.9	8.68	8.27	7.91	7.59	7.28	6.99	
1.0	8.68	8.27	7.91	7.57	7.26	6.96	
1.1	8.65	8.26	7.88	7.55	7.24	6.93	
1.2	8.63	8.23	7.86	7.52	7.21	6.89	
1.3	8.62	8.21	7.84	7.50	7.16	6.82	
1.4	8.61	8.18	7.81	7.46	7.09	6.74	
1.5	8.58	8.14	7.74	7.35	7.03	6.64	
1.6	8.52	8.07	7.66	7.29	6.93	6.52	

[1]) Interpolated from neutron scattering experiments[6,8]).

energy. The values of:

$$\Sigma = \frac{s_{1r}\, T^{\frac{1}{2}} \exp(\Delta_a/kT)}{1 + \frac{3}{2}\frac{kT}{\Delta_a} + \varphi + (\frac{3}{2}\varphi + \theta\varphi')\frac{kT}{\Delta_a}} \qquad (6.9)$$

have been plotted logarithmically as a function of T^{-1} (fig. 6,4). It yields:

$$\ln \Sigma = \ln A\Delta/\rho_1 + \left(\frac{\Delta_a}{k} - \frac{\Delta}{k}\right) T^{-1}, \qquad (6.10)$$

which gives a straight line with a slope of $(\Delta_a - \Delta)/k$ if Δ is a constant. The errors indicated are such as would arise from an experimental error of 1 % in the total entropies s_1. They are only appreciable at temperatures below 0.8 K.

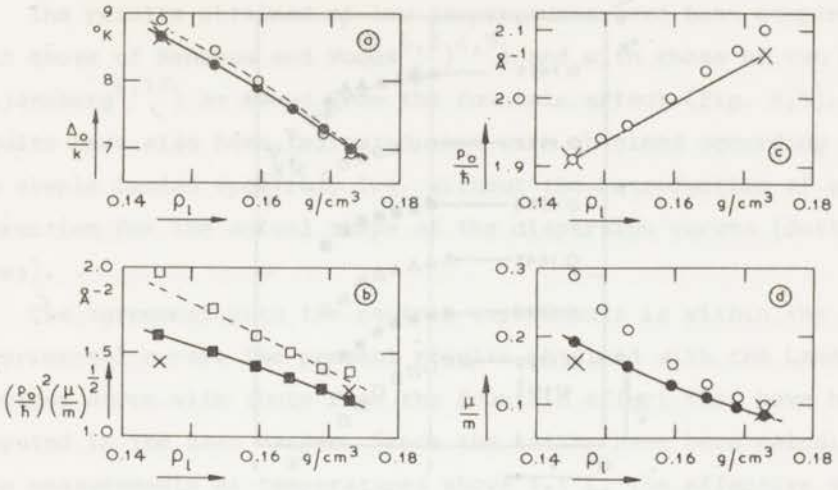

Fig. 6,5. Roton parameters as functions of the density;
● ■ : present results; × : Henshaw and Woods (1961), from neutron scattering;
- - - : results from the present entropies, obtained with the Landau approximation; O □ : van den Meijdenberg et al.(1961), from the fountain effect, obtained with the Landau approximation for the dispersion curve.

The parts at temperatures below 1.0 K can be extrapolated to T^{-1} equal to zero, giving the values of the constants A equal to:

$$A = 2^{-\frac{1}{2}} \pi^{-\frac{3}{2}} m^{\frac{1}{2}} k^{\frac{1}{2}} \hbar^{-1} (p_o/\hbar)^2 (\mu/m)^{\frac{1}{2}} . \qquad (6.11)$$

The combination of parameters $(p_o/\hbar)^2(\mu/m)^{\frac{1}{2}}$ and the value Δ_o of the minimum energy at temperatures below 1.0 K can be found directly. They have been compiled in table 6,III. Values for $p_o/\hbar$ interpolated from the data on neutron scattering at 0 and 25 atm [6,8] (see fig. 6,5c) have been used to calculate μ/m which is found within an error of 10 %. The error in Δ_o is estimated to be 0.05 to 0.10 K. The results are shown in fig. 6,5.

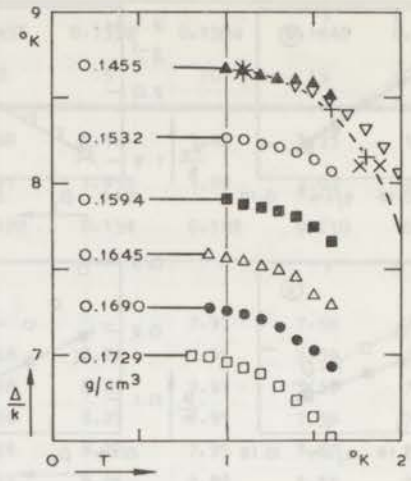

Fig. 6,6. Roton minimum energies Δ at several densities, as functions of temperature; ▲○■△●□ : present results; ▽ : Kramers et al.(1952), at SVP; + : Yarnell et al.(1959), at SVP; - - - : used by Bendt et al.(1959); × : Henshaw and Woods (1961), at SVP.

By means of the values of A and Δ_o obtained at low temperatures, the temperature dependent values of $\Delta(T)$ at temperatures above 1.0 K can now be found. In this connection it is observed that $\ln A\Delta/\rho_1$ is still nearly constant. Graphically, this means that fixed points may be found near the intersections of the extrapolated low-temperature parts with the axis at T^{-1} equal to zero (see fig. 6,4). Straight lines connecting these fixed points with the plotted points have slopes equal to the required lowerings of Δ/k. The results for Δ/k as functions of temperature have been given in table 6,III and in fig. 6,6.

6-6. Discussion and conclusion

The results obtained at low temperatures have been compared with those of Henshaw and Woods[6,8)6,9)] and with those of van den Meijdenberg[6,12)] as found from the fountain effect (fig. 6,5). Results have also been indicated that were obtained according to the simple Landau spectrum, i.e. without the introduction of a correction for the actual shape of the dispersion curves (dotted lines).

The agreement with the neutron experiments is within the experimental error. The present results obtained with the Landau spectrum agree with those from the fountain effect that have been computed in the same manner. Since the latter have been calculated from measurements at temperatures above 1.1 K, the effective values of Δ_o and $(p_o/\hbar)^2(\mu/m)^{\frac{1}{2}}$ must be expected to be higher than the actual ones. This can be seen from fig. 6,4; according to eq. (6.10), extrapolation of data at temperatures higher than 1.0 K yield lines with negative slopes equal to $(\Delta_a - \Delta)/k$. Consequently, the present results obtained with the application of a correction for the shape of the dispersion curves lie systematically lower than those of van den Meijdenberg except for values for Δ_o/k at the highest pressures.

In fig. 6,6 the temperature dependent values of $\Delta(T)/k$ are compared with those obtained from neutron scattering by Yarnell et al.[6,7)] and by Henshaw and Woods. Also the values as used by Bendt et al.[6,10)] in their calculation of thermodynamic quantities have been indicated by a dashed line. Finally the results at saturated vapour pressure of Kramers et al.[6,13)] have been analysed in the same way as the present results. These points extend to 2.0 K and are also shown in the figure. The results from the experiments on neutron scattering seem to indicate a decrease of Δ towards higher temperatures somewhat steeper than do the results obtained from the measurements of the heat capacities. This is perhaps a consequence of the spread of the roton energies. However, in view

of the experimental errors in the latter determination, the differences are probably not significant.

It may be concluded that the thermodynamic properties of liquid ^{4}He under pressure at temperatures up to 1.0 K can be described within an accuracy of 2 % by five parameters that are functions of the density. The single parameter u, the velocity of sound, describes the phonons. The other four all treat the rotons and are the minimum energy Δ_o, the characteristic momentum p_o, the effective mass μ, and a parameter b correcting for the shape of the dispersion curve. At temperatures above 1.0 K, the minimum energy of the rotons can no longer be considered as a constant. By the introduction of a temperature dependancy in the roton minimum energy, the description given may be maintained up to temperatures in the vicinity of the lambda line.

REFERENCES

6,1) L.D.Landau, J.Phys.U.S.S.R.5(1941)71;11(1947)91; see also D.ter Haar in Selected Readings in Physics, Vol.I, Low Temperature and Solid State Physics; Men of Physics: L.D.Landau (Pergamum Press 1955).

6,2) M.Cohen and R.P.Feynman, Phys.Rev.107(1957)13.

6,3) H.Palevsky, K.Otnes, K.E.Larsson, R.Pauli and S.Stedman, Phys.Rev.108(1957)1346.

6,4) D.G.Henshaw, Phys.Rev.Letters 1(1958)127.

6,5) H.Palevsky, K.Otnes and K.E.Larsson, Phys.Rev.112(1958)11.

6,6) K.E.Larsson and K.Otnes, Ark.Fys.15(1959)49.

6,7) J.L.Yarnell, G.P.Arnold, P.J.Bendt and E.C.Kerr, Phys.Rev.113(1959)1379.

6,8) D.G.Henshaw and A.D.B.Woods, Proc.VIIth intern.Conf.on Low Temp.Phys.(Toronto 1961)p.539.

6,9) D.G.Henshaw and A.D.B.Woods, Phys.Rev.121(1961)1266.

6,10) P.J.Bendt, R.D.Cowan and J.L.Yarnell, Phys.Rev.113(1959)1386.

6,11) M.Cohen, Phys.Rev.118(1960)27.

6,12) C.J.N.van den Meijdenberg, K.W.Taconis and R.de Bruyn Ouboter, Commun.Kamerlingh Onnes Lab.,Leiden No.326c; Physica 27(1961)197.

6,13) H.C.Kramers, J.D.Wasscher and C.J.Gorter, Commun.Leiden No.288c; Physica 18 (1952)329.

SAMENVATTING

In dit proefschrift worden calorische metingen beschreven die zijn verricht aan ^{4}He in het temperatuurgebied van 0.3 tot 1.6 K, onder drukken variërend van die van de verzadigde damp tot de smeltdruk, i.e. van 0.0 tot 25.0 atm.

De experimenten zijn uitgevoerd in een "open" koperen kalorimeter. De magnetische thermometer is, met spoelen en ceriummagnesiumnitraat als meetzout, geheel in de kalorimeter ondergebracht om goed warmtekontakt te verzekeren. De temperaturen zijn bepaald met behulp van een nieuw ontwikkelde kompensator voor wederkerige induktie, die een vaste standaard heeft met een varieerbare primaire stroom. De druk in de kalorimeter wordt bepaald met een manometer die op het vulkapillair is aangesloten. De kalorimeter is omsloten door een vakuümmantel die is geplaatst in een bad met vloeibaar helium, dat door afpompen op een temperatuur van 1.1 K wordt gehouden. Lagere temperaturen worden bereikt door demagnetisatie van een koelzoutpil, die binnen de vakuümmantel op het vulkapillair is geplaatst en via een supergeleidende warmteschakelaar met de kalorimeter is verbonden. De koelzoutpil dient tevens als buffer tegen warmtelekken.

Met deze opstelling zijn de warmtekapaciteiten gemeten van vloeibaar helium onder verscheidene drukken, en die van twee--fasensystemen van vloeistof met gas of met vaste stof. Bovendien is de mogelijkheid van adiabatische expansie, door het aflaten van vloeistof zonder toevoer van warmte, benut om de uitzettingskoëfficiënt van de vloeistof en de helling van de smeltlijn te bepalen. Deze volgen uit de temperatuurverandering die gepaard gaat met een drukverandering veroorzaakt door aflaten van vloeistof, respektievelijk met het aflaten van een hoeveelheid helium waardoor er vaste stof smelt. Een overzicht van deze metingen wordt in

hoofdstuk I gegeven. Er moet wel op worden gewezen dat andere metingen dan die aan de vloeistof onder praktisch konstante druk, waarvoor de kalorimeter oorspronkelijk is ontworpen, te lijden kunnen hebben van onzekerheden in de kalibratie van de magnetische thermometer en andere moeilijk te vermijden systematische fouten.

In hoofdstuk II wordt de meetapparatuur beschreven. In hoofdstuk III wordt een gedetailleerde afleiding van de gebruikte formules gegeven en worden de talrijke korrekties besproken. Verder wordt een overzicht gegeven van de te gebruiken gegevens uit andere bronnen, die in sommige gevallen nader zijn bewerkt, met name de geëxtrapoleerde toestandsvergelijking bij het absolute nulpunt.

In hoofdstuk IV worden de metingen aan de vloeistof onder druk nader uitgewerkt. Berekend zijn: de soortelijke warmte bij konstante druk en die bij konstant volume; de soortelijke entropie door integreren naar de temperatuur van het kotiënt van de soortelijke warmte en de temperatuur; de uitzettingskoëfficiënt door differentiëren van de soortelijke entropie naar de druk. De soortelijke warmte sluit binnen de meetnauwkeurigheid aan bij de resultaten van Lounasmaa (1961), die in het temperatuurgebied van 1.5 tot 3.0 K heeft gemeten, en bij bestaande resultaten langs de dampspanningslijn van Kramers et al.(1952) en Wiebes et al.(1957). De entropie sluit redelijk aan bij de resultaten van van den Meijdenberg et al.(1961), verkregen uit het fonteineffekt. De resultaten voor de uitzettingskoëfficiënt, die noch via de entropie noch uit de expansiemetingen nauwkeurig kan worden bepaald, zijn niet in tegenspraak met die van Boghosian en Meyer (1966), verkregen uit metingen van de brekingsindex.

In hoofdstuk V zijn de metingen behandeld die zijn verricht aan het systeem vloeistof-vaste stof. De uitkomsten voor de soortelijke warmte van de vaste stof zijn niet bevredigend; ten gevolge van onzekerheden in de aan Swenson (1950) ontleende waarde voor het dichtheidsverschil van de vloeistof en de vaste stof, en mogelijke systematische fouten in de bepaling van de hoeveelheid vast

helium is het resultaat waarschijnlijk bij temperaturen onder ongeveer 0.7 K te laag en daarboven te hoog. De hieruit berekende diepte van het minimum in de smeltdruk is waarschijnlijk 10 % te klein. De uit de expansiemetingen gevonden waarde voor de diepte van het minimum is in overeenstemming met de resultaten van Straty en Adams (1966), verkregen uit direkte drukmeting, en die van Hoffer (1968), verkregen uit nauwkeurige metingen van de soortelijke warmte.

In hoofdstuk VI wordt de entropie van de vloeistof geanalyseerd volgens het model van de elementaire excitaties. Hiertoe worden de konstanten bepaald die de vorm van de dispersiekrommen voor de excitaties beheersen. Op de eenvoudigste parabolische benadering van het rotongedeelte volgens Landau (1947) zijn twee verfijningen aangebracht. De eerste betreft de symmetrische afwijkingen van een parabolisch verloop, die kunnen worden geschat aan de hand van de vorm van de excitatiekrommen, zoals die uit experimenten aan inelastische verstrooing van neutronen worden gevonden. De tweede behelst een manier om de wisselwerking tussen de excitaties in rekening te brengen, en resulteert in een temperatuurafhankelijkheid van de minimale energie Δ die nodig is om een roton aan te slaan. De uitkomsten sluiten goed aan bij de bestaande resultaten verkregen uit de neutronenexperimenten.